Title
Numerical Simulation of Land Subsidence in the Los Banos-Kettleman City Area, California

Authors
Larson, Keith J
Basagaoglu, Hakan
Marino, Miguel

Publication Date
2001

Numerical Simulation of Land Subsidence in the Los Banos-Kettleman City Area, California

Keith J. Larson
Hakan Basagaoglu
Department of Civil & Environmental Engineering

Miguel Mariño
Department of Land, Air and Water Resources
University of California, Davis

Technical Completion Report
Project Number UCAL-WRC-W-892

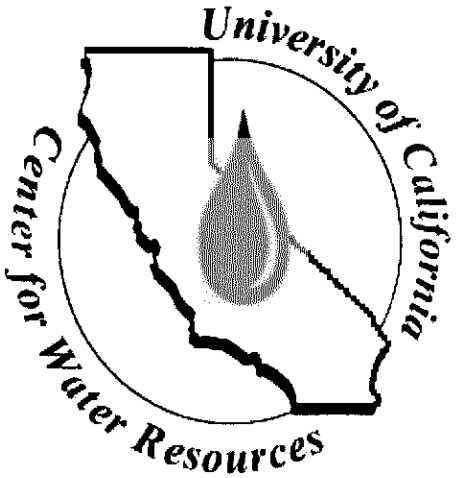

University of California
Water Resources Center

Contribution #207
ISBN 1-887192-13-1
January 2001

This publication is a continuation of the Water Resources Center Report series. It is published and distributed by the DIRECTOR'S OFFICE OF THE UC CENTER FOR WATER RESOURCES. The Center sponsors projects in water resources and related research within the state of California with funds provided by various state and federal agencies and private industry. Copies of this and other reports published by the Center may be obtained from:

UC CENTER FOR WATER RESOURCES
WATER RESOURCES CENTER
RUBIDOUX HALL - 094
UNIVERSITY OF CALIFORNIA
RIVERSIDE, CA 92521
(909) 787-4327

Copies of Center publications may be examined at the Water Resources Center Archives, 410 O'Brien Hall, University of California, Berkeley, CA 94720 (510) 642-2666.

This publication is available on the web site of the UC Center for Water Resources. The URL is http://www.waterresources.ucr.edu.

Funding for this publication is provided by the University of California. It is available to the general public free of charge.

Abstract

Land subsidence caused by the excessive use of groundwater resources has traditionally caused serious and costly damage to the Los Banos-Kettleman City area of California's San Joaquin Valley. Although the arrival of surface water from the Central Valley Project has reduced subsidence in recent decades, the growing instability of surface water supplies has refocused attention on the future of land subsidence in the region. This report develops a three-dimensional, numerical simulation model for both groundwater flow and land subsidence. The simulation model is calibrated using observed data from 1972 to 1998. A probable future drought scenario is used to consider the effect on land subsidence of three management alternatives over the next thirty years. Maintaining present practices virtually eliminates unrecoverable land subsidence, but with a growing urban population to the south and concern over the ecological implications of water exportation from the north, it does not appear that the delivery of surface water can be sustained at current levels. The two other proposed management alternatives reduce the dependency on surface water by increasing groundwater withdrawl. Land subsidence is confined to tolerable levels in the more moderate of these proposals, while the more aggressive produces significant long-term subsidence. Finally, an optimization model is formulated to determine maximum groundwater withdrawl from nine water sub-basins without causing irrecoverable subsidence over the forecasted period. The optimization reveals that withdrawl of groundwater supplies can be increased in certain areas in the eastern side of the study area without causing significant subsidence.

KEY WORDS: Subsidence, groundwater and groundwater hydrology, optimization, systems modeling, environmental impacts.

Table of Contents

List of Tables

List of Figures

1. Introduction

The San Joaquin Valley is an important agricultural region in California, contributing billions of dollars to the state's economy and providing jobs and food for the state's growing population. As such, providing affordable water for agriculture has traditionally been a high priority for water managers in the region. In recent years, however, economic and environmental concerns over a limited water supply have threatened the viability of agriculture in portions of the Valley.

One of the more subtle of these concerns is land subsidence. Land subsidence is defined as a lowering of the land surface elevation. Although this hydrogeological hazard progresses slowly, it can result in significant economic losses over time (Hua et al., 1993). In the San Joaquin Valley, land subsidence has caused serious and costly damage to highways, water-transport structures and deep water wells (Ireland et al., 1984). Although there are several causes of land subsidence, the majority of subsidence in the Valley can be attributed to overpumping of the aquifer system underlying the region (Ireland et al., 1984).

Prior to 1967, the main source of irrigation water was groundwater. As unregulated pumping accompanied rapid agricultural development, dramatic drawdown occurred in the aquifers underlying the region. One result of this drawdown was severe land subsidence throughout much of the Valley. In 1967, the completion of the California Aqueduct provided a new source of water for irrigation. As canals and delivery systems were completed, the demand for groundwater was reduced and land subsidence rates correspondingly decreased. However, the inevitability of drought and the continued growth of urban areas to the south made the aqueduct a less than reliable alternative. This was evident in 1977 and the early 1990s as drought forced a renewed dependence on groundwater and the return of subsidence (California Department of Water Resources, 1998).

The goal of this research is to evaluate the effects of existing and proposed water management plans on land subsidence in the Los Banos-Kettleman City region of the San Joaquin Valley. This will be accomplished through: (1) employment of existing numerical models to simulate groundwater flow and land subsidence over the Los Banos-Kettleman City region; (2) calibration of the overall model using observed groundwater and subsidence data for the years 1972 to 1999; (3) identification of the most influential aquifer parameters and their roles in model calibration (4) construction of future water availability scenarios; and (5) implementation of the calibrated model to estimate future land subsidence for the existing and proposed management alternatives.

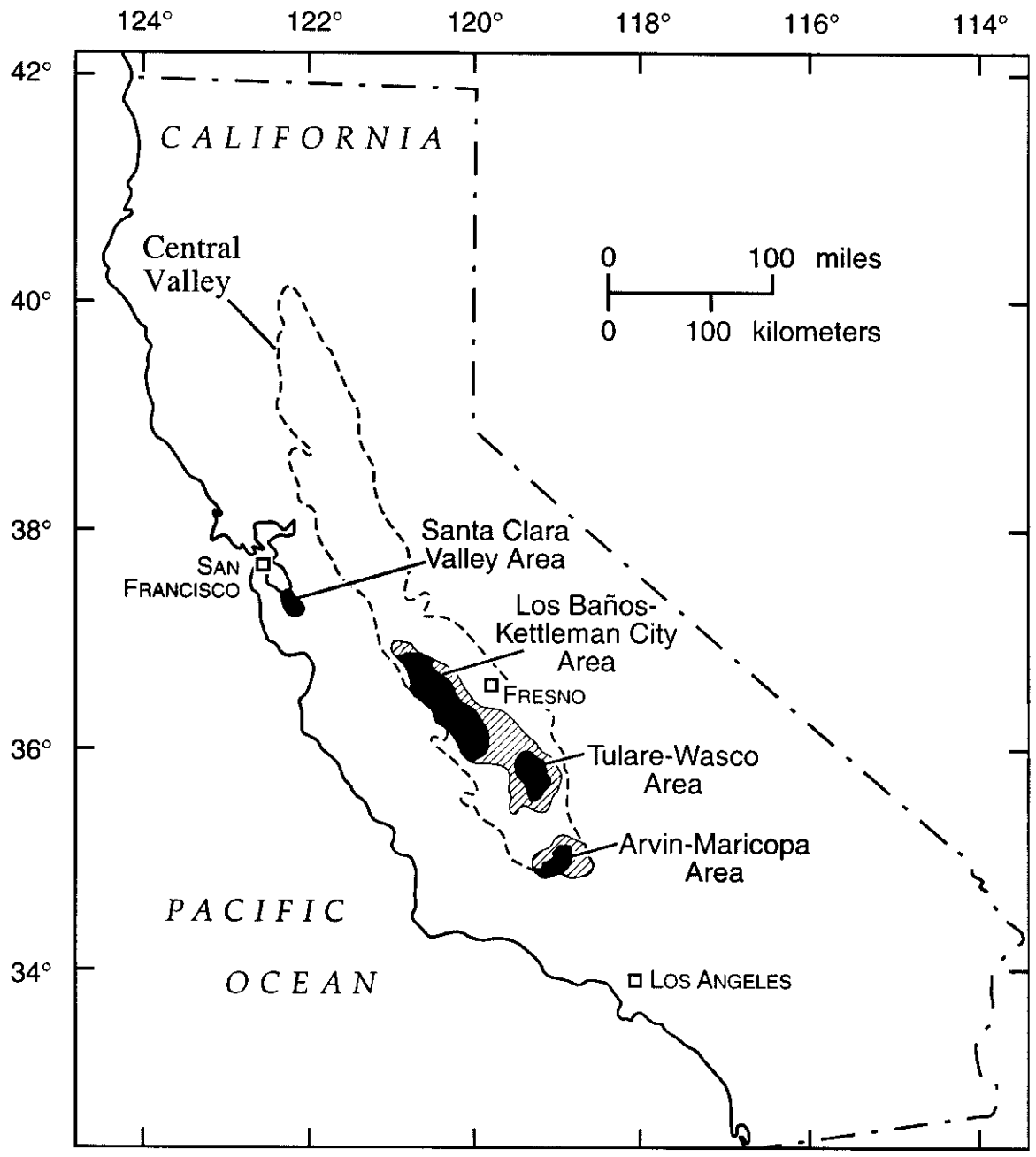

Figure 1 - Areas of observed land subsidence in the Central Valley and vicinity.

2. Background

2.1 Subsidence in the San Joaquin Valley

California's San Joaquin Valley (Figure 1) is one of the most productive and intensely farmed agricultural areas in the world (American Farmland Trust, 1995). As early as the 1920s, intense abstractions of groundwater in excess of natural recharge began to cause groundwater storage depletion and corresponding land subsidence across the Valley (Ireland et al., 1984). By 1969, subsidence reached nearly 29 feet in one location with a total volume of 15.5 MAF for the entire San Joaquin Valley (Poland, 1981).

Subsidence can have several negative economic, social and technical implications. Problems associated with land subsidence include: (1) changes in groundwater and surface water flow patterns (e.g., Lofgren, 1979); (2) decline in aquifer storage capacity (e.g., Belitz and Phillips, 1995); (3) localized flooding (e.g., Hua et al., 1993); (4) failure of well casings and changes in channel gradient (e.g., Holzer, 1989); (5) damage to highways, buildings, and other structures (e.g., Ireland et al., 1984); etc. By the mid 1960s, several regions in the San Joaquin Valley were facing many of these problems. Millions of dollars had been spent repairing damage to structures and deep water wells, while continually changing gradients caused farmers to spend additional dollars on recurrent land leveling (e.g., Ireland, 1986).

The arrival of imported surface water supplies in the late 1960s greatly reduced the amount of groundwater withdrawn from the region. With the reduction in pumping, the rate of land subsidence also declined. During droughts in 1976-77 and 1987-1993, however, groundwater supplies were pumped heavily to meed demand as surface water deliveries were reduced. In the Los Banos-Kettleman City area, pumping increased to an estimated 470,000 acre-feet in 1977 compared to a yearly average of less than 100,000 acre-feet between 1974 and 1976 (Ireland et al., 1984). The result was the return of significant subsidence, although rates only reached about half of those before the arrival of surface water (see Figure 8).

In addition to drought, several other factors threaten future surface water supplies to the San Joaquin Valley. The implementation of the Central Valley Project Improvement Act (CVPIA) will transfer 800,000 acre-feet of surface water to augment instream flow and meet other environmental purposes. The growth of urban populations to the south will place an additional strain on existing imported water supplies. The surface water for the Valley remains precariously balanced between competing urban, environmental, and agricultural interests. Although recent measurments reveal that annual average land subsidence rates have declined over the last three decades, the volatile future of imported surface water in the region maintains land subsidence as a serious concern to local and state water agencies (California DWR, 1998).

2.2 The Los Banos-Kettleman City Region

Three areas of the San Joaquin Valley exhibit especially severe subsidence: the Los Banos-Kettleman City area, the Tulare-Wasco area, and the Arvin-Maricopa area. The area chosen for this research comprises the northern portion of the Los Banos-Kettleman

City area. This 550-square mile region of western Fresno County (Figure 2) has been chosen because of the large amount of available groundwater and land subsidence data. Additionally, several previous studies have been conducted in the region, providing important insight into several aspects of this research.

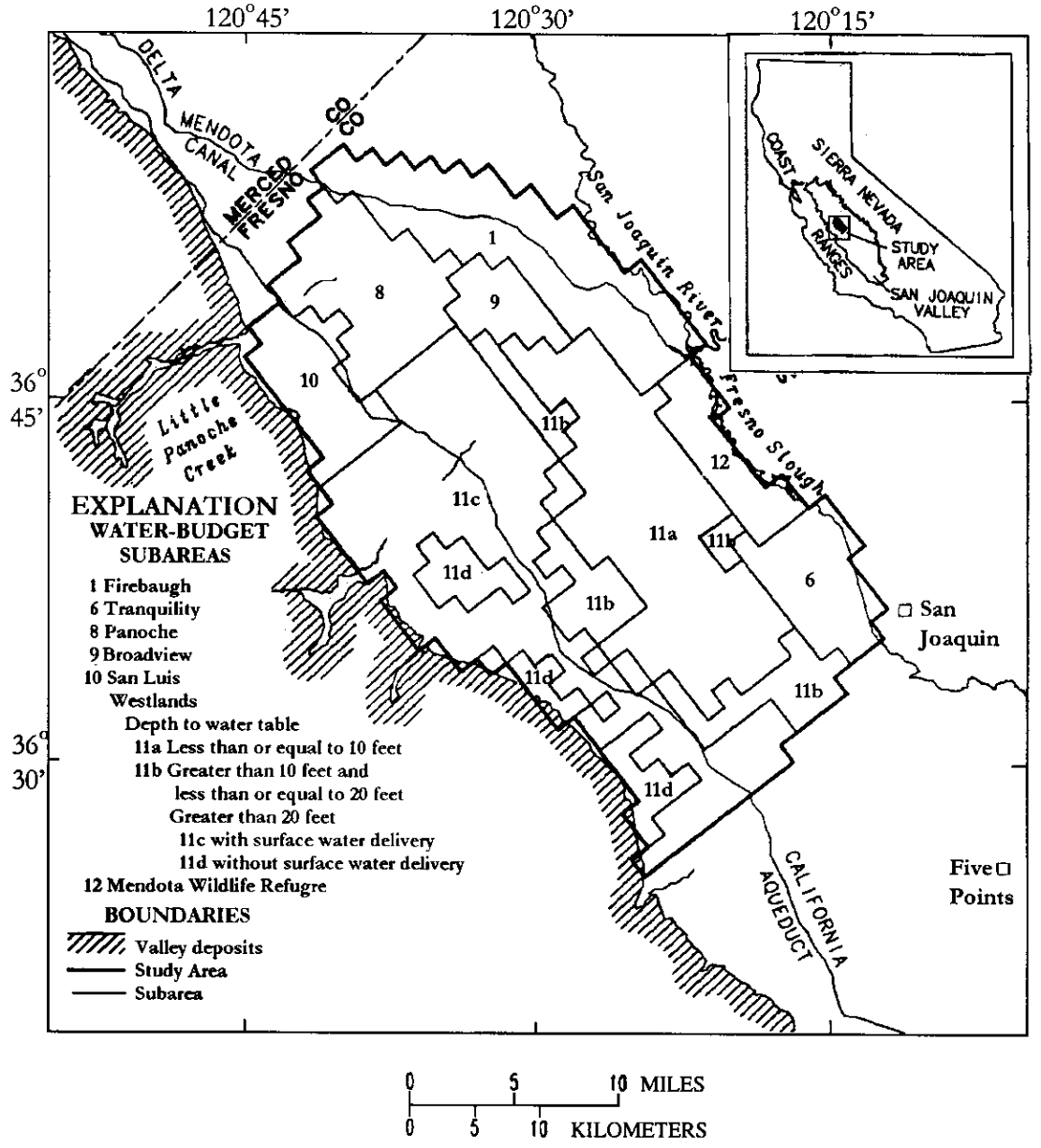

Figure 2 - Location of Study Area and Water Budget Subareas (Modified from Gronberg and Belitz, 1992).

2.2.1 Hydrogeology

The hydrogeology of the Los Banos-Kettleman City area was previously documented by Miller et al. (1971) and Belitz and Heimes (1990). From their reports, the subsurface flow system is divided into upper and lower water-bearing zones, which are separated by the Corcoran Clay Member of the Tulare Formation (Figure 3). The Corcoran Clay Member has a thickness ranging from 20 to 120 ft (Page, 1986) and consists of low-conductivity lacustrine deposits (Johnson et al., 1968).

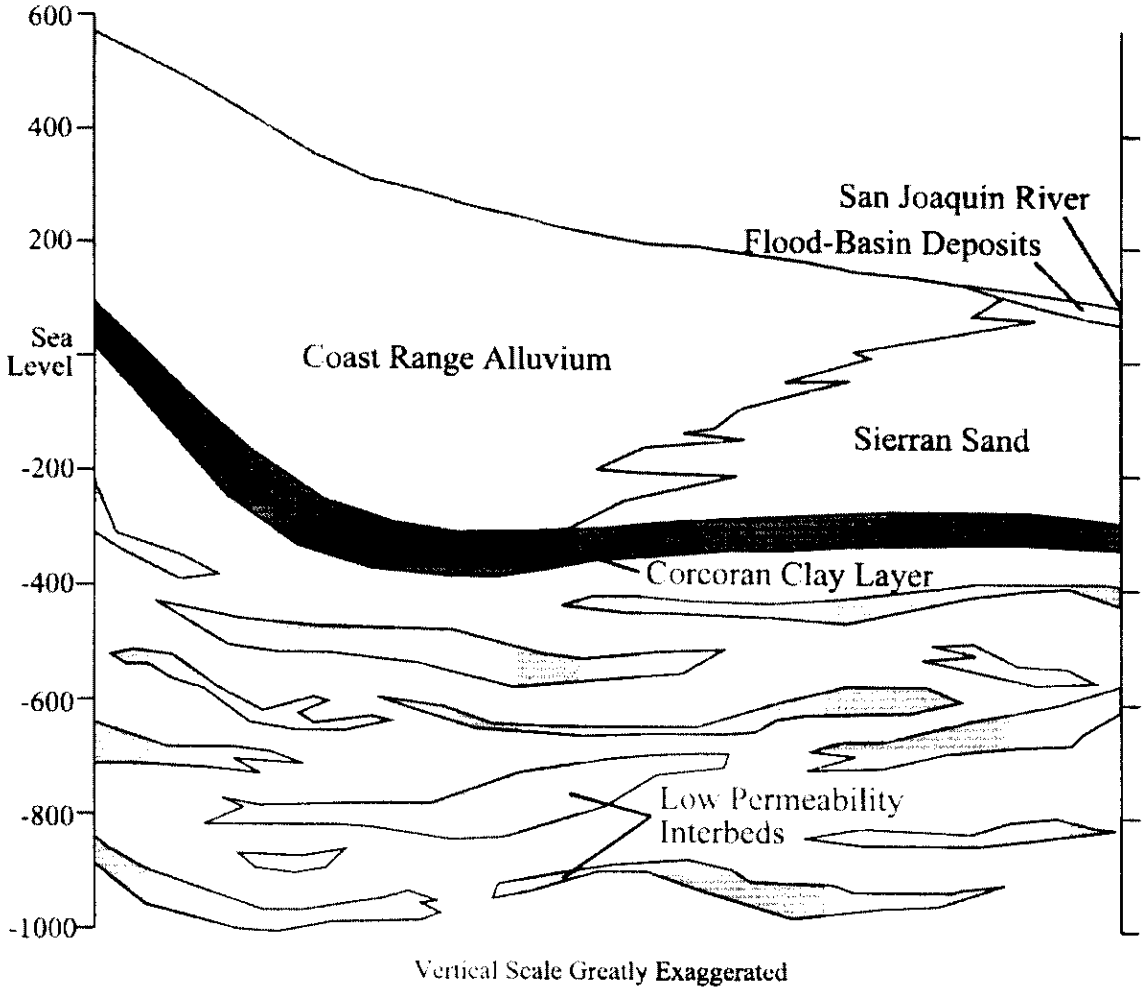

Figure 3 - Hydrogeologic Cross-section of the Study Area (Modified from Belitz et al., 1992).

The unconfined to semi-confined zone above the Corcoran Clay Member consists of Coast Range alluvium, Sierran sand, and flood basin deposits. The Coast Range alluvium reaches a thickness of more than 800 ft near the western edge of the valley. It is composed of sand and gravel along the stream channels and at the fan heads, and of clay and silt in the distal fan areas (Laudon and Belitz, 1991). The Coast Range alluvium is interfingered laterally with the Sierran sand, which consists of well-sorted medium to coarse-grained fluvial sand reaching a thickness of 400-500 ft in the valley trough (Miller

et al., 1971). Flood-basin deposits overlie the Sierran sand at the Valley trough and have a thickness of 5-35 ft (Laudon and Belitz, 1991). The quality of groundwater in the upper water-bearing zone is generally poor with high concentrations of calcium, magnesium, and sulfate, except near the Fresno Slough (Bull and Miller, 1975).

The lower water-bearing zone is locally less permeable than the upper-water bearing zone. It is also much thicker, ranging from 570 to 2460 ft (Williamson et al., 1989). It is composed of poorly consolidated flood-basin, deltaic, alluvial-fan, and lacustrine deposits of the Tulare formation (Bull and Heimes, 1990). Before surface water supplies were made available to the Los Banos-Kettleman City area, 75-80% of irrigation water was pumped from the lower water-bearing zone due to its greater thickness and superior water quality (Bull and Miller, 1975; Ireland et al., 1984).

2.2.2 Water Budget

Gronberg and Belitz (1992) performed an analysis of groundwater pumping, recharge, and irrigation efficiency for the Los Banos-Kettleman City region. This analysis resulted in two water budgets for the years 1980 and 1984. The Los Banos-Kettleman City area is divided into nine water-budget subareas based on water district boundaries and depth to water table (Figure 2). An area-weighted average irrigation efficiency is calculated for each subarea as a function of depth to water table. The irrigation efficiency is subsequently used to compute the irrigation requirement for each water budget subarea. If the computed irrigation requirement exceeds surface water delivery, the unmet water requirement is supplied from the groundwater reservoir; otherwise no pumping takes place. The required volume of groundwater withdrawl is spread uniformly over each subarea.

Gronberg and Belitz (1992) did not consider drought in their water budget analysis. However, drought will have a substantial influence on the rate and magnitude of land subsidence. During normal water years, this report adopts the same pumping rates and spatial distribution between subareas as those computed by Gronberg and Belitz (1992) for the year 1980 (Table 1). For drought periods, however, groundwater pumping rates will be a function of available surface water supplies. This will be discussed in greater detail in subsequent sections.

2.2.3 Surface Water Supplies

The State Water Resources Control Board (SWRCB) issued the first water rights to the U.S. Bureau of Reclamation (USBR) for operation in the Central Valley Project (CVP) in 1958 and to the California Department of Water Resources (DWR) for operation of the State Water Project (SWP) in 1967. Principal facilities of the SWP include Oroville Dam, Delta facilities, the California Aqueduct, and North and South Aqueducts. Principal facilities of CVP include Shasta, Trinity, Folsom, Friant, Clair Engle, Whiskeytown, and New Melones dams, Delta facilities, and the Delta Mendota Canal. Joint SWP/CVP facilities include San Luis Reservoir and Canal and various Delta facilities (California DWR, 1999). Although it arrives through a SWP facility (the California Aqueduct), all of the surface water used in the study region is contracted through the CVP and delivery rates are determined by the USBR.

Table 1 - Revised Water Budget for 1980
(Modified from Gronberg and Belitz, 1992)

Subarea	Area (mi^2)	Surface Water Delivery (ft/yr)	Groundwater Pumpage (ft/yr)	Groundwater Recharge (ft/yr)
Firebaugh	73	2.63	0.0	0.75
Panoche	48	2.48	0.0	0.96
Broadview	16	2.75	0.0	0.78
Tranquility	30	2.51	0.30	0.84
San Luis	30	1.86	0.40	0.79
Westlands				
Depth to Water<10 ft	97	1.90	0.40	0.46
10 ft< Depth to Water < 20 ft	42	2.19	0.46	0.74
Depth to Water > 20 ft				
with surface water	163	2.43	0.25	0.94
without surface water (1980)	30	0.0	2.46	0.86

2.3 Numerical Models

2.3.1 The Groundwater Flow Model

Groundwater flow in the Los Banos-Kettleman City area was previously modeled by Belitz et al. (1992) using MODFLOW, a modular finite-difference flow model developed by McDonald and Harbaugh (1988). MODFLOW is a three-dimensional groundwater simulation model that has been successfully used in real world problems (e.g., Sophocleuos and Perkins, 1993; Reynolds and Spruill, 1995; Bumb et al., 1997; Hubbel et al., 1997). It can simulate anistrophic and heterogeneous aquifer systems with various boundary conditions.

MODFLOW's structure is described as modular because it consists of one main program surrounded by a group of "modules" or packages. This modular structure is advantageous because it allows for the addition of new features without much alteration of the existing code. Packages are available to evaluate evapotranspiration, recharge, drainage, and land subsidence to name a few.

The focus of the research by Belitz et al. (1992) and Belitz and Phillips (1995) was the management of the shallow water table and associated drainage discharge in the aquifer above the Corcoran layer. It was the culmination of a series of studies motivated by the occurrence of selenium toxicity in nearby Kesterson Wildlife Refuge. A number of earlier studies had examined the presence of selenium in drain water coming from the study area. The purpose of Belitz et al.'s (1992) work was to present a regional hydrogeologic approach to the evaluation of management alternatives (Belitz and Phillips, 1995).

The Belitz et al. (1992) finite difference model was discretized laterally with a 36 row by 20 column grid, with each model cell one mile on a side (Figure 4). Vertically, the upper semi-confince zone was divided into five layers, while the lower confined zone was represented by a single layer (Figure 5). The bottom of the confined zone was assumed to be impermeable. The western boundary of the grid approximates the contact between the Coast Ranges and the unconsolidated alluvium, and was modeled as a no-flow boundary. The northwest and southern boundaries approximate flow lines and were also treated as no-flow boundaries. The boundaries along the valley trough and to the northeast are modeled as Fourier or general-head boundaries to capture lateral flow from the east (Belitz and Phillips, 1995).

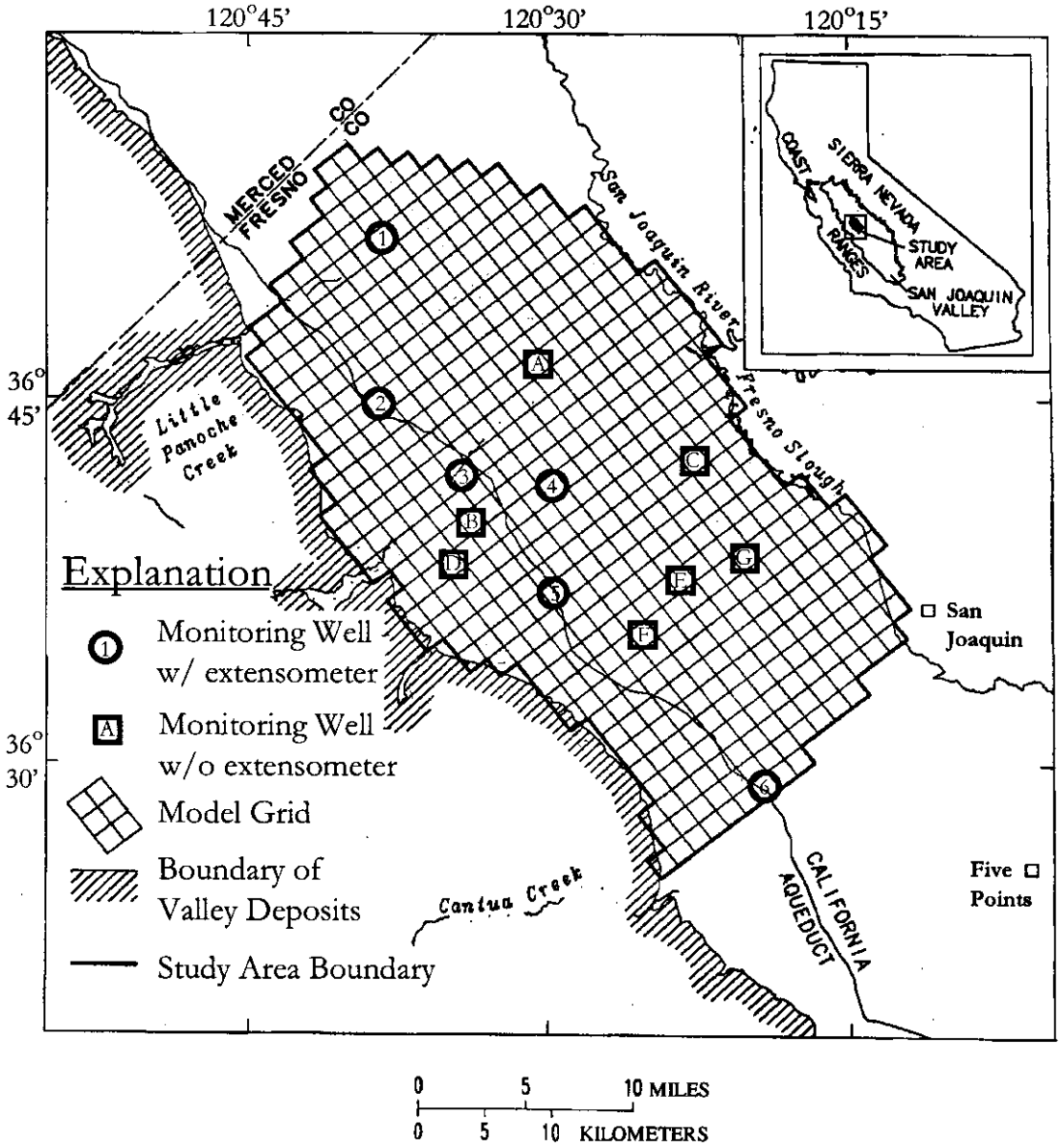

Figure 4 - Model Grid and Location of Observation Wells.

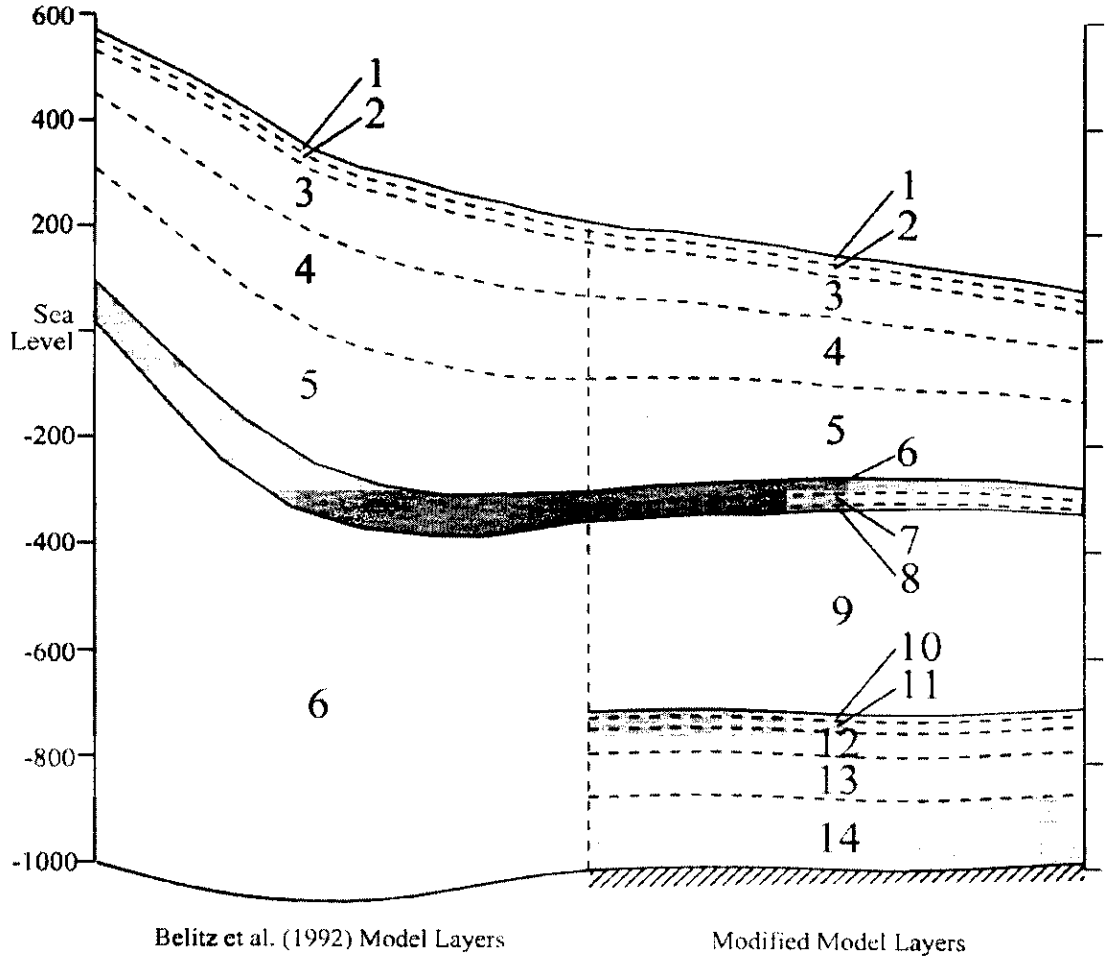

Figure 5 - Modifications to Belitz et al. (1992) Model Layers.

The hydraulic properties of the model were the combined result of field measurements and calibration. The hydraulic conductivity of coarse-grained deposits from the Coast Ranges (3.6 x 10^{-4} ft/sec) and Sierra Nevadas (1.2 x 10^{-3} ft/sec) were determined from slug test data. Specific storage (3.0 x 10^{-6} ft^{-1}) was specified on the basis of a previous study (Ireland et al., 1984). The hydraulic conductivity of the fine-grained deposits of the semi-confined zone (4.6 x 10^{-8} ft/sec), the hydraulic conductivity of the Corcoran Clay layer (6.0 x 10^{-9} ft/sec), the transmissivity of the confined zones (0.20 ft^2/sec), and specific yield (0.30 for layer 1 and 0.20 for layers 2-6) were calibration variables. Sources and sinks for the model included recharge, groundwater pumping, drains, and bare-soil evaporation. Recharge and pumping in the model were spatially distributed, but temporally constant. Drains and bare-soil evaporation were modeled using linear head-dependent functions (Belitz and Phillips, 1995).

The Belitz et al. (1992) model forecasts the effects on the groundwater table of various management alternatives using yearly time steps. This has been done because most of the the data (water table levels, subsidence rates, CVP deliveries, etc.) are only

available at yearly intervals. The major weakness of this approach is its effect on pumping. By averaging the pumping out over the entire year, the higher drawdowns occurring during the summer months are lost. This is significant for the land subsidence portion of the model because most of the subsidence actually occurs during these periods of high drawdown. This can be compensated for by altering some of the other model parameters, but it should be noted that the piezometric heads predicted by the model are artificially high during the summer months.

Although it does not simulate land subsidence, the model provides a calibrated estimate of groundwater flow in the Los Banos-Kettleman City area from 1972 to 1988. This report adopts the Belitz et al. (1992) groundwater model to simulate flow in the upper and lower aquifer; however, modifications are made to the model in order to consider groundwater flow and subsidence in the aquifer system's low-conductivity layers.

2.3.2 The Land Subsidence Model

The relationship between groundwater movement and land subsidence was not well understood at the beginning of the century. In the 1920s, Karl Terzaghi began investigating the relationship between stress and the compression of soils. His one-dimensional consolidation theory (Terzaghi, 1925) became the foundation for almost all current subsidence models, including the IBS1 model used for this report. This theory encompasses the following principles (Holtz and Kovacs, 1981).

As a saturated soil is loaded, it can change volume through three mechanisms: (1) compression of the soil particles; (2) compression of the water within the soil; and (3) expulsion of water from the soil and the resulting deformation of the soil matrix. The first two processes can easily be explained using simple stress-strain relationships, but their contribution to overall compression is small. The third process, the release of water from the soil matrix, dominates the compression of soil. Consequently, the rate of soil compression is governed by the rate at which water can leave the soil matrix. Low-conductivity soils such as clays can continue to compress for years after being loaded because the water in the clay escapes very slowly.

Underlying this observation is the concept of effective stress. As a load is applied to a saturated soil, water pressure develops instantaneously as the soil matrix tries to compress. In a coarse-grained soil, this increase in pressure expels water quickly. In fine-grained soils, however, the drainage of water is retarded by the soils' low conductivity. The pressure that remains supports the soil matrix and is called pore pressure. No compression will occur until the pore pressure dissipates as the water slowly flows out of the soil. To account for the presence and effects of pore pressure, Terzaghi (1925) defined an effective stress. This is the stress transmitted from grain to grain in the soil matrix (de Marsily, 1986), and can be written as:

$$\sigma' = \sigma - u \qquad (1)$$

in which σ' is the effective stress; σ is the total stress; and u is the pore water pressure.

The principle of effective stress provides the link between groundwater withdrawl and subsidence. Within an aquifer, the pore water pressure is equivalent to the pressure

head. As water is withdrawn from the aquifer and piezometric head drops, the effective stress on the aquifer increases even though the total stress remains constant. It is this increase in effective stress that causes the compression of the soil leading to subsidence.

Further study of compression revealed a highly nonlinear relationship between effective stress and the compression of clays. Fine-grained soils exhibit a "memory" of past exposure to stress (Casagrande, 1932). The past maximum stress is recorded in the soil's structure and is called its preconsolidation stress, σ_p'. At stresses less than the preconsolidation stress, the magnitude of compression is much smaller than it is for stresses that exceed this past minimum. Additionally, compression is elastic (recoverable) at stresses less than the preconsolidation stress while the compression beyond the preconsolidation stress is inelastic (unrecoverable). This inelastic compression of clay is called consolidation. It is the consolidation of the fine-grained aquifer interbeds that causes the vast majority of subsidence problems in the San Joaquin Valley (Poland, 1981; Ireland et al., 1984).

Several models exist for calculating each layer's magnitude of compression (referred to as compaction) according to Terzaghi's one-dimensional consolidation theory (1925). For this report, land subsidence is modeled by coupling the Interbed Storage Package-1 (IBS1) of Leake (1991a) with the modified groundwater simulation model of Belitz et al. (1992).

The IBS1 package assumes that a change in piezometric head produces an equal but opposite change in effective stress in the aquifer. In other words, even as the piezometric head fluctuates, the total stress (i.e., geostatic load) remains constant. This assumption introduces error in shallow unconfined aquifers (e.g., Leake, 1991a), but holds for deep or confined aquifers.

The package also assumes that the inelastic and elastic storage coefficients are constant. The values of these coefficients are actually functions of effective stress, however, the assumption introduces little error if changes in effective stress are small in relation to the total effective stress. Again, this assumption is problematic for shallow aquifers, but satisfactory for deeper ones (e.g., Leake, 1991a).

An alternative land subsidence package, ISB3 (Leake 1991b), eliminates the above assumptions by calculating changes in the storage coeffiecients and geostatic load. Although this would be a valuable improvement for a shallow aquifer, the subsidence model in this report only considers consolidation occurring in the Corcoran clay layer and the lower confined aquifer. Compaction in the upper aquifer is neglected. Extensometer data have shown that almost all the consolidation-induced subsidence in the valley occurs at depths between 350 and 2000 feet (Ireland et at., 1984). This roughly corresponds to the range depths for the Corcoran clay layer and confined aquifer and justifies the exclusion of compaction occurring in the upper, semi-confined aquifer. Additionally, low water quality in the upper aquifer has restricted the majority of groundwater pumping to the lower aquifer. With the exception of the Firebaugh and Tranquility water districts, approximately 86 percent of the wells in the study area pump from the confined aquifer (Gronberg and Belitz, 1992). Large head changes resulting in subsidence are not likely to be seen above the Corcoran clay layer. Hence, the additional complexity of the IBS3 package is not merited because it would perform very similarly to the IBS1 model.

Using the above assumptions, the IBS1 package calculates the compaction of each model layer as:

$$\Delta b_e = S_{ske} b_0 \Delta h \tag{2}$$

$$\Delta b_i = S_{ski} b_0 \Delta h \tag{3}$$

in which Δb_e and Δb_i are the elastic and inelastic compaction, respectively; Δh is the change in head at the center of the layer; b_0 is the original thickness of the layer; and S_{ske} and S_{ski} are the elastic and inelastic storage coefficients per unit thickness, respectively.

For all layers included in the IBS1 package, the preconsolidation stress is actually recorded as a preconsolidation head, $h_p = \sigma_P'/\gamma_{water}$. Inelastic compaction occurs when the piezometric head in a model layer drops below its preconsolidation head. The amount of each type of compaction is based on the change in head in relationship to the preconsolidation head. For each time step, the total elastic and inelastic compaction is recorded and the amount of water released due to compaction is returned to the model water balance. Finally, if inelastic compaction has occurred, a new value of preconsolidation head is recorded.

The major weakness of the ISB1 package is its inability to directly consider the time delay of consolidation. The ISB1 package assumes that consolidation occurs instantaneously with change in head. This approach is sufficient for aquifer systems with very thin compressible units and large model time steps, but thicker clay layers require a significant amount of time for pore pressure to dissipate (Leake, 1991a).

Figure 6 illustrates the role of pore pressure in the time delay of consolidation. The line to the left represents the pressure in the aquifer system at a point of equilibrium before any change in stress occurs. As the effective stress in the aquifer increases, the low hydraulic conductivity of the clay layer results in a parabolic profile of residual pore pressure. Complete consolidation will not occur until all of the pore pressure dissipates and equilibrium is again achieved.

There are two viable techniques for representing the time delay of consolidation. The first is to consider the delay in the analytical derivation of the land subsidence model as illustrated by Shearer and Kitching (1994). In their Interbed Drainage Package (IDP), each model element is split into two sub-elements, one for the coarse aquifer material and one for the fine-grained interbeds. Flow between them is controlled by: (1) a parameter called vertical interbed conductance, which is analogous to the conductance term in the stream-routing package of MODFLOW (McDonald and Harbaugh, 1988); and (2) the head difference between the sub-elements. Leake's ISB2 package (1998, personal communication) uses a similar procedure to represent the delayed release of water from compressible, discontinuous clay beds within an aquifer.

The same result can be achieved numerically by dividing the larger low-conductivity units vertically into a number of smaller units. The residual pore pressure profile is then represented step-wise across each compressible unit (Leake, 1990; Onta and Gupta, 1995). This second approach has been employed in this model and allows for representation

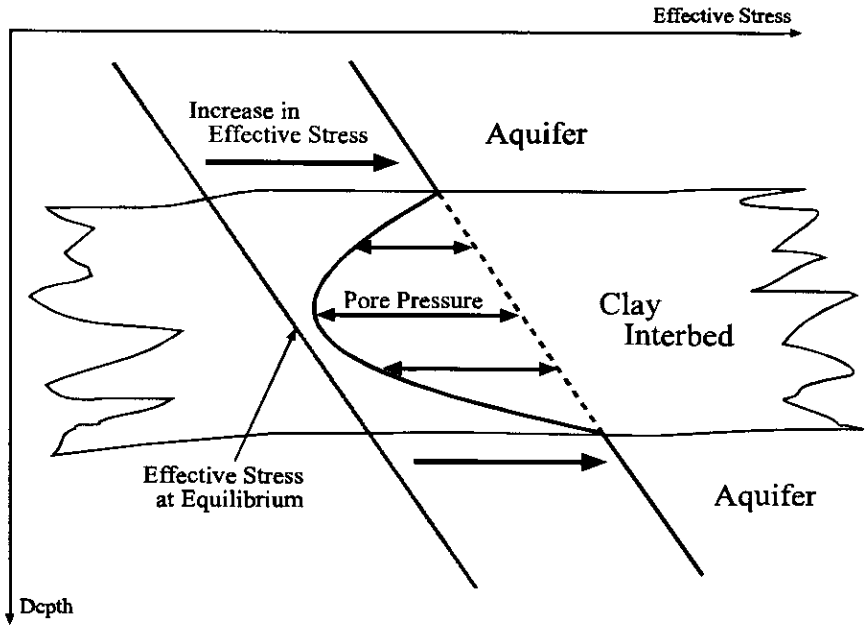

Figure 6 - Role of Pore Pressure in the Time Delay of Consolidation.

of the time delay using the IBS1 package. The actual implementation of this model will be discussed in further detail in the following section.

It should be emphasized that the IBS1 subsidence model only considers subsidence due to increased effective stress caused by changing groundwater levels. It does not consider subsidence due to hydrocompaction, withdrawl of gas and oil, deep-seated tectonic movement, or the dewatering of organic soils. Of these alternative causes of subsidence, only hydrocompaction has been significantly observed in the study area (Ireland, 1984).

Hydrocompaction is subsidence that occurs as shallow, low-density soils are wetted for the first time. In the Los Banos-Kettleman City area, initial farmland irrigation revealed that debris flow deposits associated with interfan areas were susceptible to this kind of compaction (Phillips, 2000, personal communication). In the study region, two sections along the California Aqueduct alignment, miles 98-103 and 114-129 (corresponding to the Coast Range interfan areas), were especially sensitive to hydrocompaction. Water was applied to these areas in the mid-1960s to exhaust the majority of hydrocompaction before the aqueduct was constructed. It has been assumed that all significant hydrocompaction occurred at that time or during initial irrigation and that it does not significantly contribute to subsidence during the modeling period (1972-2028).

3. Application of the Model

3.1 Modification of the Belitz et al. (1992) Model

3.1.1 Geometry

As indicated previously, the model used in this report is an adaptation of the Belitz et al. (1992) model. Modifications have been made in order to simulate land subsidence due to groundwater withdrawl. No changes were made to the horizontal dimensions, model grid, and boundary conditions as shown in Figure 4. Each grid cell continues to represent a one-square-mile area with uniform hydrologic and hydrogeologic parameters. The only significant change in geometry occurs in the representation of the vertical model layers. Figure 5 shows the conceptual modifications made to the Belitz et al. (1992) model. Most notably there is a change in how the low-conductivity layers (the Corcoran clay layer and clay interbeds) are represented. In the Belitz et al. (1992) model, both the high-conductivity deposits as well as the clay interbeds in the confined aquifer system have been represented as one composite unit. Additionally, the Corcoran clay layer has not been directly included. Instead, its presence is accounted for by reducing the vertical conductivity between layers 5 and 6. The model was satisfactory for assessing alternatives to agricultural drains, but is inadequate for modeling land subsidence.

In order to model subsidence, two major changes have been made regarding the compressible, low-conductivity layers. First, the larger clay layers have been divided into several smaller modeling layers. As discussed previously, this modification allows a head gradient to develop between each clay modeling layer to mimic the presence of residual pore pressure and capture the time delay of consolidation. The Corcoran layer is represented in this way. It was divided into three modeling layers comprising 55, 30, and 15 percent of the layer thickness (layers 6, 7 and 8, respectively).

The thickness of the layers decreases with depth to capture the large head changes occurring in the underlying confined aquifer. As the head in the lower aquifer changes, the steepest head gradients in the Corcoran clay layer occur near the outer edge. The thinner layers are better able to capture this gradient. Thinner layers were not placed at the top of the Corcoran layer because it is assumed that only small changes will be observed in the water table. Although the water table is relatively stable during the modeling period, a gradient does exist throughout the semiconfined uper aquifer and heads in the lower modeling layers can fluctucate substantially. This may be one limitation of the model. The top modeling layer for the Corcorn clay unit is affected by head changes in the upper aquifer, but because of its greater thickness, it may not adequately capture the time delay of consolidation associated with head changes in the upper aquifer. This may result in more subsidence occurring during each time step and an overestimate of total subsidence.

The Corcoran layer can be modeled as described above because both its depth and thickness are relatively well known. For the discontinuous interbed layers of the confined aquifer, however, far less information is available. Although previous work explores the nature and general distribution of these interbeds (Ireland, 1986; Belitz and Heimes, 1990), their extent and location are not well documented. Even if the location of each interbed were known, the large number of interbeds would make modeling each seperately

a computationally impractical approach. The second major modification to the model incorporates a possible solution to this problem suggested by Ireland (1986). Instead of trying to map all the major interbeds in the confined aquifer, the interbeds are removed from the confined layer and replaced by one large low-permeability layer at the bottom of the aquifer.

This bottom layer is assumed to have uniform thickness of 310 feet (after model calibration), located 1000 feet below the Corcoran. It is divided into five modeling layers with thicknesses (for increasing depth) of 10, 20, 40, 80, and 160 ft. There is a no-flow boundary at the bottom of the layer, allowing drainage to occur only in the direction of the confined aquifer. This assumption has a strong effect on the time delay of consolidation because it replaces many doubly draining layers with a single drainage face. This is compensated for by modifying the modeling layer's parameters during calibration (e.g., increasing vertical hydraulic conductivity). The goal is to find parameters such that the effect of the fictional model layer on land subsidence is equivalent to the composite effect of the actual interbeds.

This approach has one major disadvantage. Characteristics of the layer such as storage coefficients (elastic and inelastic) and vertical hydraulic conductivity are a product of calibration and thus, cannot be verified by any field measurements. This means the validity of the layer's parameters can only be measured by their ability to simulate past and predict future subsidence.

3.1.2 Pumping

The other major modification to the Belitz et al. (1992) model occurs in the representation of groundwater pumping. The pumping of groundwater from the aquifer system is one of the most important components of the groundwater model, affecting piezometric head in the confined aquifer more than any other single variable. It is also one of the most difficult components to model because it has never been directly measured.

The Belitz et al. (1992) model estimated pumping magnitudes using the same nine subareas designated in the water budget by Gronberg and Belitz (1992). Pumping rates are allowed to vary between subareas, but are uniform within each subarea. Well depths and perforation lengths were used to determine the percentage of pumping from upper and lower water-bearing units. The 1980 water budget values (Gronberg and Belitz, 1992) were adopted for all model years.

This model adopts the spatial distribution of pumping in the Belitz et al. (1992) model, but alters the yearly magnitude estimates. The major limitation of Belitz et al. (1992) approach is that the magnitude of pumping for all model years was assumed to be constant. The was satisfactory for the purposes of their work (Belitz et al., 1992; Belitz and Phillips, 1995), but does not capture the pore pressure fluctuation necessary to model land subsidence.

There are two major sources of water in the Los Banos-Kettleman City region, surface water fromthe CVP and groundwater. Although groundwater pumping has not been measured, some records of water delivery from the CVP are available. Records from the Westlands and Panoche Water Districts are summarized in Table 2. These rates have been used to construct an estimation of the pumping rate for each model year.

Table 2 - Yearly CVP Deliveries for Westlands and Panoche Water Districts

Water Year	Westlands CVP Delivery (acre-ft)	Panoche CVP Delivery (acre-ft)	Model Percent
1972	*1,150,000**	*104.600*	100%
1973	*1,150,000*	*104.600*	100%
1974	*1,150,000*	*104.600*	100%
1975	*1,150,000*	*104.600*	100%
1976	*1,150,000*	*104.600*	100%
1977	*230,000*	*20,920*	20%
1978	*1,150,000*	*104.600*	100%
1979	*1,150,000*	*104.600*	100%
1980	*1,150,000*	*104.600*	100%
1981	*1,150,000*	*104.600*	100%
1982	*1,150,000*	*104.600*	100%
1983	*1,150,000*	*104.600*	100%
1984	*1,150,000*	*104.600*	100%
1985	*1,150,000*	*104.600*	100%
1986	**1,150,000**	**101,600**	100%
1987	**1,150,000**	**111,800**	100%
1988	**1,150,000**	**107,000**	100%
1989	**1,150,000**	**97,900**	100%
1990	**575,000**	**63,600**	51%
1991	**287,500**	**36,900**	26%
1992	**287,500**	**41,100**	26%
1993	**575,000**	**80,500**	52%
1994	**402,500**	*52,500*	36%
1995	**1,150,000**	*104,600*	100%
1996	**1,092,500**	*98,200*	94%
1997	**1,035,000**	*94,100*	90%
1998	**1,150,000**	*104,600*	100%

* Recorded values in bold, approximations italicized

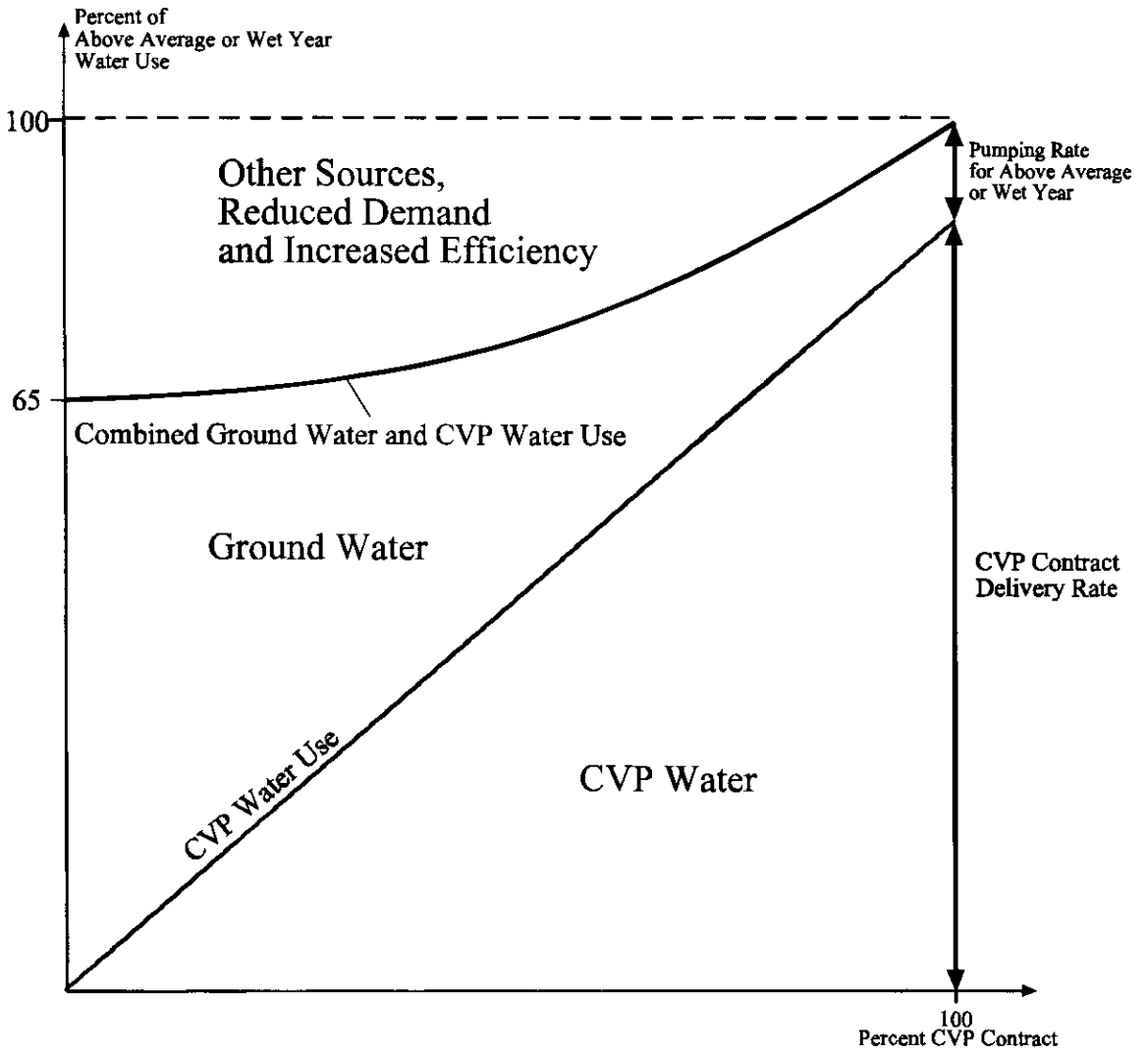

Figure 7 - Relationship between CVP Delivery and Groundwater Pumping Rates.

Figure 7 illustrates the relationship adopted between CVP water delivery and groundwater pumping rates. Although not done in this report, the relationship shown in Figure 7 can be improved by using crop, or some surrogate, data.

Several assumptions have been made in creating this figure. First, it is assumed that the Gronberg and Belitz (1992) water budget is appropriate for years in which 100 percent of the CVP contract water is available. During years of reduced surface water availability, the shortage can be met by reducing demand (leaving land fallow), increasing irrigation efficiency, procuring other sources, or increasing groundwater pumping. The line of combined groundwater and CVP water use is assumed to be concave up. This is because increasing efficiency and the use of other sources are inexpensive alternatives for years with small reductions in CVP water. For increasing levels of drought, however, these options become very costly or unavailable. Thus, an increasing amount of the shortage must be met with groundwater. The actual shape of the line of combined groundwater and CVP water use was determined through trial and error during the model

calibration and can be mathematically described as:

$$\Phi_c = 0.0022\Phi_s^2 + 0.13\Phi_s + 65 \quad (4)$$

in which Φ_c is the percent of normal, combined groundwater and surface water use; and Φ_s is the percent of contracted surface water.

One method of verifying equation four is highlighted by a similar approach of estimating groundwater pumping employed by Leighton and Fio (1995). In their water budget, groundwater pumping is estimated as the difference between crop water requirement and conveyed surface water. In this approach, the yearly crop water requirement serves a similar function to that of equation four. Crop water requirement is used to indicate changes in total water demand during drought years. Thus some relationship should exist between crop water requirement (or irrigated acreage) and the total water use predicted by equation four. Crop water requirement is used to indicate changes in total water demand during drought years. Thus, some relationship should exist between crop water requirement (or irrigated acreage) and the total water use predicted by equation four.

Figure 8 shows a comparison of the combine surface and groundwater estimated by equation four and the crop water requirement (CWR) for two of the water districts in the study area. CWR for the Panoche Water District was estimated from irrigated acreage for the years 1990-92 (California Polytechnic State University, Irrigation Training and Research Center, 1994). CWR is also shown for the Westlands Water District for the years 1977 and 1990-94 (Westlands Water District, 1998).

Although the relatively few droughts on record limit what can be concluded from the figure, several interesting observations can still be made. First, the model's estimate includes reductions made for increased irrigation efficiency and procurement of other sources as well as reduced acreage. Although the magnitude of these other sources is unknown, the CWR can be viewed as an upper bound with additional reductions coming from these sources. Figure 8 is fairly consistent with this assumption with only one of the observed CWR levels falling below the prediction of equation four. Second, given the assumption above, equation four looks to be a reasonable estimate of the combined surface and groundwater use in the region. Unfortunately, because of the limited amount of data, a number of other relationships could also produce reasonable estimates. It is difficult to say if the relationship in equation four is better than one produced by linear or concave down relationship. Finally, even within the same water district, similar droughts produce a wide range of crop water requirements. Equation four oversimplifies the system by predicting that a given level of drought will always produce the same level of required water. Even with these limitations, the relationship given in equation four is useful because it assures consistent estimation of pumping rates throughout the calibration period. It also provides a method of estimating future pumping rates based on the availability of surface water.

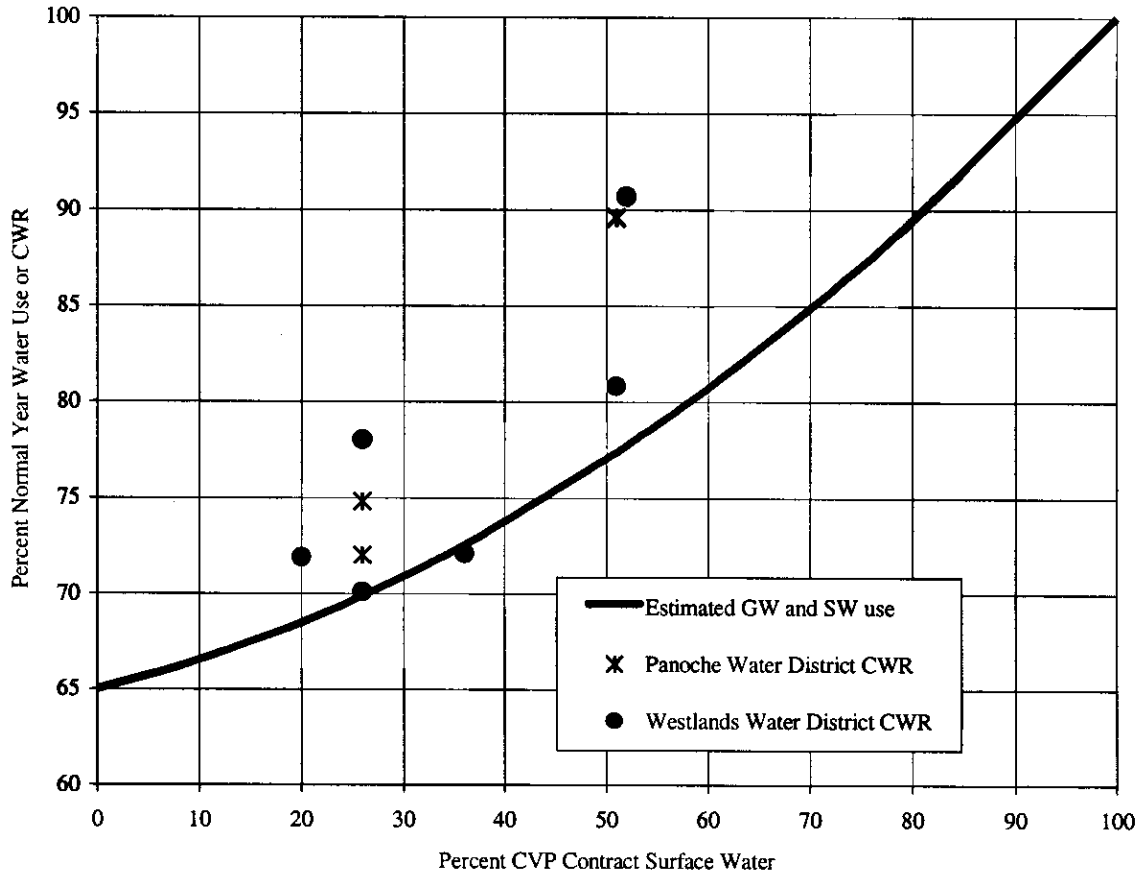

Figure 8 - Comparison of Estimated Combined Surface and Groundwater Use and Observed Crop Water Requirements During Drought Years.

3.1.3 Initial and Preconsolidation Heads

Initial heads in the aquifers remain largely unchanged from the Belitz et al. (1992) model. Modifications were made only where large jumps were observed in the initial time steps. This was particularly prevalent in the bottom layers of the upper, semi-confined aquifer (Belitz and Phillips, 1995). This is because the Belitz et al. (1992) model used the 1972 observed water table data as the initial head for all model layers of the upper aquifer. This assumption ignores the presence of a head gradient in the aquifer. During the first few time steps, heads in the lower layers jump to approximate the gradient in the aquifer. Although these jumps have little effect on the long-term accuracy of the groundwater flow portion of the model, they can cause large fictional jumps in land subsidence. For this reason, model head values for the bottom layers of the semi-confined aquifer were chosen after two years (1974) of a preliminary model run. This allowed sufficient time for a gradient to stabilize.

The IBS1 package requires the entry of a preconsolidation head for each element of the model for which compaction will be monitored. Since the Belitz et al. (1992) model did not include any consideration of subsidence, all preconsolidation files are original to this model. Additionally, the initial heads for both the Corcoran and the clay interbed layers are newly generated. The estimates for both initial and preconsolidation heads in the clay layers are the result of each layer's pressure history.

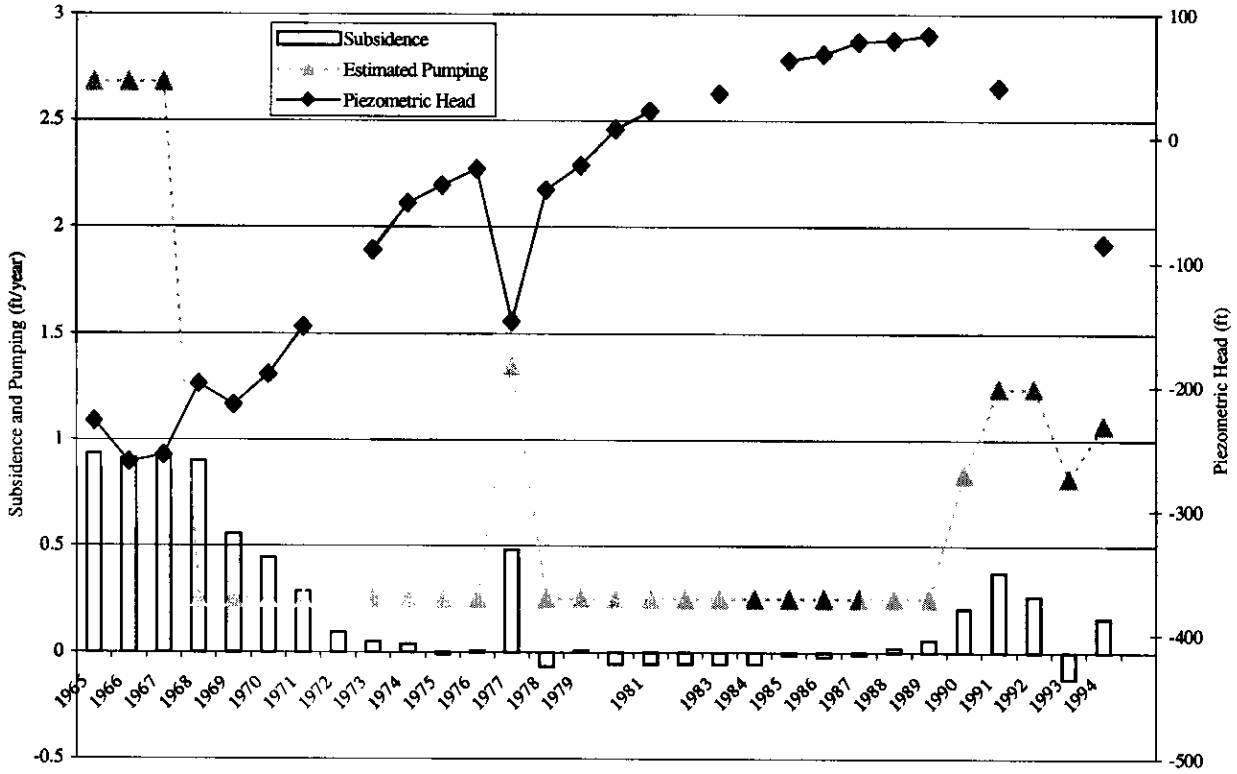

Figure 9 - Subsidence, Estimated Pumping Rate, and Piezometric Head at an Observation Well Near Cantua Creek (Modified from Ireland et al., 1984).

From the historical record it is apparent that piezometric head levels were dropping prior to the arrival of the California Aqueduct. This suggests that when head levels were at a minimum in the aquifers, some amount of residual pore pressure probably remained in the thicker clay layers. The extensometer record supports this observation. Figure 9 shows subsidence, estimated pumping rate, and piezometric head for an observation well near Cantua Creek. Typical of the study area, this observation well shows inelastic compaction occurred well after head levels in the confined layer began to recover in 1969. This is evidence that pore pressure was still dissipating from the clay layers at the beginning of the modeling period.

Given this information, it is possible to create a schematic drawing of heads in the model for the time of maximum drawdown (Figure 10). Heads in the lower, confined aquifer are based on potentiometric surface maps from 1972 (after Belitz et al., 1992). Heads at the bottom of the upper aquifer are approximated as described above. Heads in the low-conductivity layers are equal to the equilibrium piezometric head plus the residual pore pressure. The equilibrium head is determined from the initial heads in each aquifer. The shape of the residual pore pressure profile is assumed to be parabolic. The magnitude of the residual pore pressure is a function of past changes in piezometric head and the thickness and hydraulic conductivity of the clay layers. Since this information is unknown, the magnitude of residual pore pressure is treated as a calibration parameter.

The above observations are only applicable for the time of maximum drawdown. The time of maximum drawdown is also a convenient time period to consider head levels

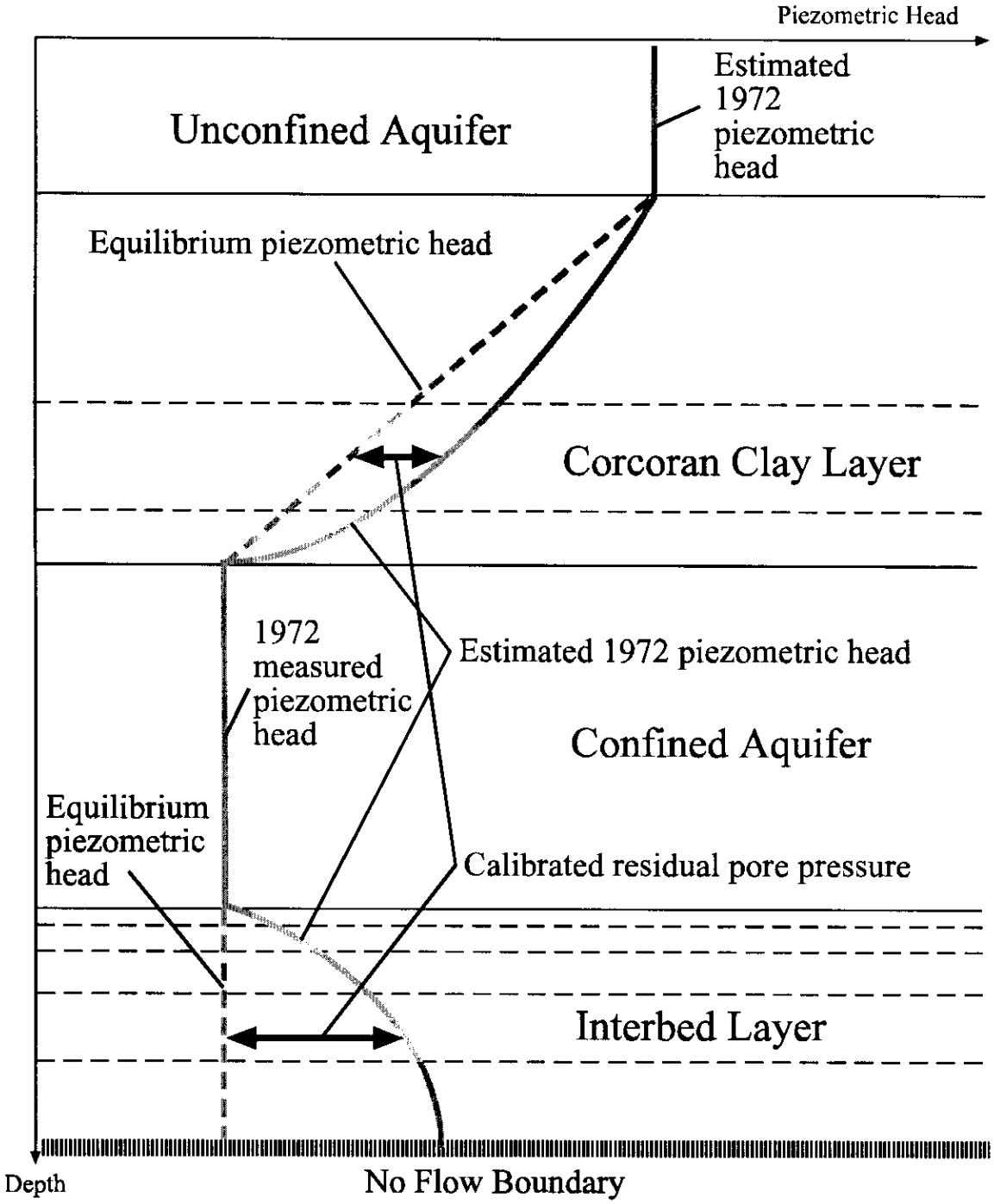

Figure 10 - Schematic Drawing of Initial Heads.

because initial and preconsolidation heads will be equal to each other. For this reason, it is assumed that the initial model heads in the aquifer are equal to the maximum historical drawdowns. Although some amount of recovery occurred between the arrival of the aqueduct (approximately 1967) and the beginning of the model (1972), the initial heads in the confined aquifer are sufficiently close to the historic minimum for this

assumption to produce acceptable results. Additionally, the assumption affects only the outermost portions of the Corcoran and clay interbed layers, resulting in minimal effect to overall land subsidence.

3.1.4 Other Modifications

All other aspects of the model have not been significantly changed from the model developed by Belitz et al. (1992), including the use of yearly stress periods. For information on the selection of parameters for drainage, evapotranspiration, recharge, and boundary conditions, the reader should consult Phillips and Belitz (1991), Belitz et al. (1992), and Belitz and Phillips (1995).

3.2 Calibration

3.2.1 Piezometric Head

Calibration of the model encompasses matching simulated piezometric head levels and land subsidence with corresponding observed values across the study area. The DWR monitors piezometric head levels at observation wells throughout the San Joaquin Valley. Figures 11-23 show the model results following calibration plotted against the observed piezometric head for thirteen monitoring locations. Each location is shown on Figure 4, while the actual well numbers are given in Table 3. All the wells in Table 3 monitor piezometric head in the lower confined aquifer although not all the screen intervals could be given. Some of the locations include more than one monitoring well and each well may be located anywhere within the model cell. Since the model simulates head at the middle of the grid cell, it is possible for observation wells to be more than a half-mile away from the location of simulated head. Thus, small differences should be expected between observed and simulated piezometric head values, as well as between head values at different observation wells within the same grid cell.

By using the aquifer parameters found by Belitz et al. (1992), it was possible to produce relatively accurate results for piezometric head with modification to the pumping rates only. Proper drawdown during years of drought was achieved using the scheme described in Section 3.1.2. In addition to determining the best equation to define combined groundwater and surface water (see equation 4), the calibration dictated two other significant changes.

The water budget for the Belitz et al. (1992) model includes a portion of the Westlands Water District that relies strictly on groundwater. Following construction of the water budget, however, improvements were made in the delivery system to bring CVP water to portions of this area. This was evident during the calibration trials when predicted head levels were significantly below those observed in these portions of the Westlands Water District. To address this problem, the original water budget is retained for the model years up to 1980, but is assumed that CVP water replaces 25 percent of the pumping in 1981 and replaces 50 percent in 1986.

The second significant change to the pumping scheme occurs along the southern edge of the study area. Observed head values suggest that more groundwater is removed from this area during periods of drought than predicted by the model. By increasing the

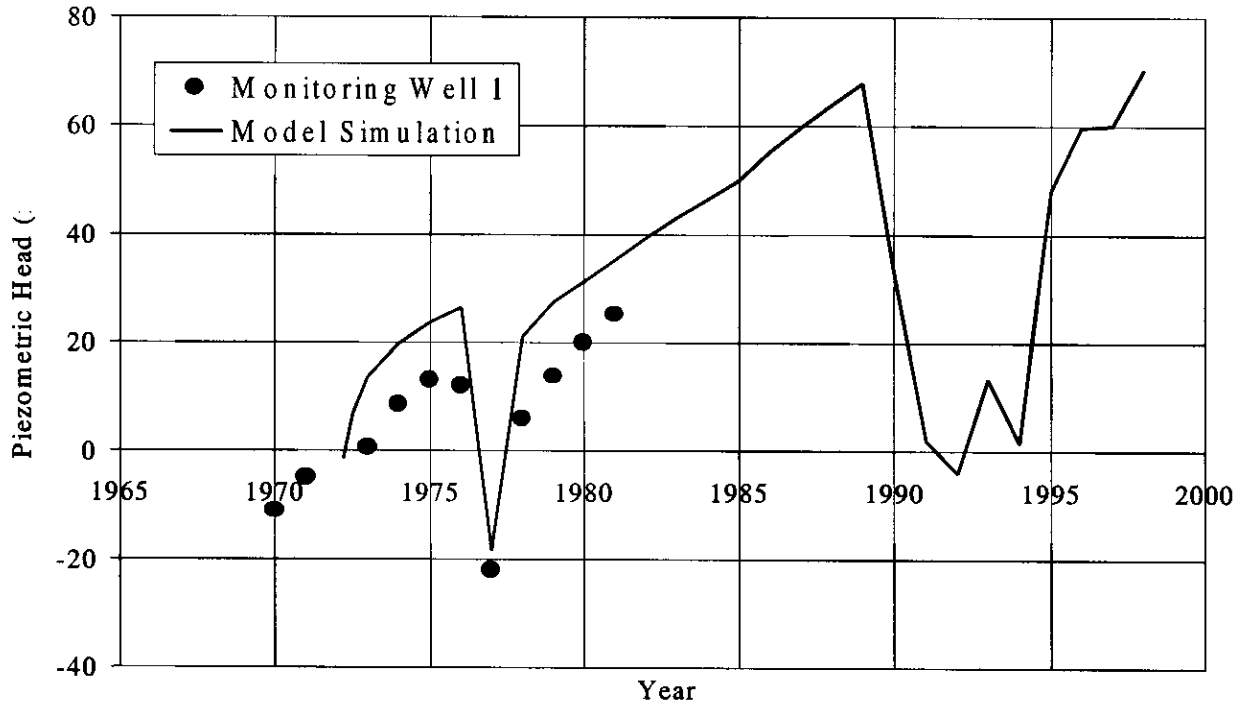

Figure 11 - Observed and Simulated Piezometric Head for Observation Location 1.

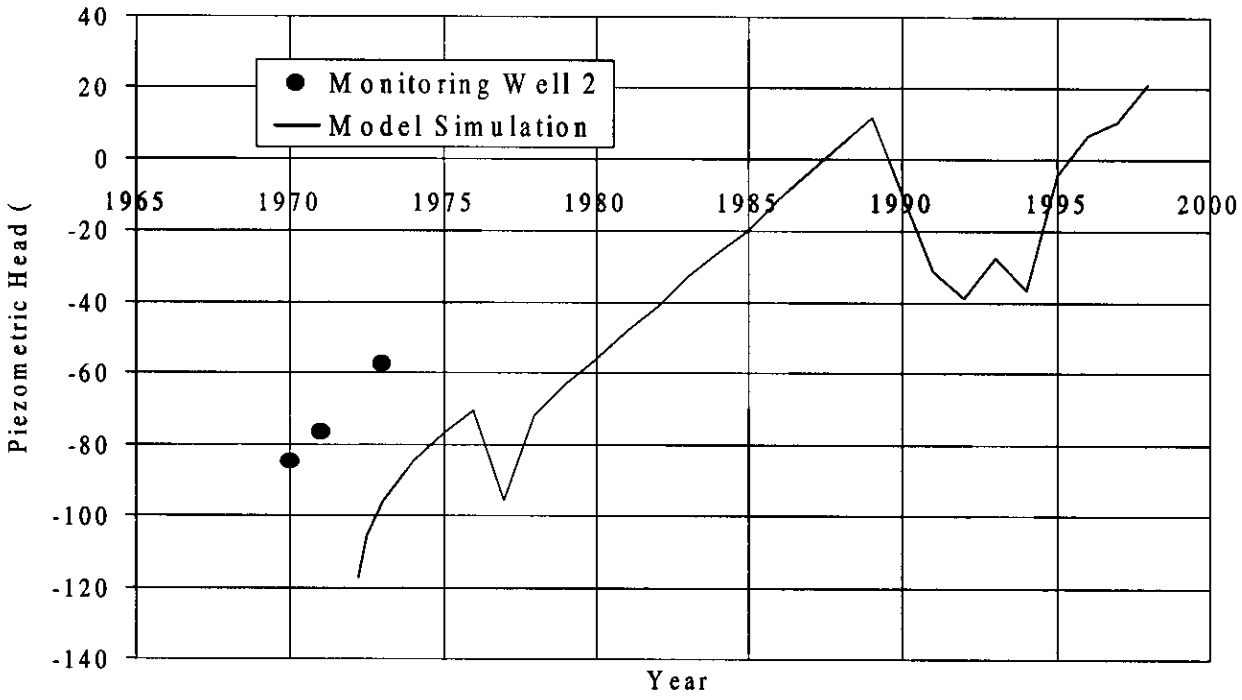

Figure 12 - Observed and Simulated Piezometric Head for Observation Location 2.

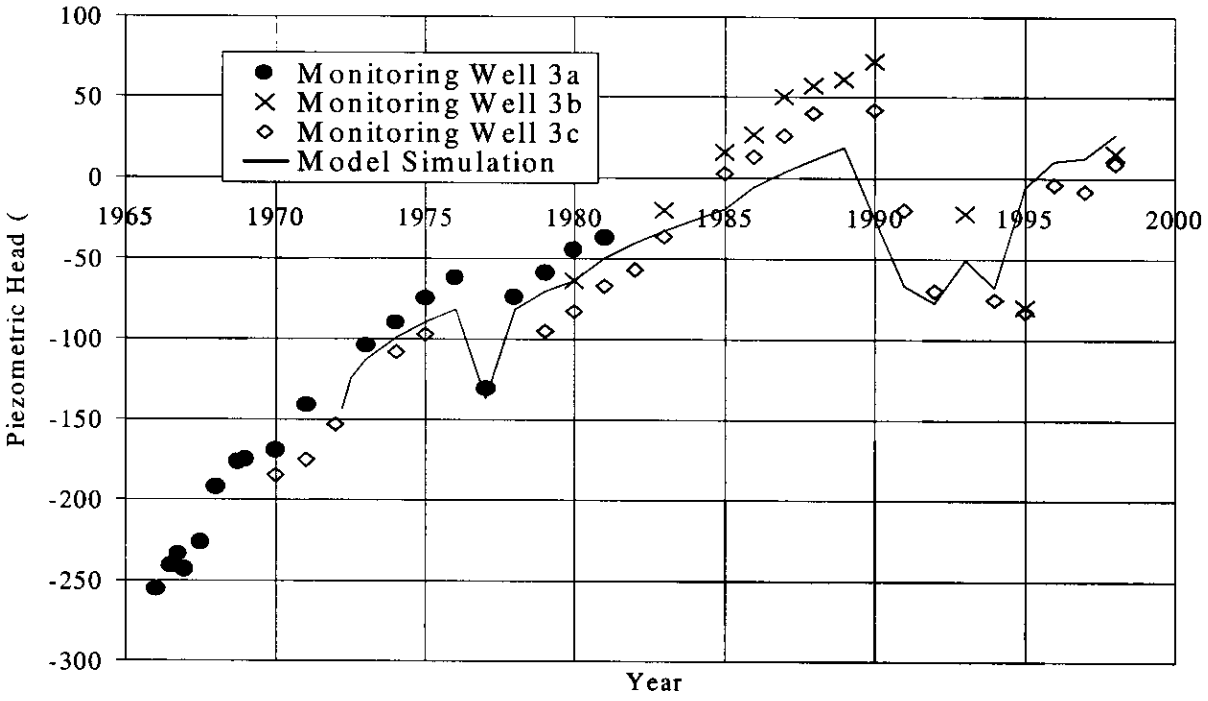

Figure 13 - Observed and Simulated Piezometric Head for Observation Location 3.

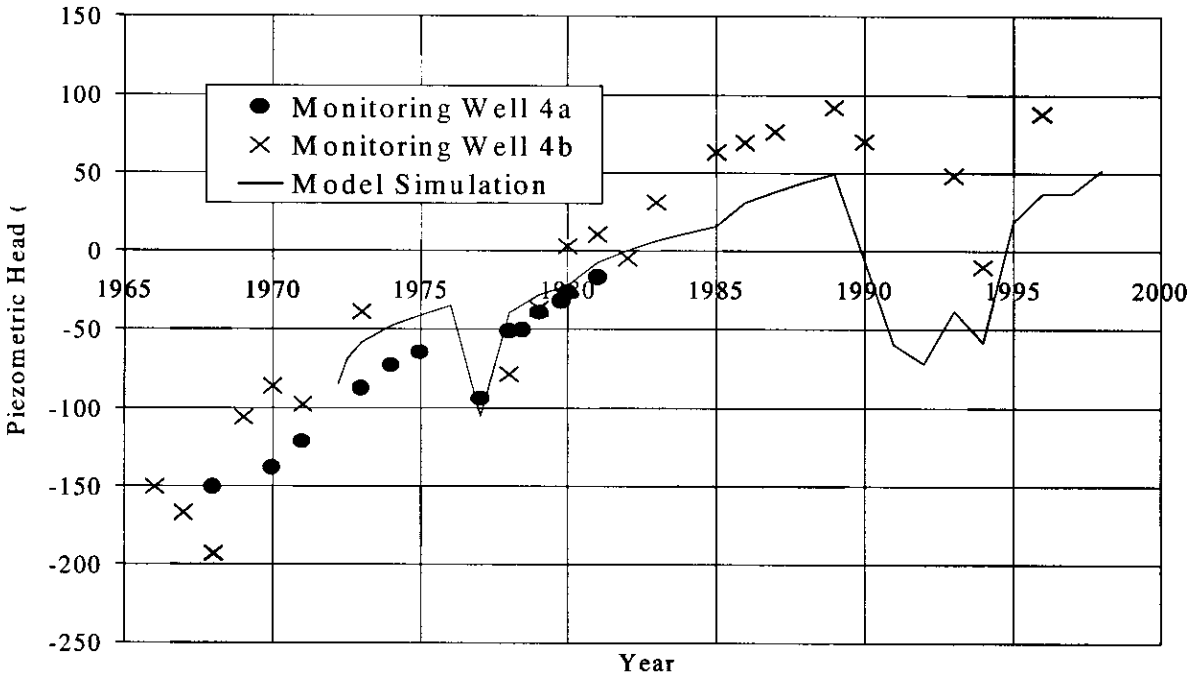

Figure 14 - Observed and Simulated Piezometric Head for Observation Location 4.

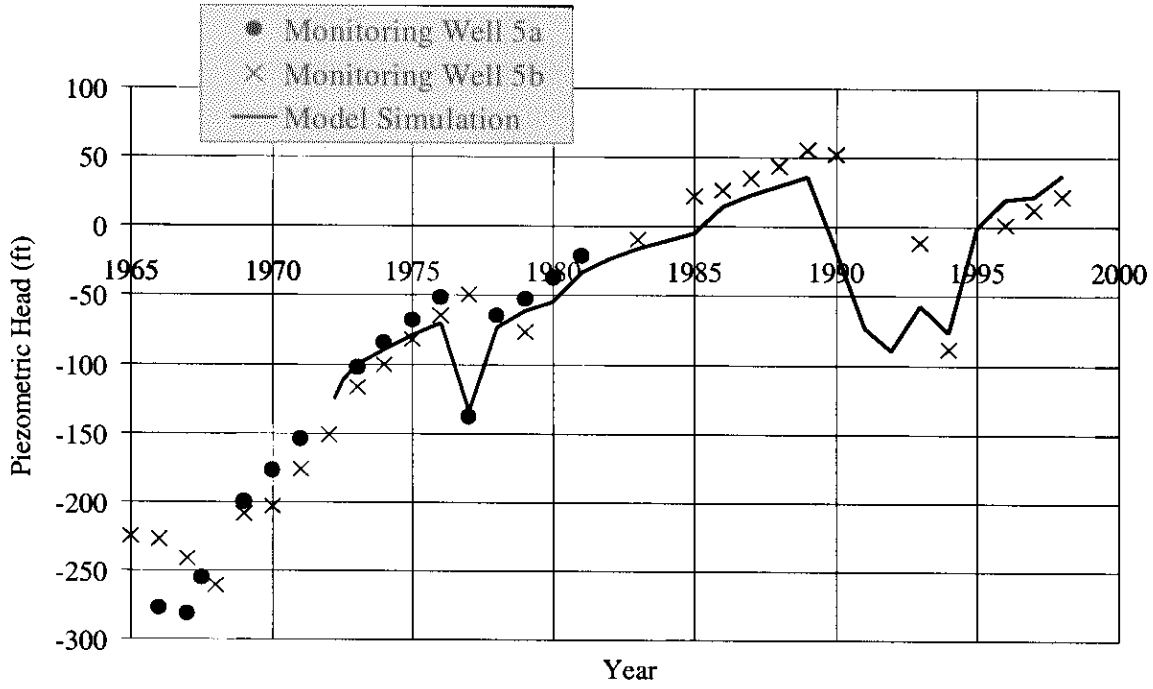

Figure 15 - Observed and Simulated Piezometric Head for Observation Location 5.

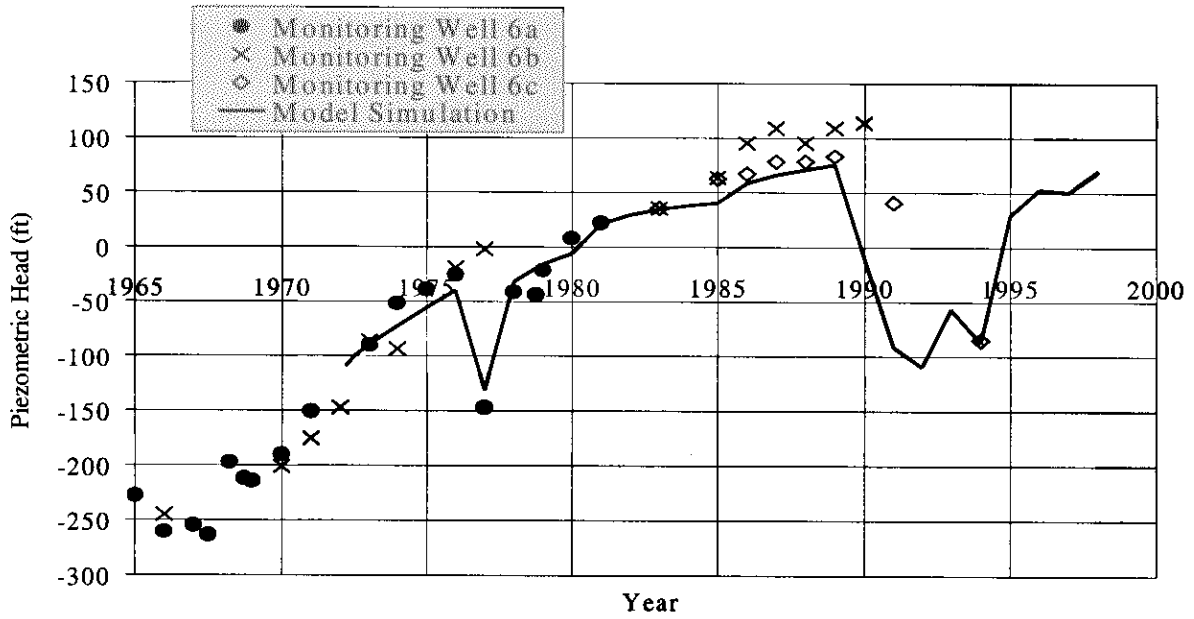

Figure 16 - Observed and Simulated Piezometric Head for Observation Location 6.

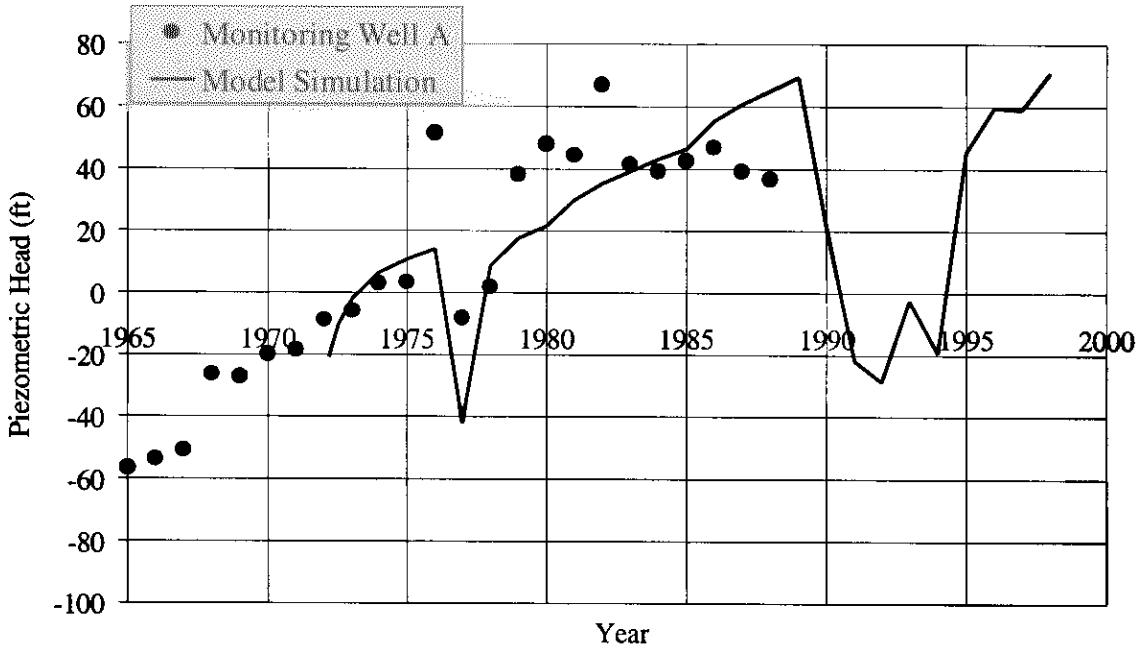

Figure 17 - Observed and Simulated Piezometric Head for Observation Location A.

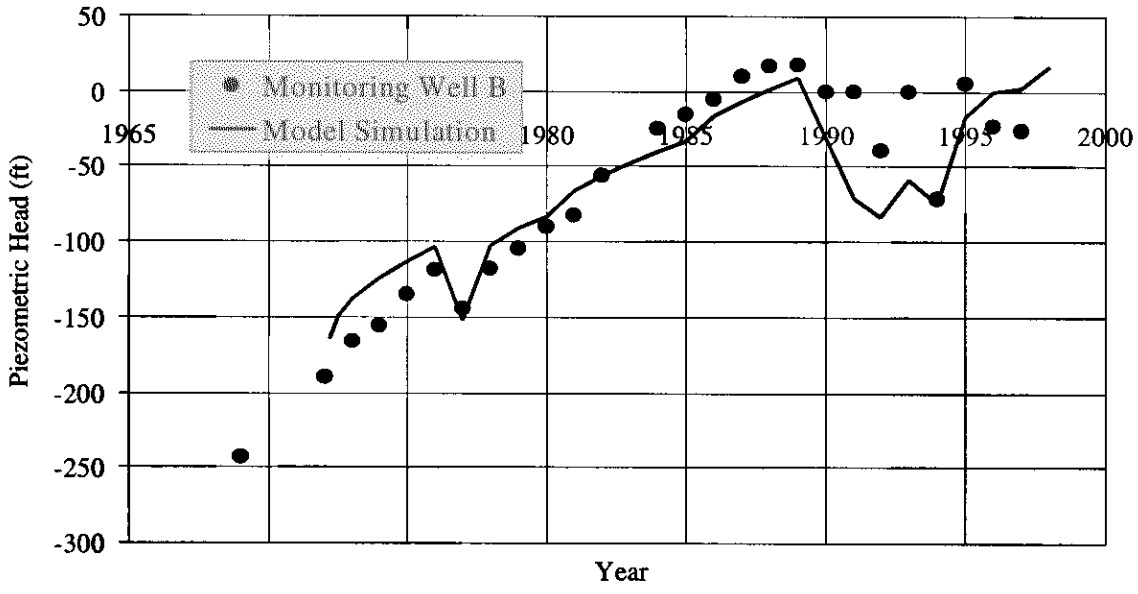

Figure 18 - Observed and Simulated Piezometric Head for Observation Location B.

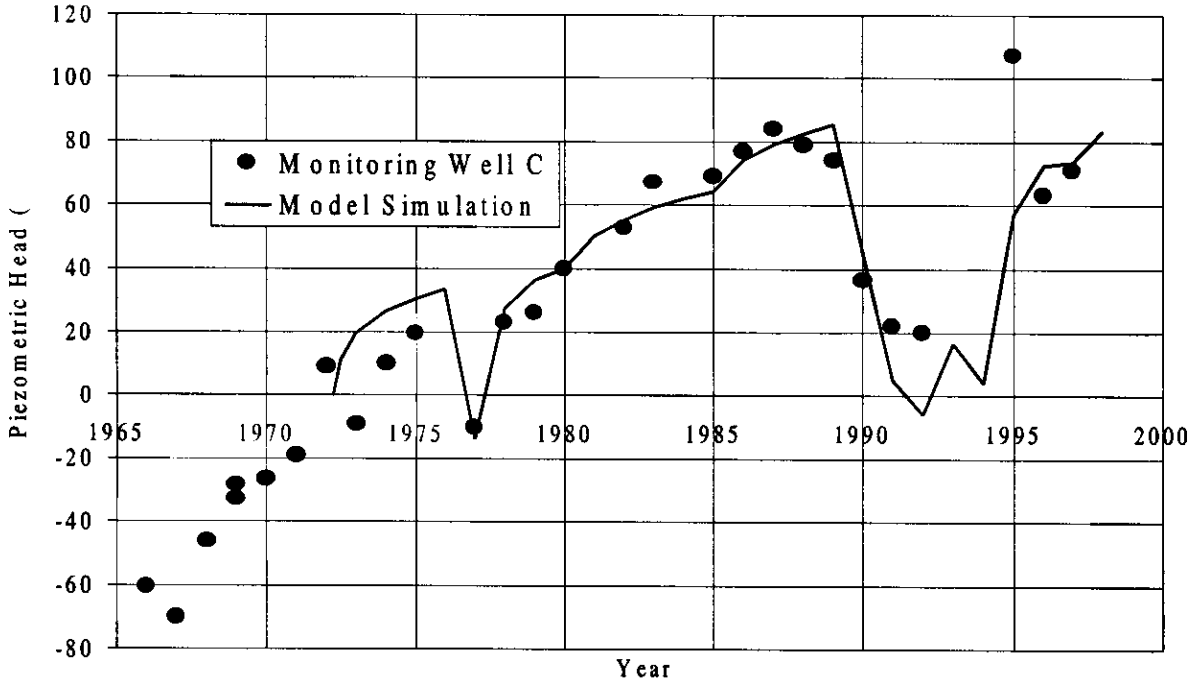

Figure 19 - Observed and Simulated Piezometric Head for Observation Location C.

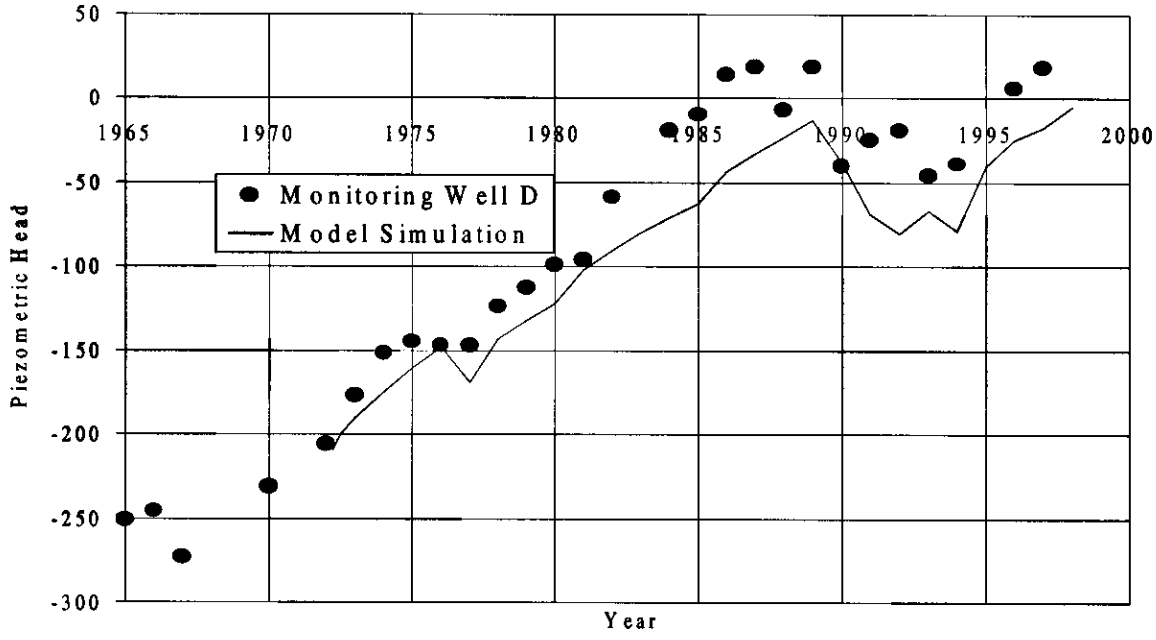

Figure 20 - Observed and Simulated Piezometric Head for Observation Location D.

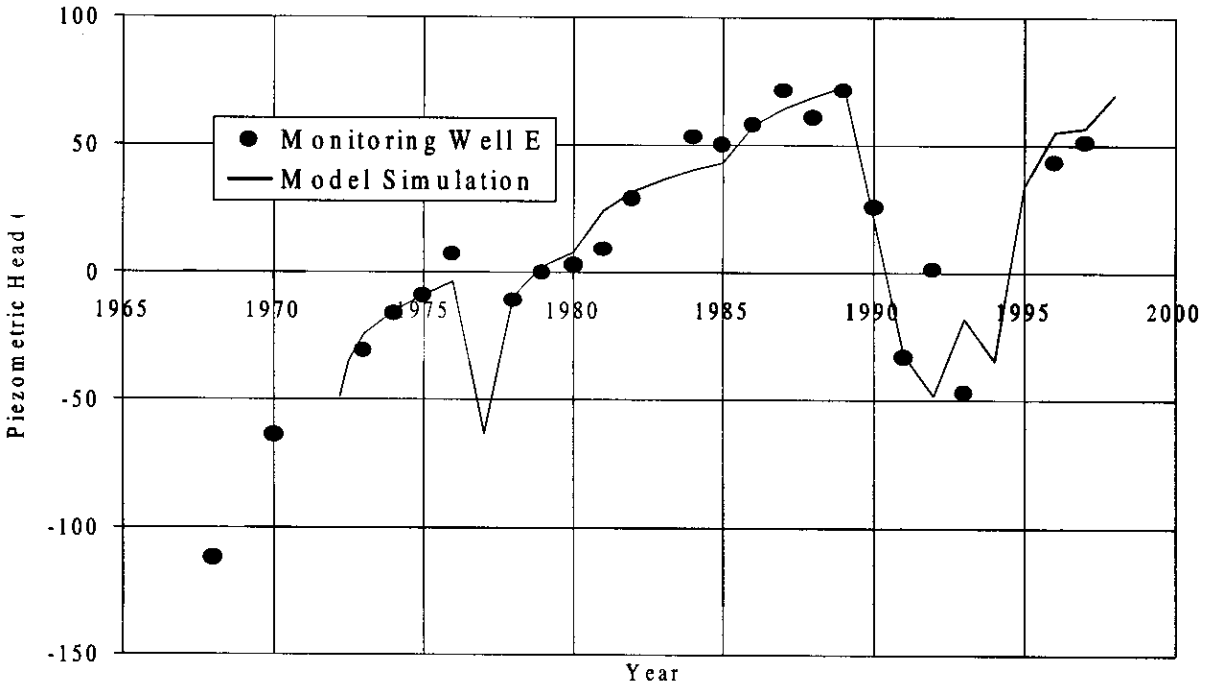

Figure 21 - Observed and Simulated Piezometric Head for Observation Location E.

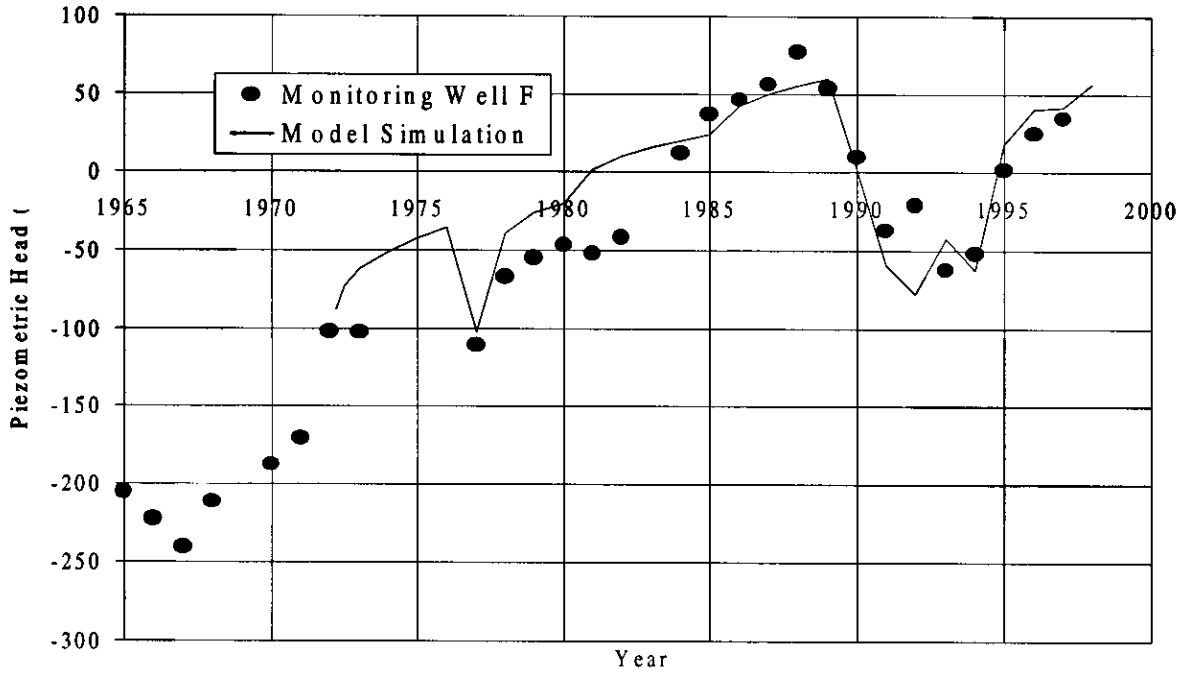

Figure 22 - Observed and Simulated Piezometric Head for Observation Location F.

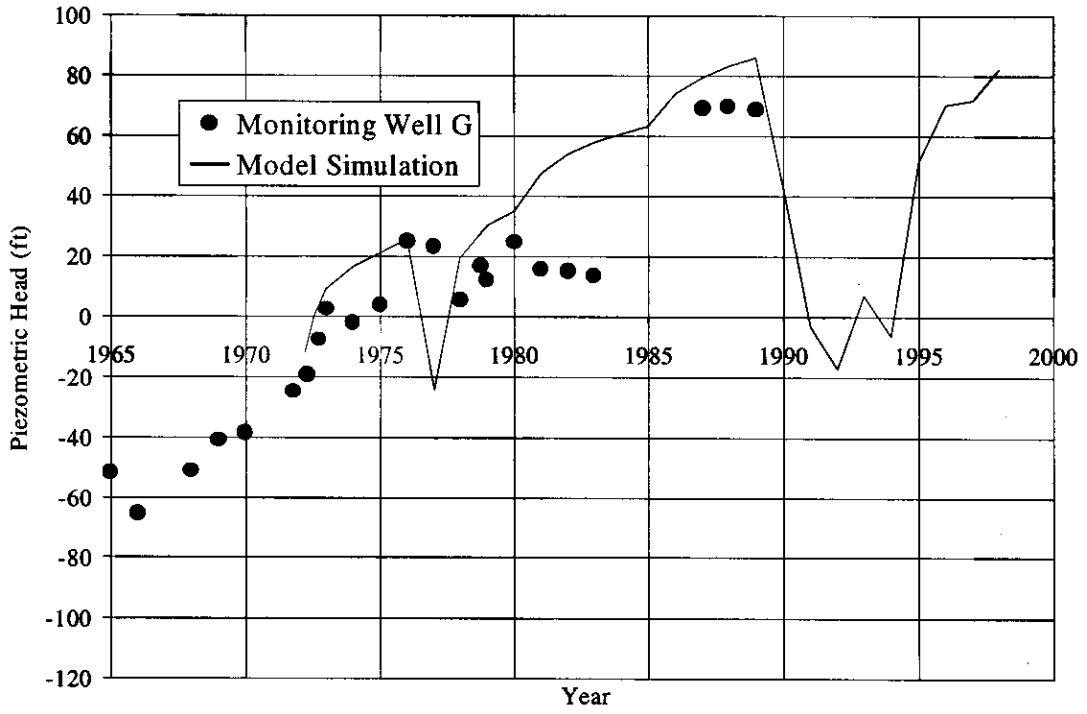

Figure 23 - Observed and Simulated Piezometric Head for Observation Location G.

pumping 150 percent during periods of drought, the head levels in the model appear to better match the observed data in the region.

3.2.2 Land Subsidence

Land subsidence in the San Joaquin Valley has been documented using both extensometers located at wells throughout the Valley and level runs along the California Aqueduct. An extensometer consists of a cable or pipe that is lowered into a well and set below the bottom of the well casing. As the aquifer system compacts, an equivalent length of cable or pipe appears to emerge from the well. By measuring the movement of the land surface relative to the fixed cable or pipe, the total compaction of the aquifer system for the length of the well can be found (Ireland et al., 1984).

Extensometers provide the most detailed measurement of compaction. Annual extensometer measurements can be plotted directly versus model predictions. Unfortunately, each extensometer only records compaction at one point, and only six are located in the study area. Level runs provide a better indication of subsidence trends spatially. Although they are conducted only once every four years, they measure subsidence along a path line.

The six extensometers included in this study (Figure 4) were installed by the U.S. Geological Survey (USGS) and are now monitored by the San Joaquin district of the California DWR. Three of the extensometers were abandoned in the 1970s and thus provide only a partial record for the calibration period. For those extensometers that continue through the entire time interval (1972-1998), a small portion of the data is

Table 3 - Well Numbers for Extensometers and Monitoring Wells

Observation Location		Well Number	Year of Installation	Screen Interval (ft)	Monitored Interval by Extensometer (ft)
Extensometer and Monitoring Wells					
	1	12/12-16H2	1958	770-909	0-1000
	2	13/12-20D1	1691	425-665	0-681
	3	14/12-12H1	1965	740-936	0-973
	4	14/13-11D6	1961	1133-1196	0-1358
	5	15/13-11D2	1965	900-960	0-958
	6	16/15-34N1	1958	1052-1112	0-2000
Monitoring Wells Only					
	3b	14/12-01Q1	*	*	--
	3c	14/13-07E3	*	*	--
	4b	14/13-11R1	*	*	--
	5b	15/13-02N2	*	*	--
	6b	16/15-33J1	*	*	--
	6c	17/15-03E1	*	*	--
	A	13/13-10R1	*	*	--
	B	14/12-25D1	*	*	--
	C	14/14-02N2	*	*	--
	D	15/12-01R1	*	*	--
	E	15/14-02B1	*	*	--
	F	15/14-21E1	*	*	--
	G	14/15-32N3	*	*	--

* Information considerd confidential by the California DWR. Contact owner of individual well for more information.

missing from the record (1974-1984). Fortunately, the missing portion corresponds to a time of relatively uniform rebound. For this portion, rebound is assumed at a rate equal to the average of the rebound in the years 1978 and 1985.

Extensometers only measure compaction across a monitored depth. As a result, additional compaction can occur below the monitored interval and surface subsidence will usually be greater than the compaction measured by the extensometer. Compaction is transformed to subsidence by multiplying the observed compaction by the extensometer's

average ratio of subsidence to compaction (Ireland et al., 1984). These ratios were calculated for data observed through 1980. Changes in well fields since 1980 may affect these ratios and represent a potential source of error. Figures 24-29 show the model results following calibration plotted directly against the transformed extensometer data. Results are for the same model run as shown in Figures 11-23.

Extensive level runs were conducted for the Los Banos-Kettleman City region throughout the 1950s and 1960s. Although more recent data could not be accessed for this report, the previous level runs give a good indication of subsidence trends for the area. Figure 30(a) is a contour map of the measured subsidence from 1926 to 1972, while Figure 30(b) shows the predicted subsidence from 1972 to 1998. Although the difference in observation periods do not allow for direct comparison, the subsidence trends for each period are similar. There appears to be a small shift in the peak of subsidence or is related to the choice of calibration parameters.

There are four major subsidence parameters determined during the calibration processes: vertical hydraulic conductivity, elastic storage coefficient, inelastic storage coefficient, and preconsolidation head. For the Corcoran layer, the storage and conductivity parameters are taken as the average of measured values from Ireland et al. (1984). They vary spatially with the thickness of the Corcoran, but are constant in time. Because field measurements are available for these parameters, only the preconsolidation heads are modified during calibration. Because of the fictional nature of the interbed layer, however, there is no correlation between its storage parameters and values measured in the field. All four major parameters for this layer can only be determined through calibration.

For the interbed layer, the hydraulic conductivity and storage coeffiecients are assumed to be constant in space and time. This leaves preconsolidation head alone as a mechanism for spatial variation. Preconsolidation head is given this distinction because there is a moderate amount of well data to aid in its selection while there is very little information available on the spatial variation of the other parameters.

The final subsidence parameters (i.e., vertical hydraulic conductivity, storage coefficients, and preconsolidation head) were achieved through trial and error. Although the computational effort required to run the model makes a statistically rigorous calibration numerically impractical, a sensitivity analysis has been performed to aid in the selection of model parameters.

3.3 Sensitivity Analysis

3.3.1 Hydraulic Conductivity

Hydraulic conductivity is represented in two directions, vertical and horizontal. The horizontal conductivity is of little interest in the interbed layers because small head gradients and long flow paths result in insignificant horizontal flow. Additionally, the horizontal flow should not be significantly changed by the new model arrangement. Hence, it is acceptable to adopt the average horizontal hydraulic conductivity in the interbed layers as measured in the field by Ireland et al. (1984).

Conversely, the vertical conductivity greatly affects the performance of the model. For a given hydraulic gradient, it determines the rate pore pressure leaves the fine-grained

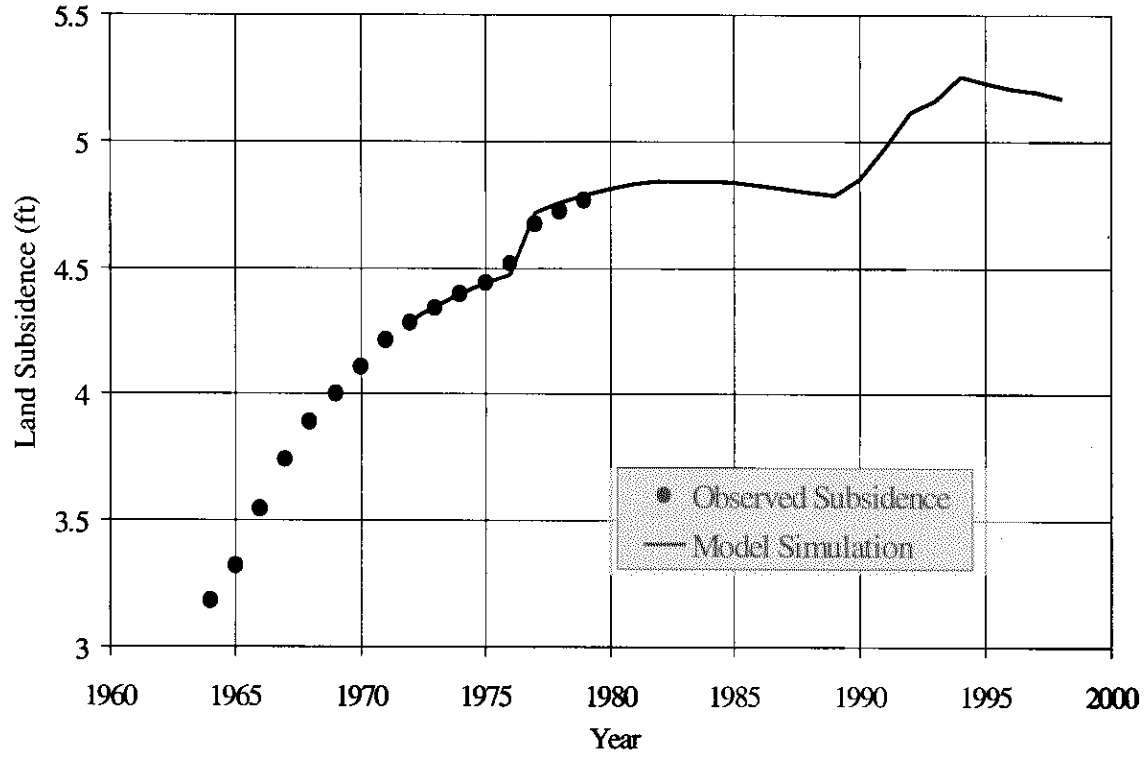

Figure 24 - Observed and Simulated Land Subsidence for Extensometer 1.

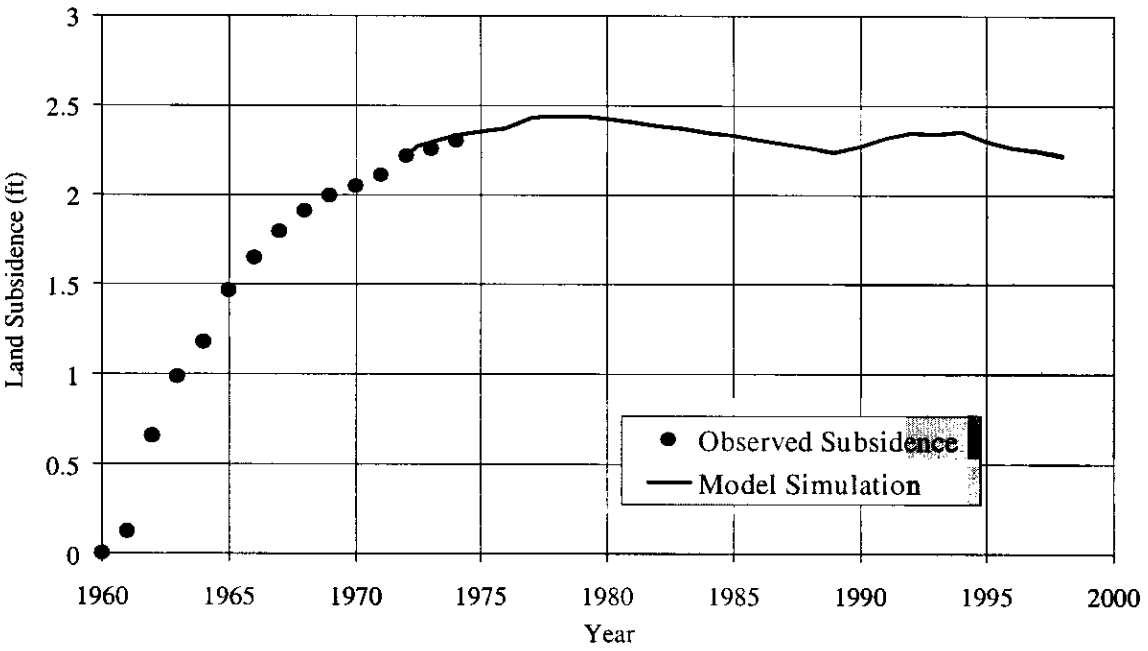

Figure 25 - Observed and Simulated Land Subsidence for Extensometer 2.

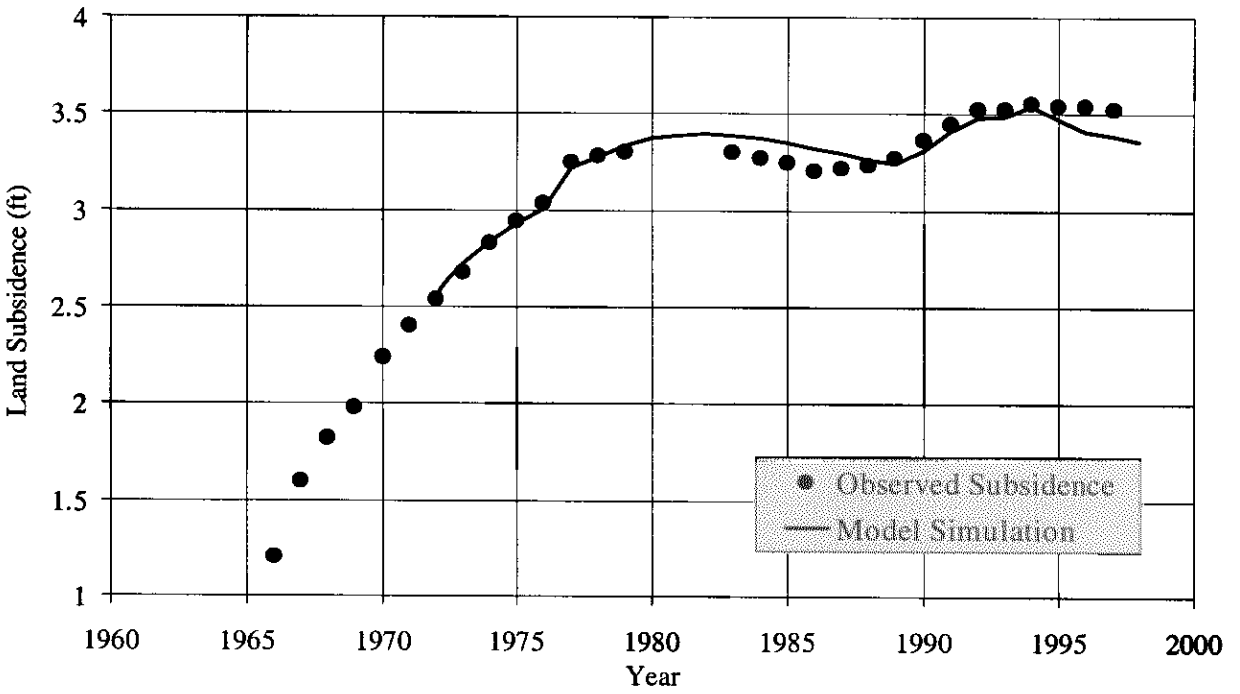

Figure 26 - Observed and Simulated Land Subsidence for Extensometer 3.

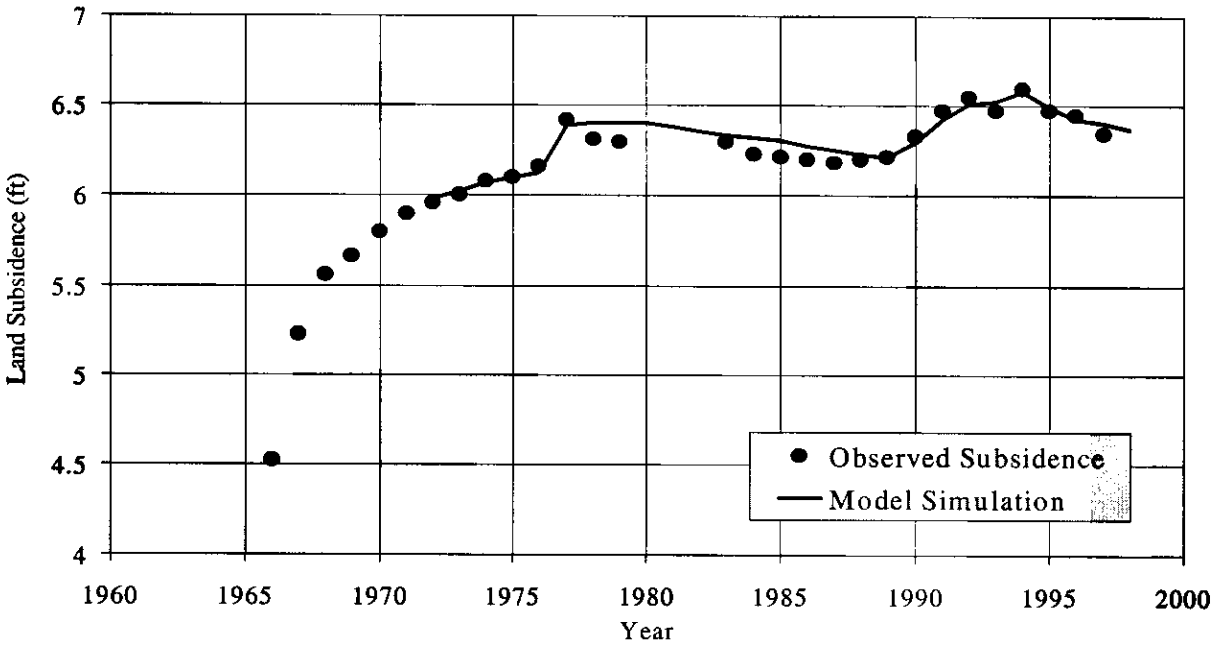

Figure 27 - Observed and Simulated Land Subsidence for Extensometer 4.

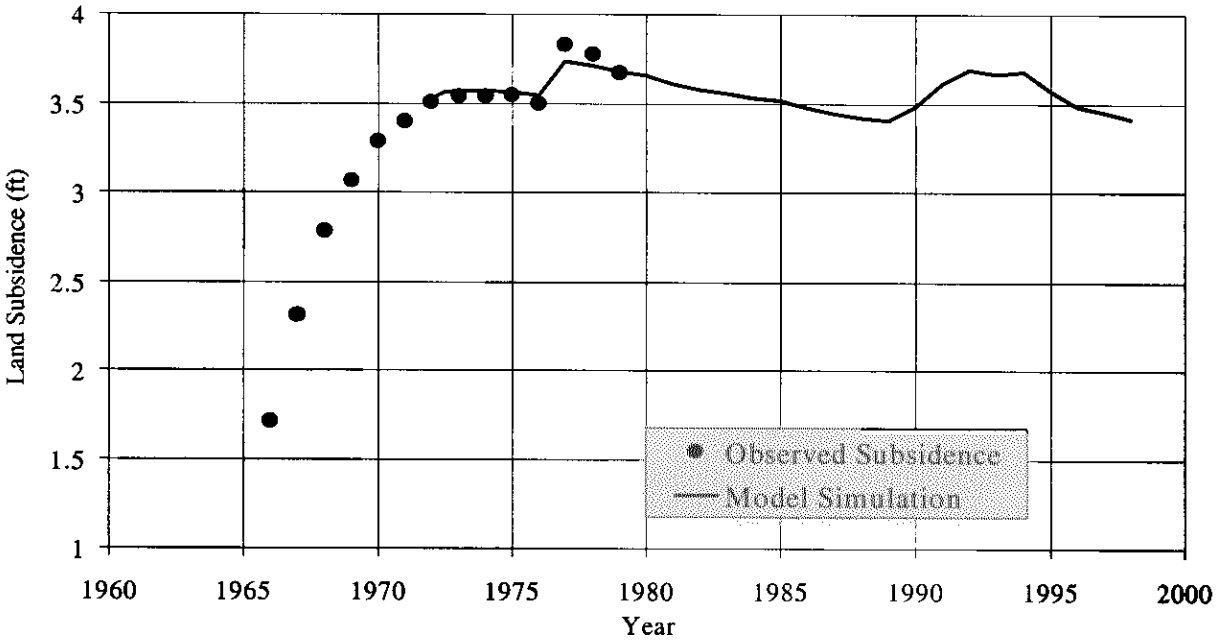

Figure 28 - Observed and Simulated Land Subsidence for Extensometer 5.

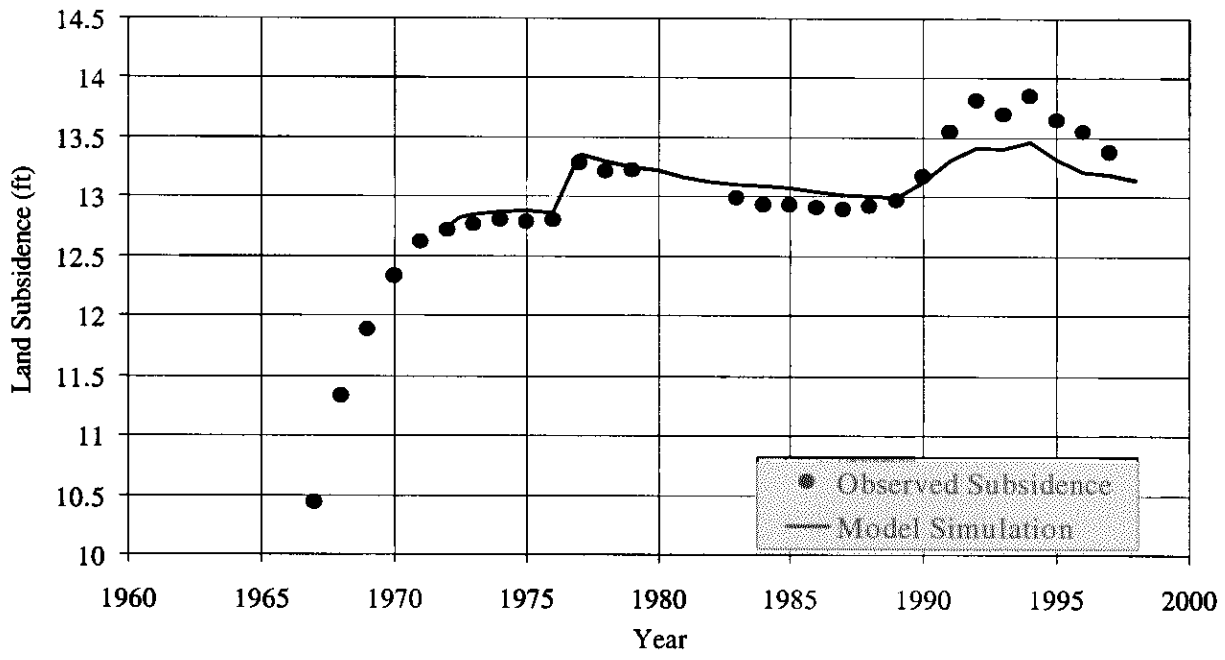

Figure 29 - Observed and Simulated Land Subsidence for Extensometer 6.

layers and hence, the rate of subsidence. Figure 31(a)-(f) show the model results obtained using four-fold and one-fourth of the interbed layer's calibrated vertical hydraulic conductivity (0.25 ft/yr). As predicted, the rate of subsidence is very dependent upon the vertical hydraulic conductivity while the general trend of the subsidence is not greatly affected. The results of the sensitivity analysis appear asymmetrical; however, during periods of subsidence, the rates of subsidence are roughly proportional to the hydraulic conductivity values. This is as expected. For a given head gradient, four times the hydraulic conductivity will release four times the amount of water from a compressible layer and will correspondingly produce four times the subsidence. Subsidence is not directly proportional to hydraulic conductivity, however, because the release of water from the compressible layers changes the head gradients during each scenario. It is also interesting to note that after the effects of delayed drainage have passed, the rate of rebound is relatively unaffected by changes in hydraulic conductivity.

3.3.2 Elastic and Inelastic Storage Coefficients

The elastic and inelastic storage coefficients determine the magnitude of subsidence for a given change in hydraulic head. During long periods of rebound (e.g., 1978-1989), the elastic coefficient can be examined independently of the inelastic coefficient since all rebound is elastic. As observed in Figure 31, after the effects of delayed drainage have passed, the rate of rebound is also mostly independent of hydraulic conductivity. This makes the elastic coefficient the easiest parameter to calibrate because it can be chosen, virtually independent of the other parameters, to match the observed rebound rate.

The contribution of the inelastic coefficient is much more difficult to isolate. It has the least visible effect on the performance of the model. During inelastic compression a significant volume of water is expelled from the compressible model layers. Because the rate of this expulsion is governed by the vertical hydraulic conductivity, the rate of inelastic compression is dominated by the vertical conductivity, not the inelastic storage coefficient. Instead, the latter coefficient determines the rate at which the preconsolidation head falls in each layer as consolidation occurs. Thus, it is an important parameter in determining when inelastic compression starts and stops. Figures 32(a)-(f) show the model results obtained using four-fold and one-fourth of the interbed layer's calibrated elastic specific storage (8.25×10^{-6} ft^{-1}), while Figures 33(a)-(f) present the same information for inelastic specific storage (6.45×10^{-4} ft^{-1}).

Figure 32 reveals a near direct proportionality between the elastic storage coefficient and the rate of rebound, confirming the arguments above. Similarly, the difficulty isolating the effects of the inelastic storage constant is well illustrated in Figure 33. Several of the plots shown in Figure 33 show very little sensitivity to the inelastic storage coefficient. Figure 33(c) best illustrates the effect of this coefficient. Subsidence rates are roughly the same for all values of inelastic storage coefficient during the first few time steps. As groundwater levels recover, however, subsidence rates began to diminish earlier for the lower values of inelastic storage coefficient (i.e., rebound for the lowest value of inelastic storage coefficient starts in 1981, while for the highest value it does not begin until 1984).

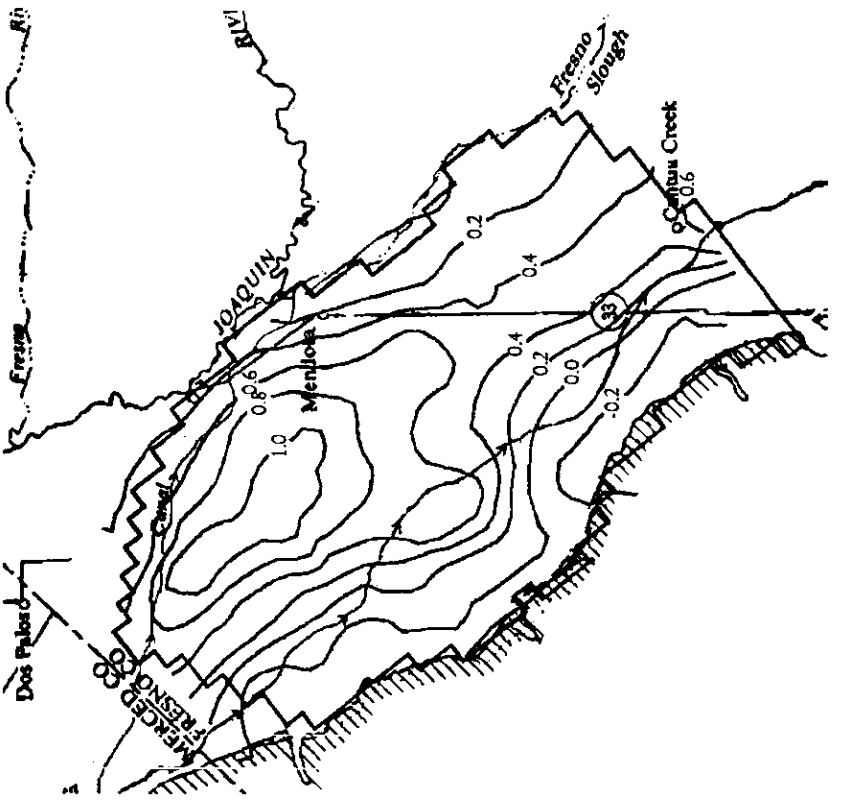

Figure 30(b) - Simulated Subsidence for Los Banos-Kettleman City, 1972-98 (in feet).

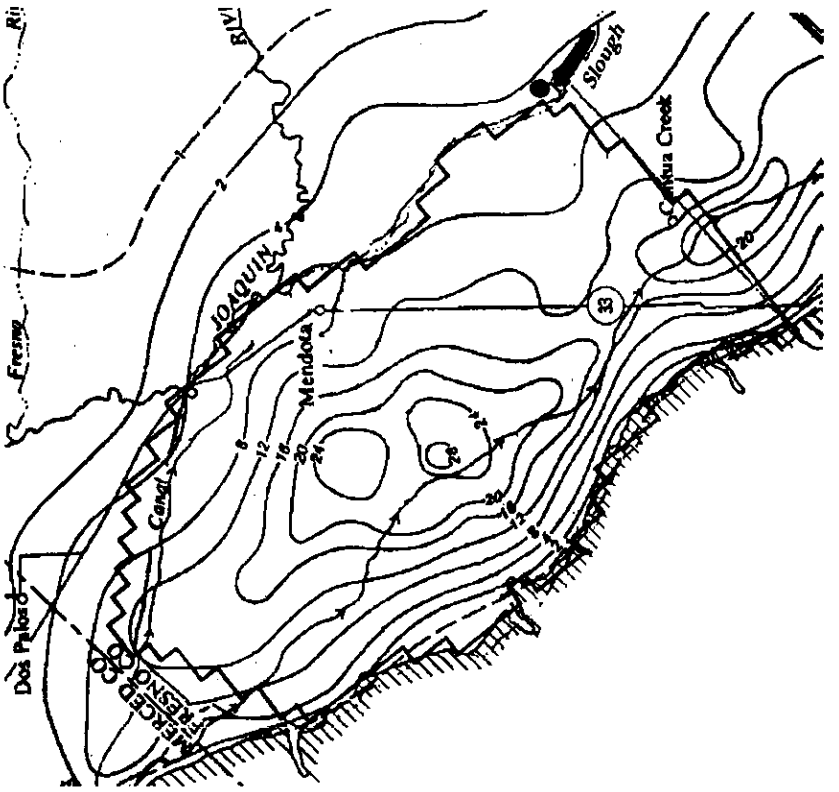

Figure 30(a) - Observed Subsidence for Los Banos-Kettleman City, 1926-72 (Ireland et al., 1984) (in feet).

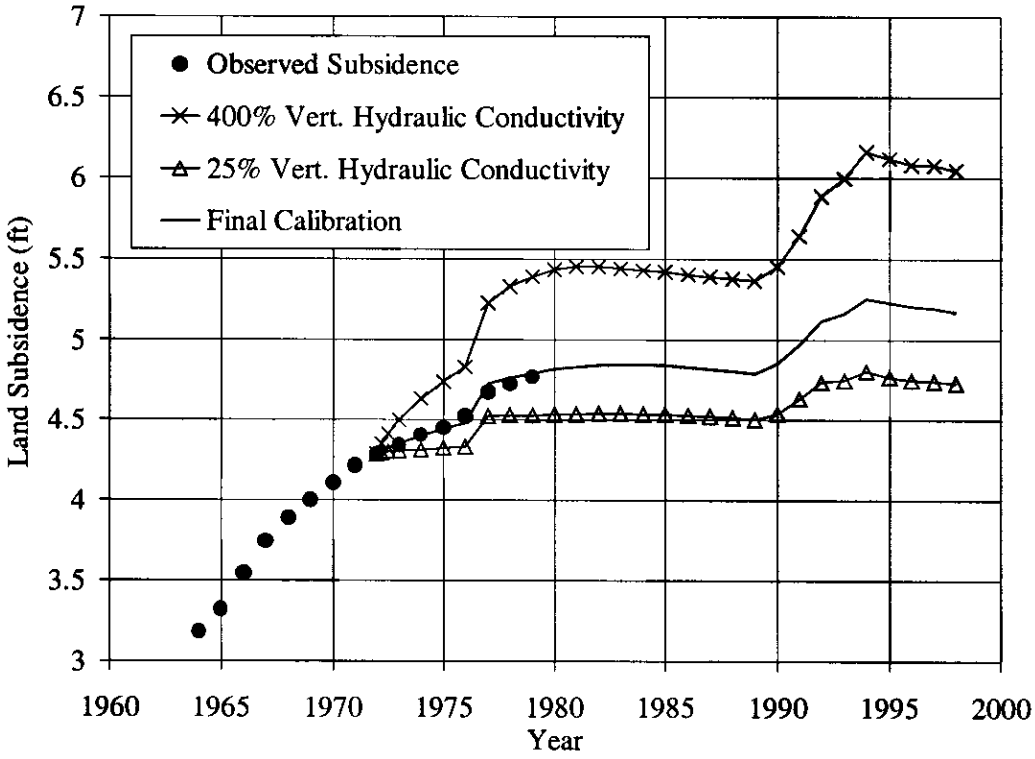

Figure 31(a) - Extensometer 1

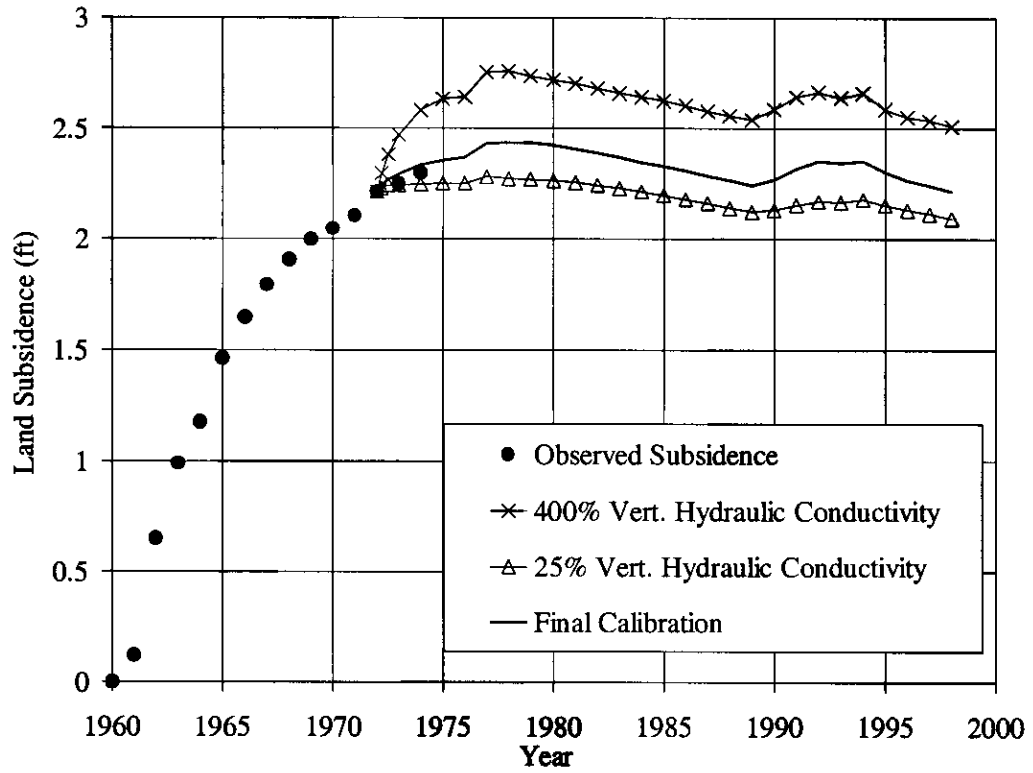

Figure 31(b) - Extensometer

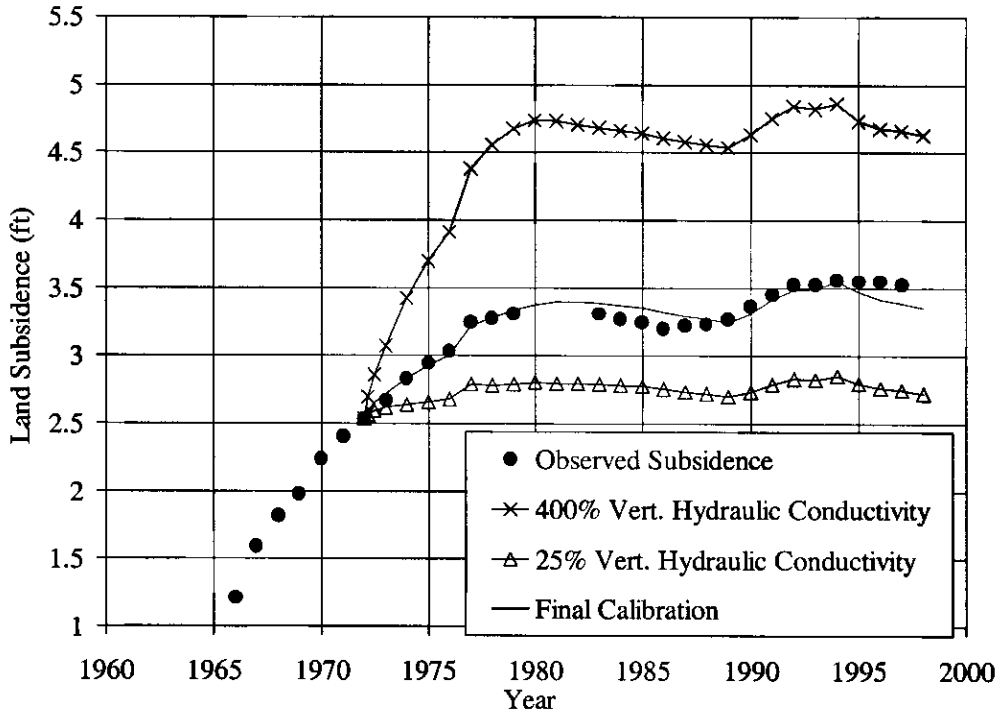

Figure 30(c) - Extensometer 3

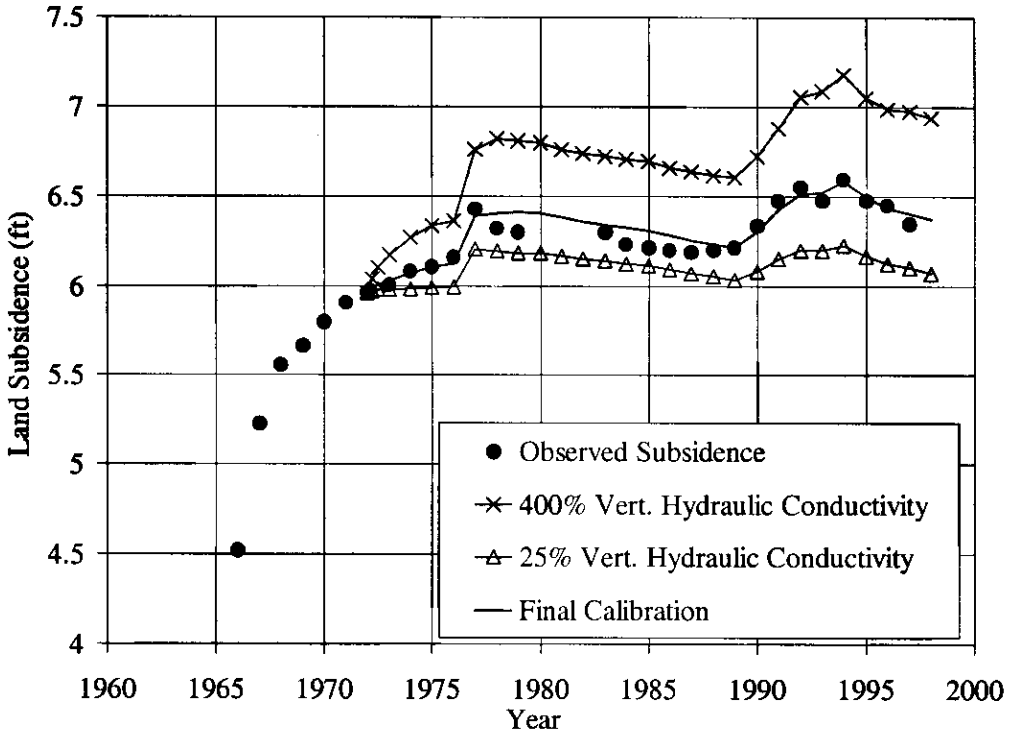

Figure 31(d) - Extensometer 4

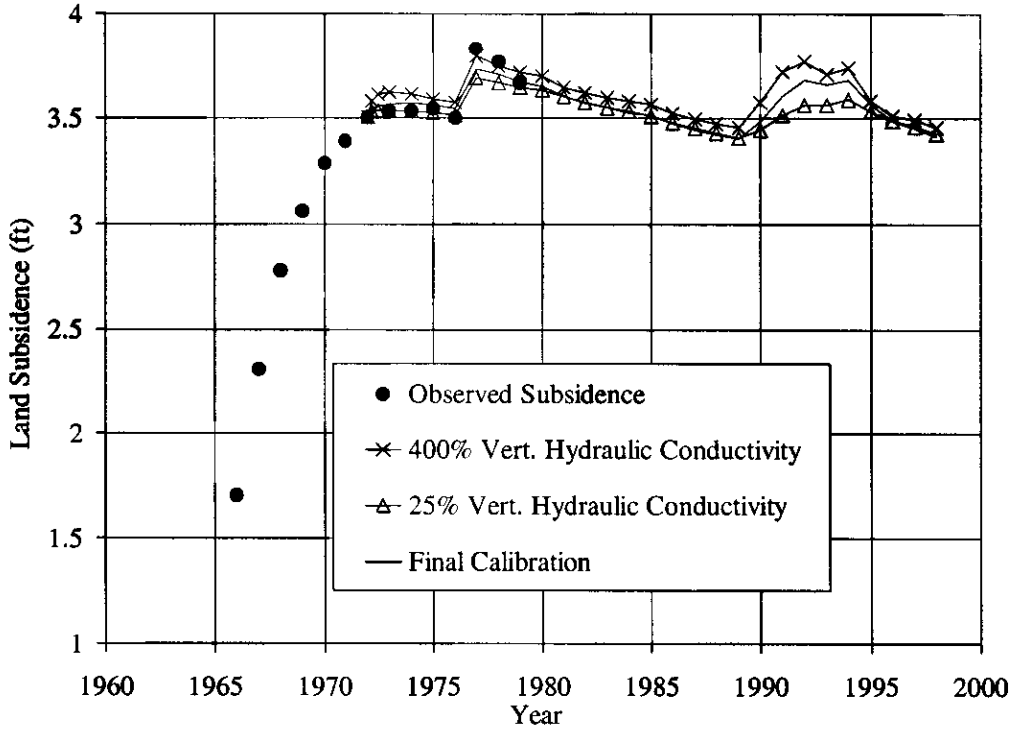

Figure 31(e) - Extensometer 5

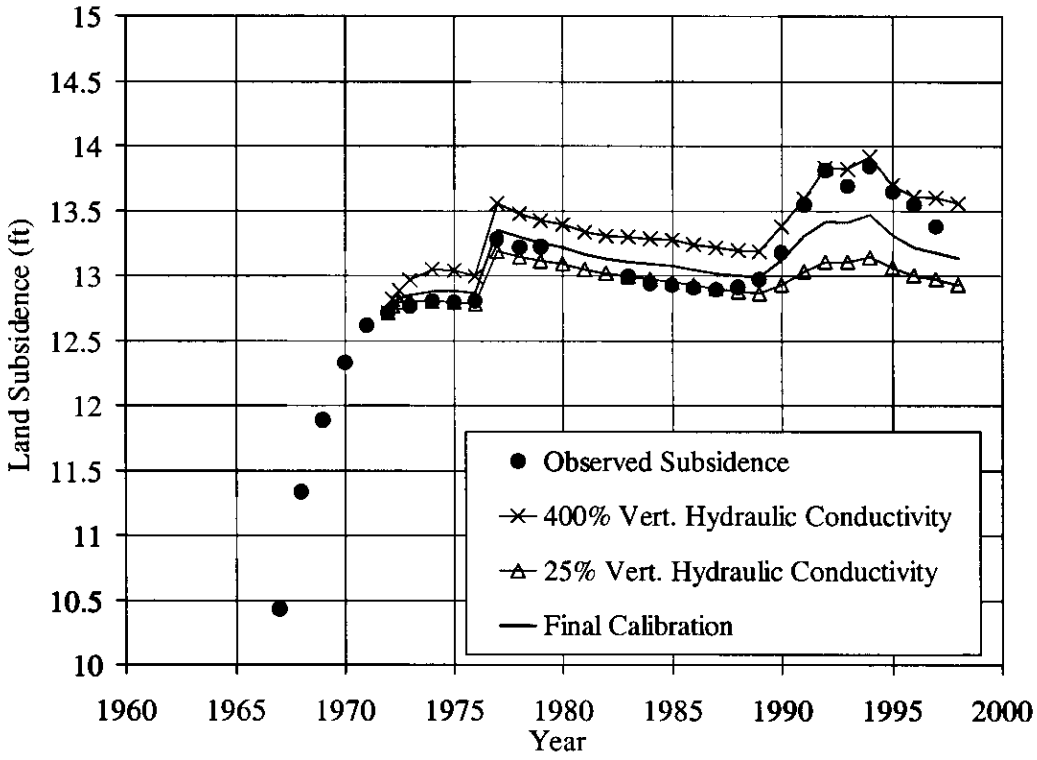

Figure 31(f) - Extensometer 6

Figures 31(a)-(f). Simulated Subsidence for 400, 100 and 25 Percent Final Calibrated Value of Vertical Hydraulic Conductivity at Six Extensometer Loca-

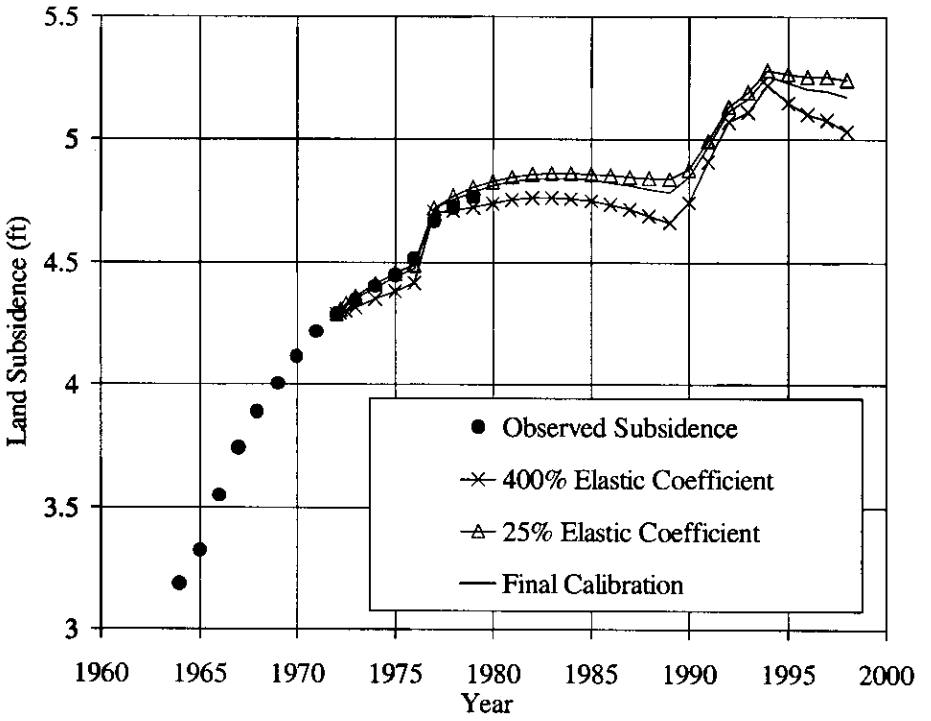

Figure 32(a) - Extensometer 1

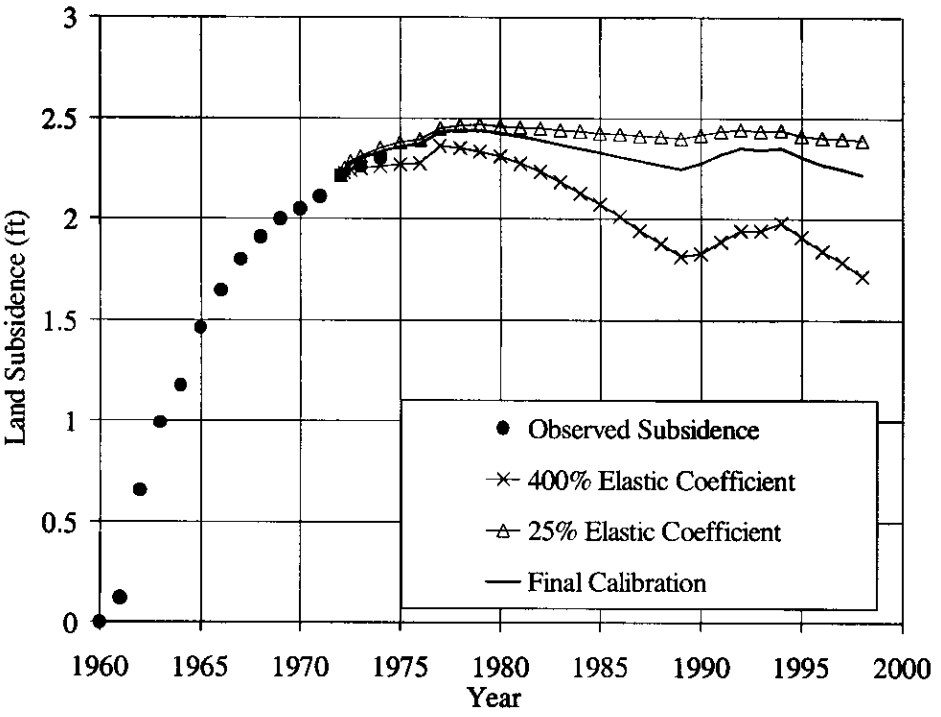

Figure 32(b) - Extensometer 2

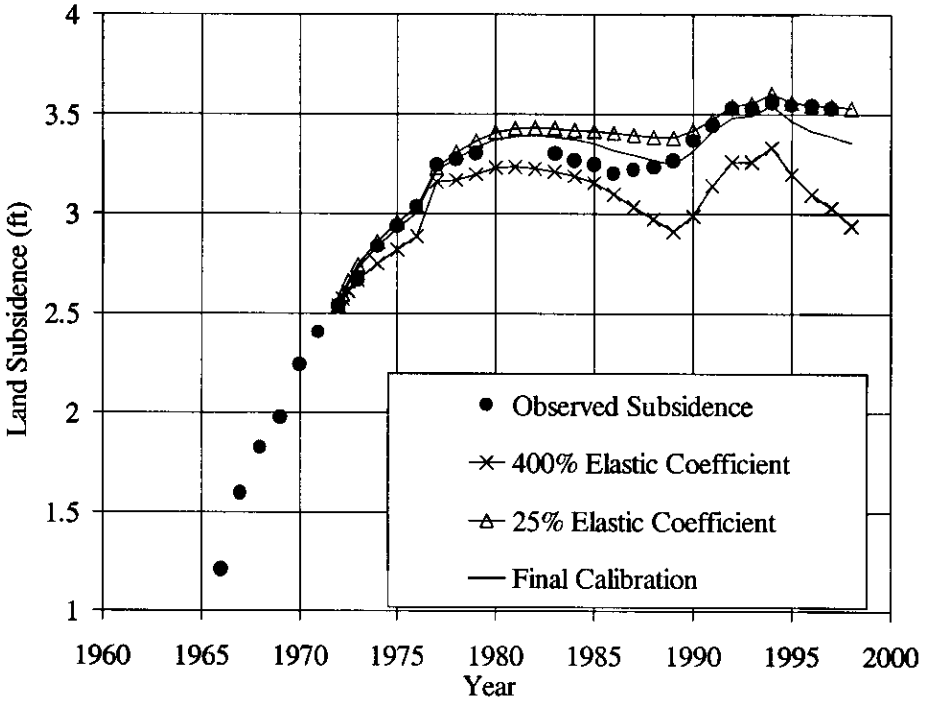

Figure 32(c) - Extensometer 3

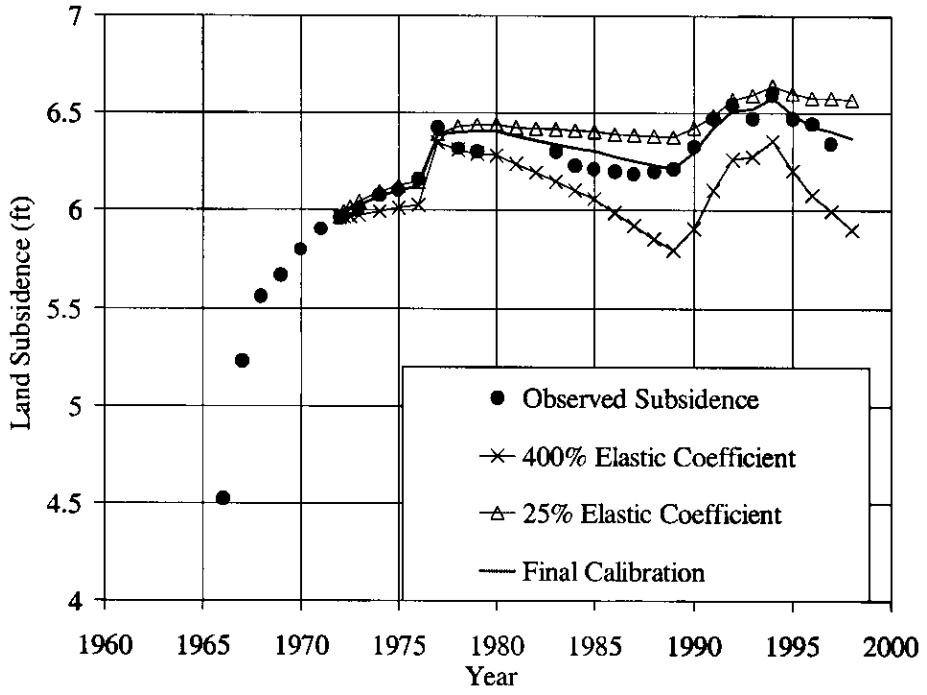

Figure 32(d) - Extensometer 4

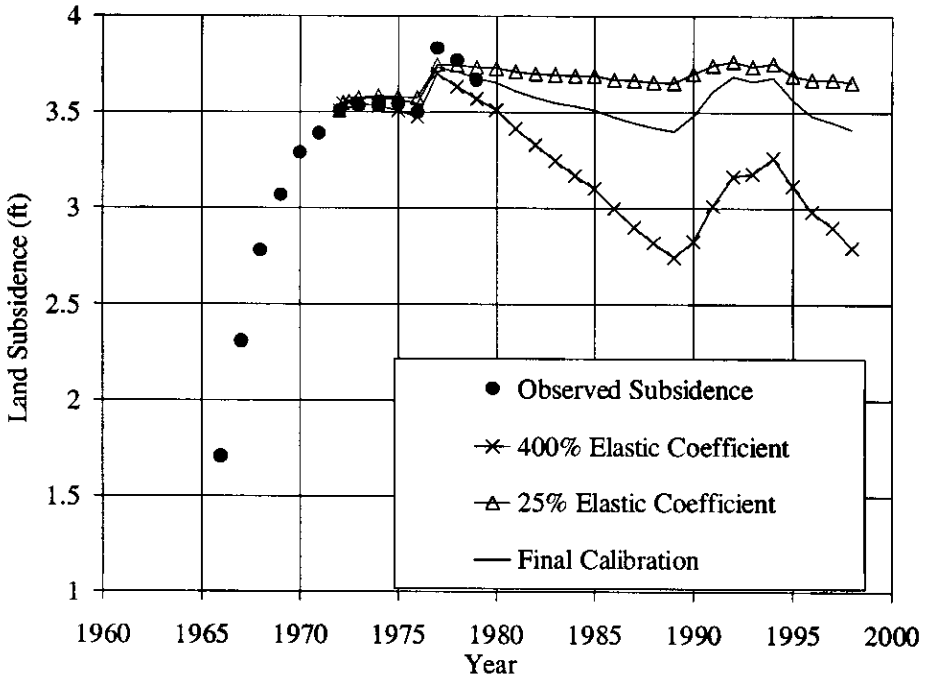

Figure 32(e) - Extensometer 5

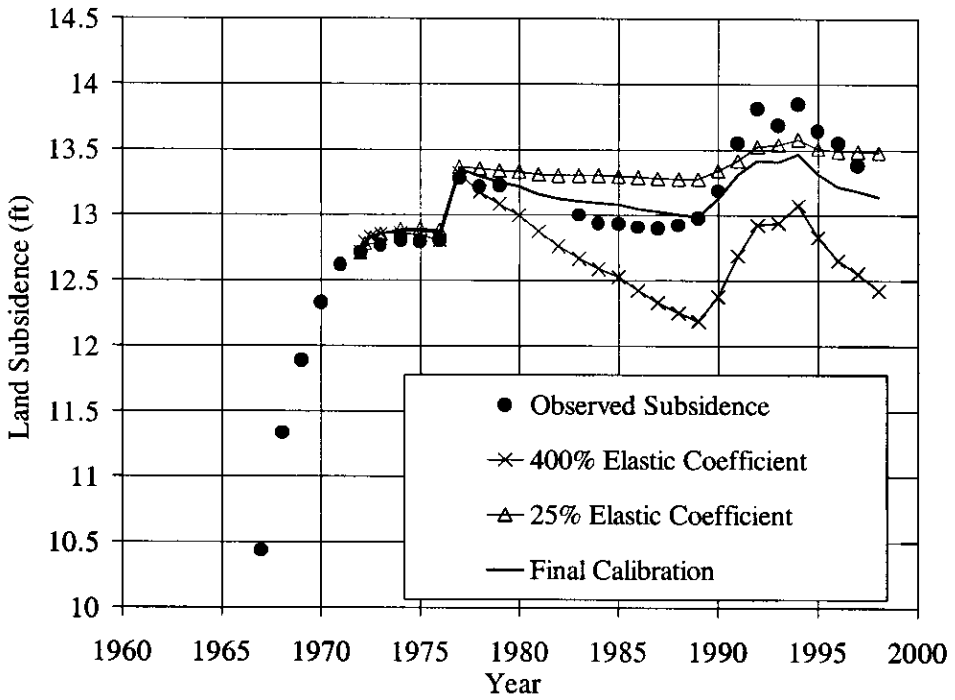

Figure 32(f) - Extensometer 6

Figures 32(a)-(f). Simulated Subsidence for 400, 100 and 25 Percent Final Calibrated Value of Elastic Storage Coefficient at Six Extensometer Locations.

3.3.3 Preconsolidation Heads

The preconsolidation heads for the Corcoran and interbed layers were determined using the process described earlier (section 3.1.3). Grids of the final preconsolidation heads for each model layer can be found in the appendix of this report. If a parabolic profile is assumed as shown in Figure 10, only the upper bound of residual pore pressure need be determined through calibration. This upper bound of residual pore pressure was first approximated using the 1943 head values in the confined aquifer. The year 1943 was chosen because it was approximately this time when intense groundwater withdrawl began to cause the most serious subsidence. These values were then adjusted during the calibration process to match observed subsidence.

Preconsolidation head has two effects on the model. First, an increase in preconsolidation head (and corresponding increase in initial head) results in an increased rate of subsidence because of the larger gradient between heads in the aquifers and in the compressible layers. Second, an increase in preconsolidation head results in longer periods of subsidence since head levels must rise higher for rebound to begin. This second characteristic makes it possible to differentiate between the effects of an increase in preconsolidation head and an increase in vertical conductivity. Figure 34(a)-(f) shows the model results obtained using 75 and 125 percent of the calibrated residual pore pressure values (preconsolidation head values given in the appendix).

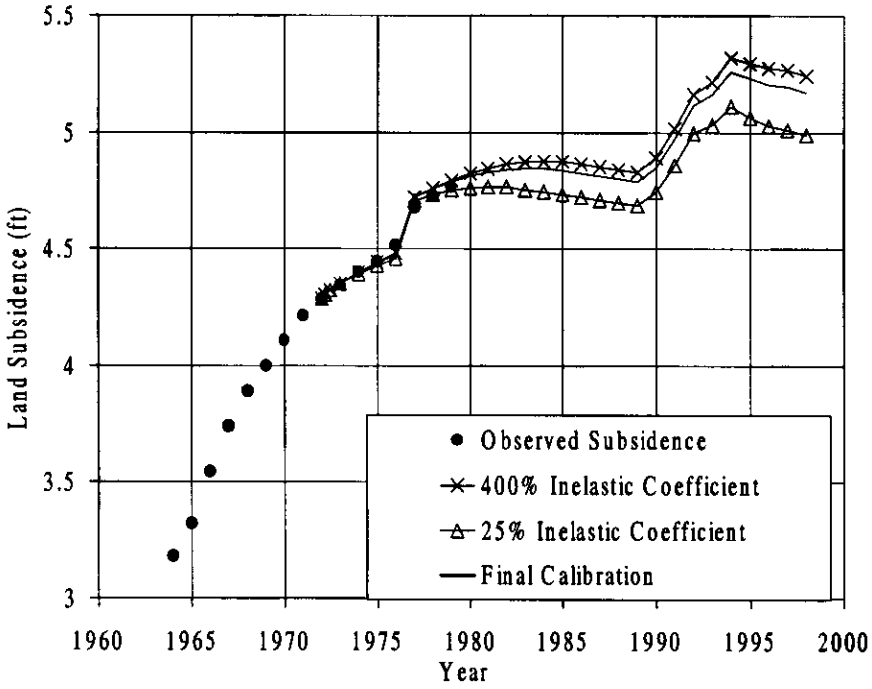

Figure 33(a) - Extensometer 1

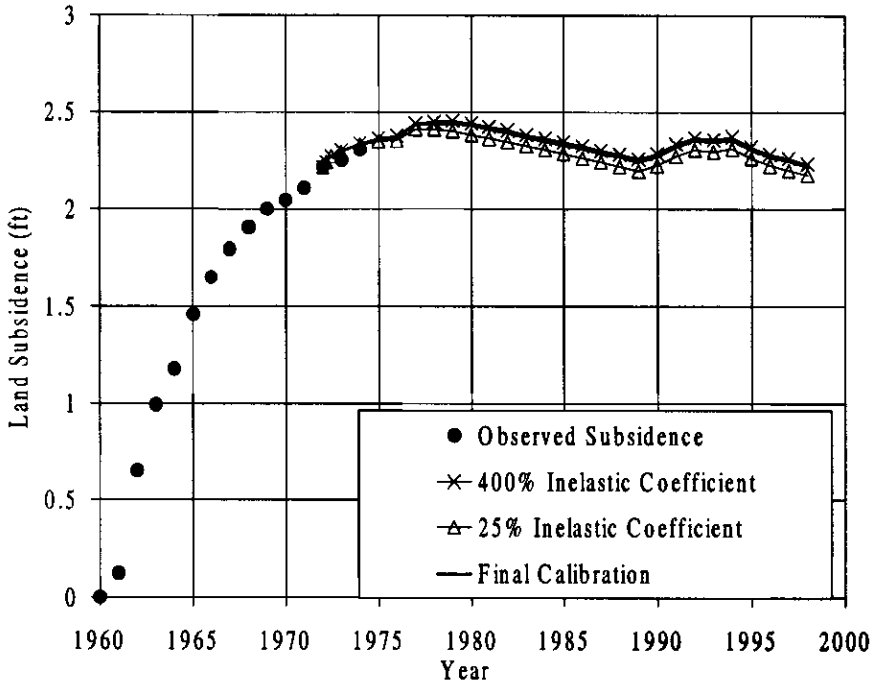

Figure 33(b) - Extensometer 2

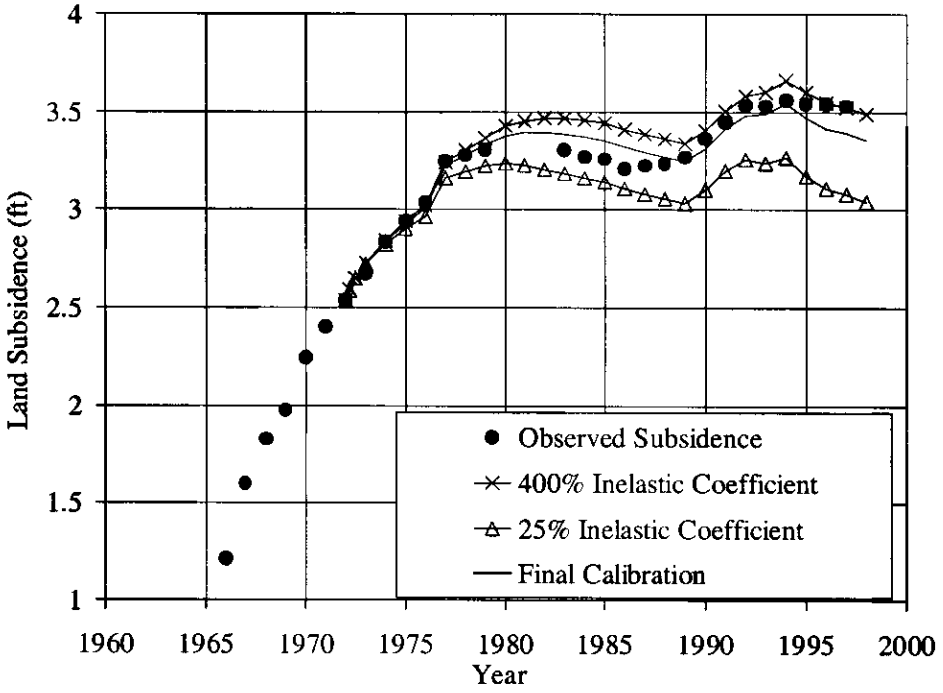

Figure 33(c) - Extensometer 3

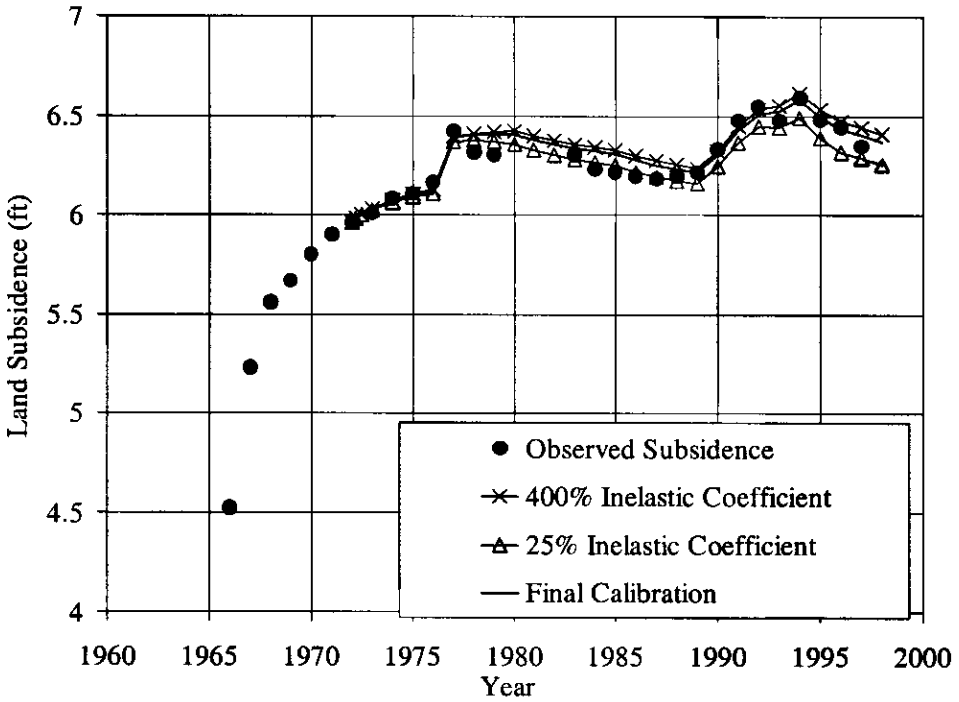

Figure 33(d) - Extensometer 4

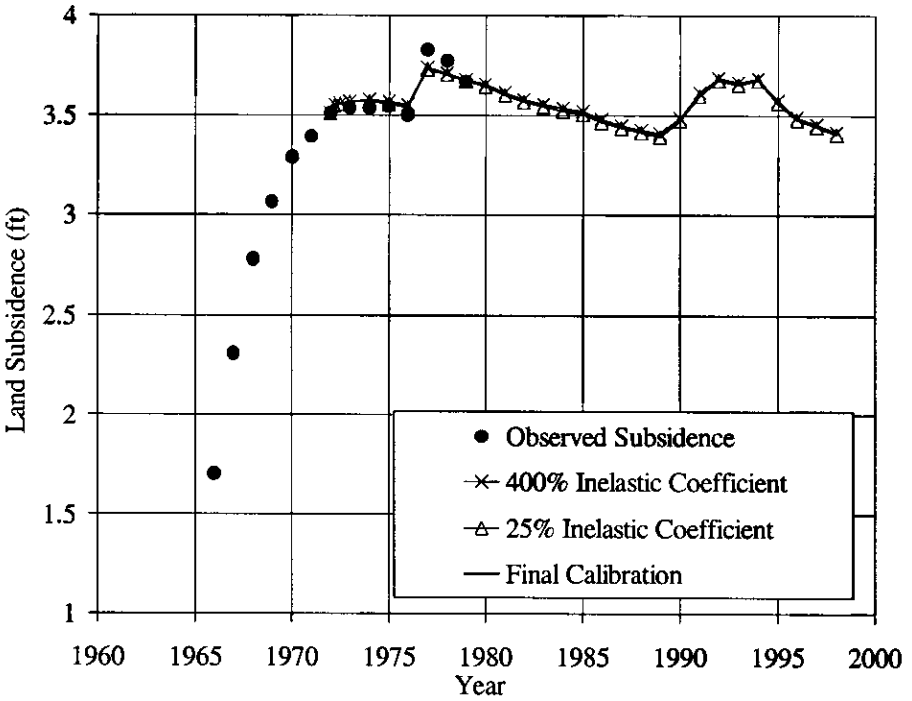

Figure 33(e) - Extensometer 5

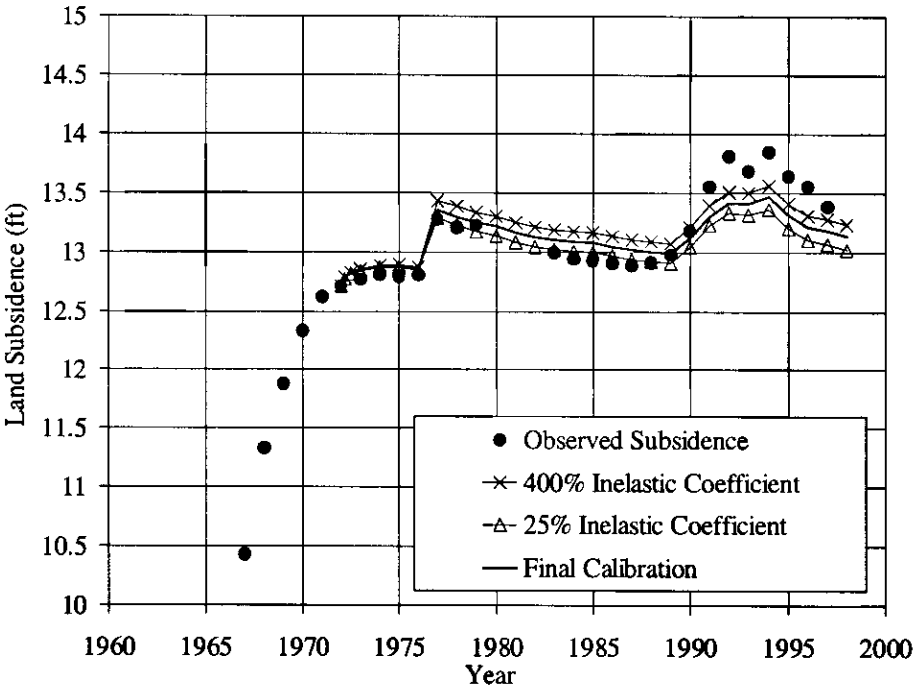

Figure 33(f) - Extensometer 6

Figures 33(a)-(f). Simulated Subsidence for 400, 100 and 25 Percent Final Calibrated Value of Inelastic Storage Coefficient at Six Extensometer Locations.

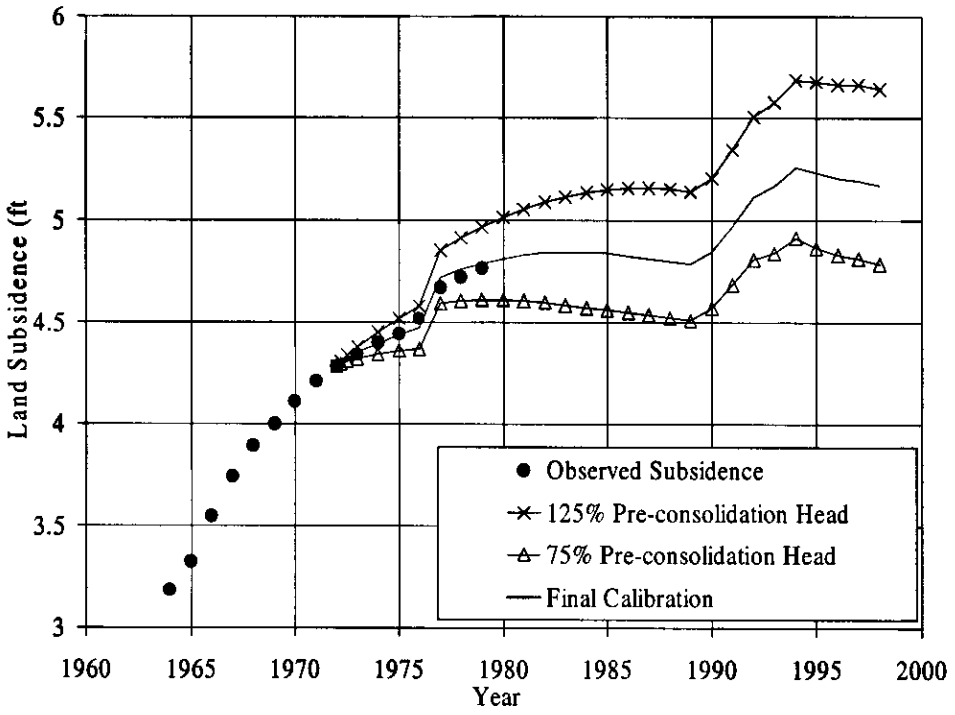

Figure 34(a) - Extensometer 1

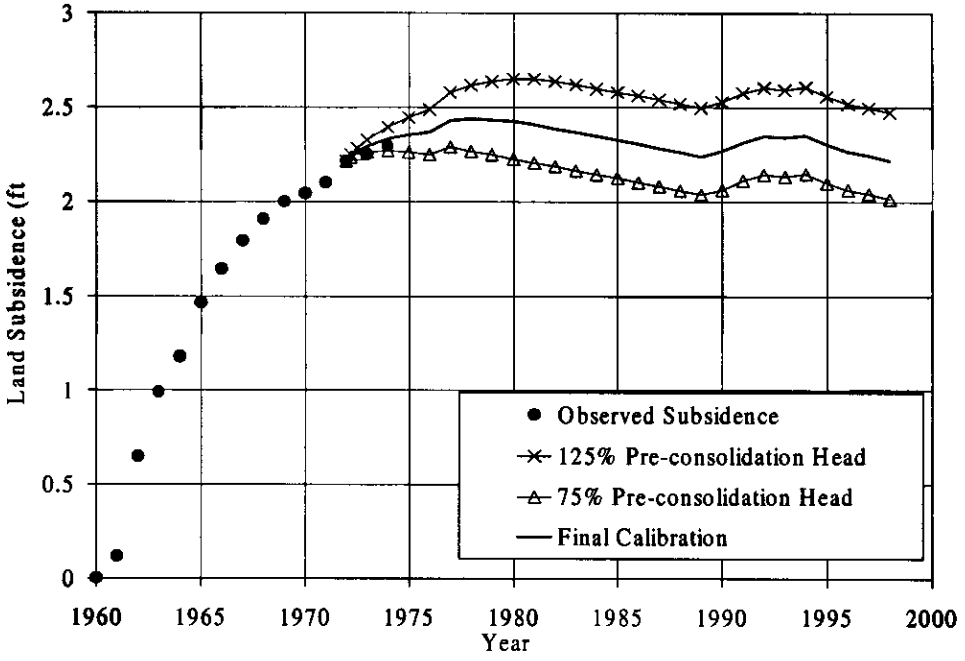

Figure 34(b) - Extensometer 2

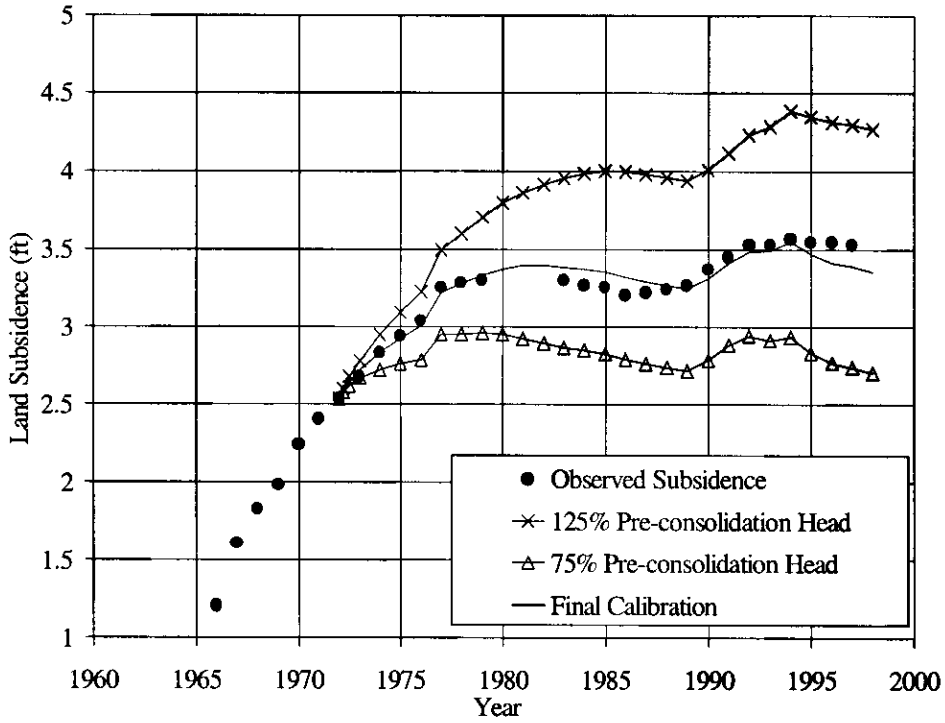

Figure 34(c) - Extensometer 3

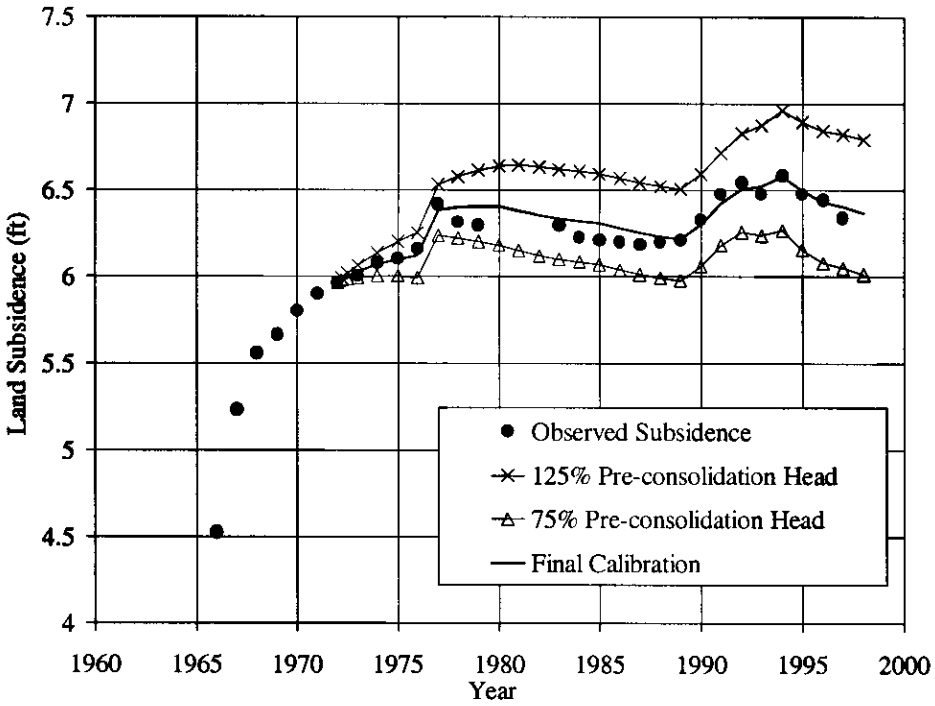

Figure 34(d) - Extensometer 4

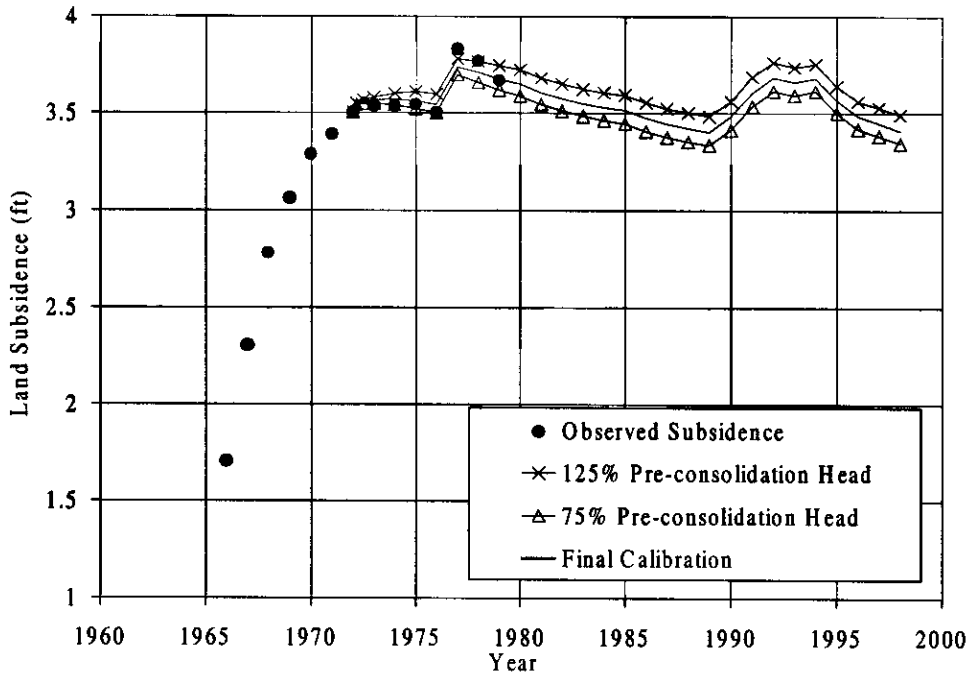

Figure 34(e) - Extensometer 5

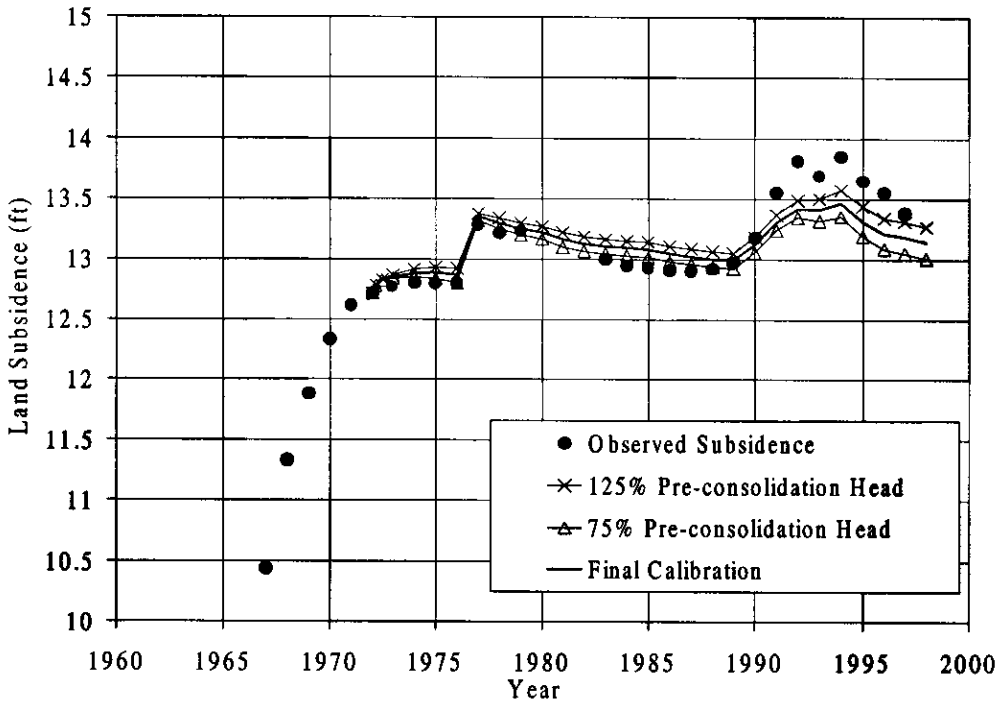

Figure 34(f) - Extensometer 6

Figures 34(a)-(f). Simulated Subsidence for 400, 100 and 25 Percent Final Calibrated Value of Residual Pore Pressure at Six Extensometer Locations.

4. Predicting Future Subsidence Potential

4.1 Development of Future Drought Scenarios

It is not currently possible to predict land subsidence for the Los Banos-Kettleman City area. As illustrated during the calibration process, groundwater levels and subsidence are highly dependent upon the rate of pumping. Because pumping rates are dependent on surface water availability, reliable long-range weather forecasting would be required before true subsidence prediction could be possible. Instead of predicting subsidence, this model estimates subsidence potential by evaluating subsidence for possible CVP water delivery scenarios.

Unfortunately, the CVP water delivery system has been in place for only 30 years. This does not provide sufficient data to statistically generate future CVP delivery scenarios. However, since the majority of the Los Banos-Kettleman City CVP water comes from the Sacramento Valley, the Sacramento 40-30-30 index can be used to estimate future surface water supplies in the Los Banos-Kettleman City area. The Sacramento 40-30-30 index, also known as the Sacramento Four-Rivers Index (SFRI), is calculated from measurements of unimpaired runoff for four major rivers in the Sacramento Valley; American, Feather, Sacramento and Yuba. The SFRI is computed as the sum of 40 percent of the current year's April-July unimpaired runoff, 30 percent of the October-March unimpaired runoff, and 30 percent of the previous year's SFRI. A cap of 10 MAF is placed on the previous year's index to account for required flood control releases during wet years (California DWR, 1999).

Figure 35 shows the best fit exponential relationship between the SFRI and the CVP delivery rates for years classified by the California Department of Water Resources as "below average," "dry," or "critical." The relationship is mathematically described ($R^2 = 0.7264$) as:

$$\Phi_s = 2 \times 10^{-7} (SFRI)^{2.2839} \quad (5)$$

in which Φ_s is the percent of contracted CVP surface water and the SFRI is in million acre-feet.

Another reasonable fit could be achieved using a step function. This would reflect a management scheme wherein water delivery is maintained at contract levels until SFRI values fall below some critical drought value. Once this occurs, delivery is dramatically cut to a lower drought level, regardless of the severity of the drought. Although this approach would closely fit the observed data and may indeed be closer to the current management practices of the USBR, there are two reasons it has not been used in this model. First, the total subsidence predicted by the model would be very sensitive to the choice of SFRI at which deliveries are reduced. A very small movement in the critical drought value of SFRI could change normal years to drought years or vice versa. A second reason for not using a step function is that Equation 5 can be viewed as an improved management plan in which deliveries are incrementally changed to reflect the magnitude of drought. Although current management practices may fall short of this

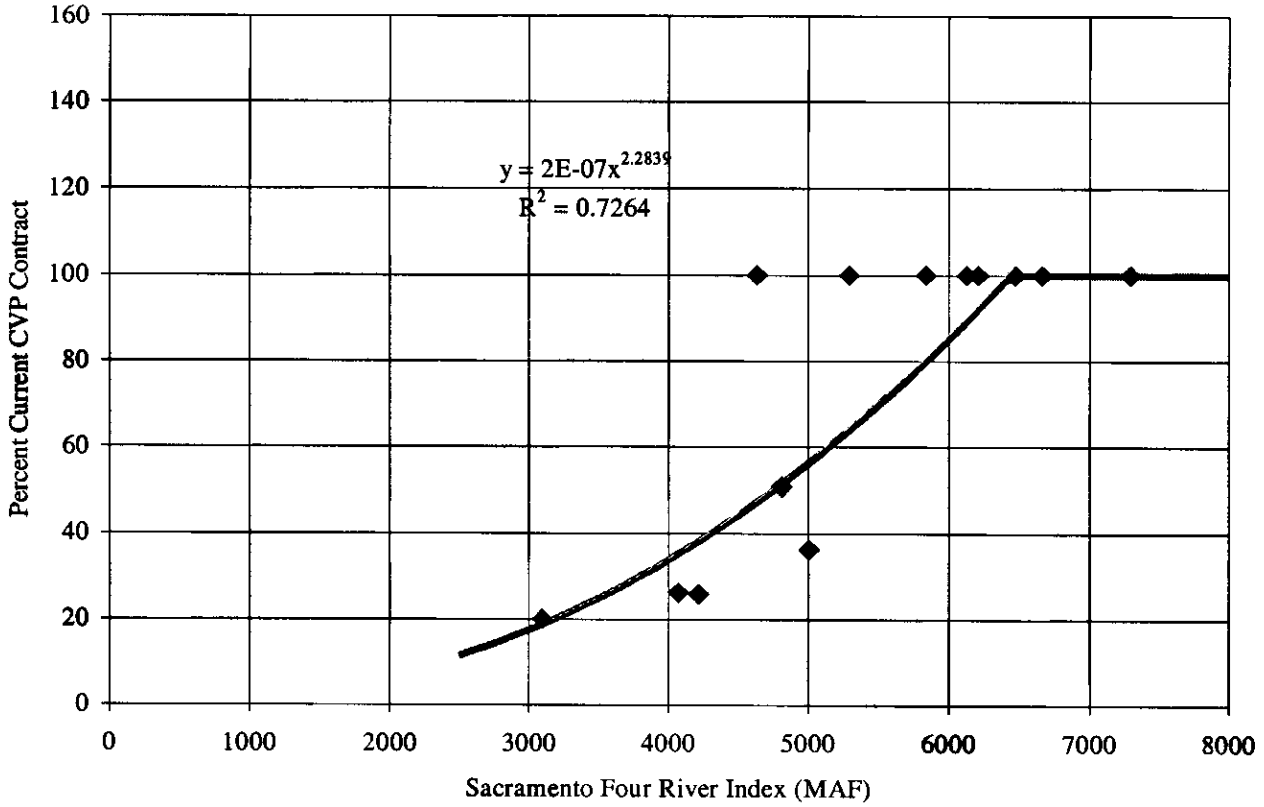

Figure 35 - Best Fit Delivery Rates for "Below Average," "Dry," and "Critical" Water Years.

goal, Equation 5 may better represent future trends as decision-making tools become more sophisticated.

Historical records of the SFRI are available from 1906 to present. Although this is still not enough data to provide any strong conclusion regarding the statistical distribution of the population, there are enought samples to generate future scenarios using the bootstrap method. The bootstrap method is based on the assumption that a sample set adequately represents the entire population and that new scenarios can be generated by sampling with replacement from the original set. The major restriction of this method is that alll sample points must be independent. Although the SFRI has an obvious one-year lag dependency, the yearly unimpaired runoff reveals no statistically significant temporal correlation. Thus, the bootstrap method may be used to generate unimpaired runoff scenarios. Sampling from the original set using randomly generated uniform deviates produces potential runoff scenarios. Each thirty-year realization represents an equally likely runoff scenario for the forecast period, 1999-2028. Each runoff scenario is then transformed to an SFRI scenario using the 40-30-30 procedure outlined earlier.

The severity of a drought forecast can be measured in several ways. Two such ways suggested by Shen and Tabios (1996) are average drought severity and cumulative deficit. Average drought severity averages the shortfall for all "drought years" occurring in the forecast, a drought year being defined as any year in which less than 100 percent of the CVP contract water is available. This criterion identifies forecasts with severe drought

events but does not consider the number of drought events. Conversely, cumulative deficit sums the shortfall for all years that fall below the critical level, giving increased weight to forecasts with additional years of drought. The disadvantage of this criterion is that forecasts with many years of minor drought are indistinguishable from forecasts with fewer years of severe drought.

Figures 36 and 37 show the cumulative distribution functions for the average drought and cumulative deficit criteria, respectively. The distribution functions were created using the drought measurements of five hundred scenarios generated using the bootstrap method. Because both criteria have advantages, a drought scenario with a five percent probability of exceedance for both categories is considered. Table 4 summarizes the SFRI for the selected scenario.

4.2 Potential Management Alternatives

The first alternative examined in this report (Alternative A) is the current best-fit relationship between surface water delivery rates and SFRI found in Figure 35. In essence, this alternative represents maintaining current management practices. For reasons given previously (Section 2.1), however, it is probably unreasonable to expect current surface water supplies will remain undiminished. Two additional alternatives are examined that reduce the region's total surface water use.

Belitz and Phillips (1995) proposed a management that involved increased groundwater pumping and reduced recharge. Although the original goal of this management plan was to reduce drainage problems in the region (see section 2.3.1), it also reduces the region's surface water use. A slightly modified version of their proposal is considered as

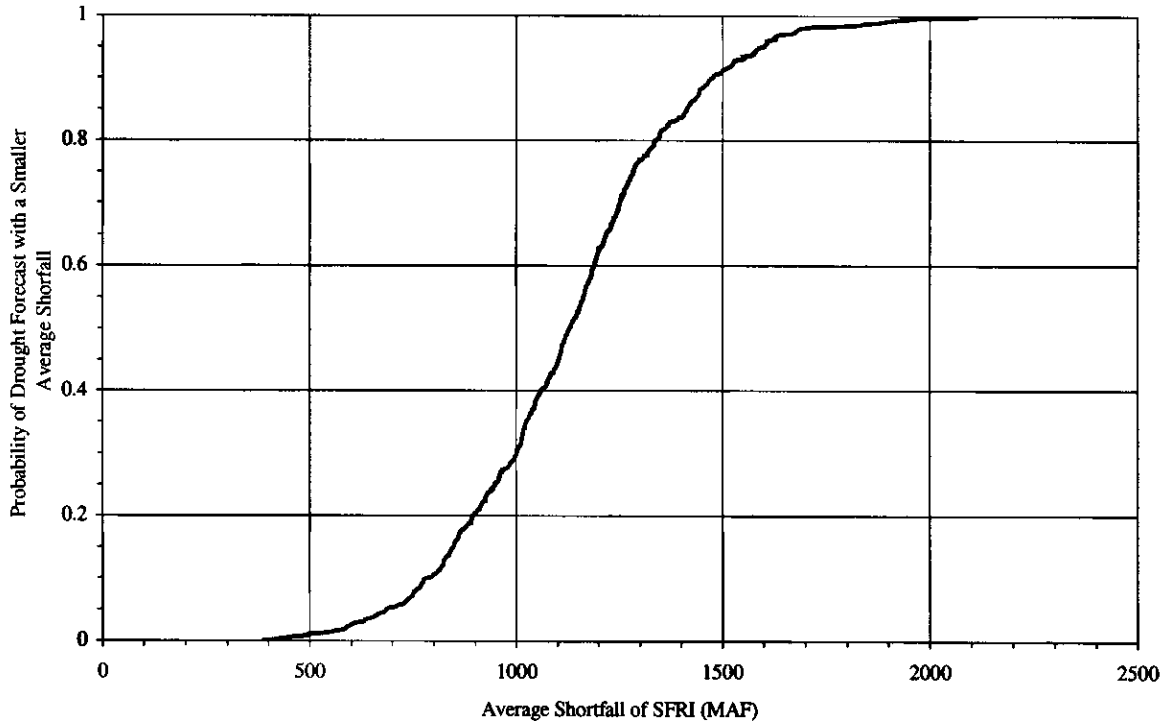

Figure 36 - Distribution Function of Average Shortfall.

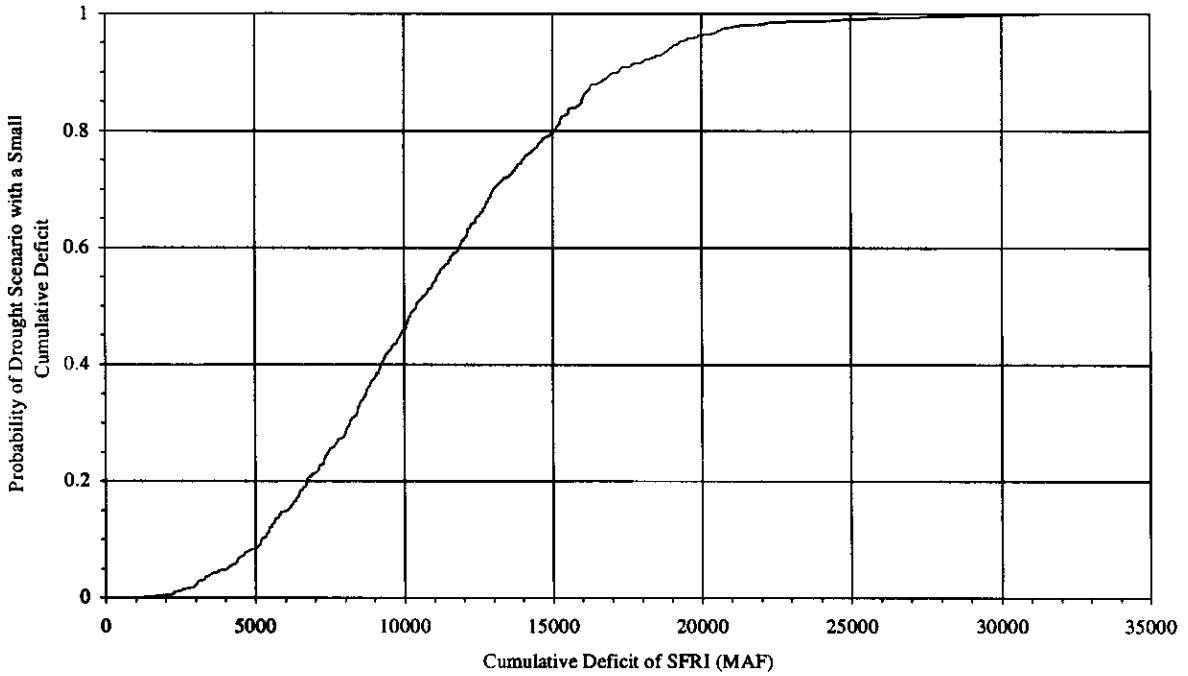

Figure 37 - Distribution Function of Cumulative Deficit.

Alternative B and is summarized by the water budget given in Table 5. It is assumed that the relationship between the percent CVP delivery rates and the SFRI remains the same as in Alternative A (see Figure 38). but that the contract delivery rate for each subarea is reduced to the rate proposed in the Belitz and Phillips (1995) water budget (Table 5). During normal water years, Alternative B would reduce the surface water required buy the study area by 214,000 acre-feet during normal water years with decreasing reductions during drought years.

Alternative C also reduces surface water demand, not by reducing the total amount of contracted surface water, but by changing the relationship between the percent delivery rates and the SFRI. By increasing the SFRI required to result in a 100 percent CVP delivery rate, Alternative C reduces the surface water used during drought years even more than the reduced deliveries of Alternative A (see Figure 38). During wet years there is no reduction in total surface water use. During drier years, however, surface water use is reduced to between 80 and 85 percent of Alternative A. This would reduce the levels of surface water required in Alternative A by up to 153,000 acre-feet (at SFRI = 6400) during years of drought. The major limitation of this alternative is that it does not address the dainage and water quality problems facing the region. Although it is beyond the scope of this report, any management scheme ultimately implemented in the region must address both the subsidence and drainage problems facing the region.

Table 6 presents parital water budgets for each of the alternatives during a normal water year (SFRI > 7000 MAF) and a sample drought year (SFRI = 4600 MAF). For all three alternatives, a drought of this severity results in applied water being reduced to 76% of normal levels. CVP surface water levels are reduced to 46% of normal levels for

Table 4 - Future Water Delivery Scenario

Year	SFRI (MAF)	CVP Delivery Rate	CVP Delivery Rate Alternative C
1999	5,806	79%	64.7%
2000	4,325	40.3%	33.4%
2001	4,599	46.4%	38.3%
2002	9,363	100%	100%
2003	9,023	100%	100%
2004	7,084	100%	100%
2005	9,776	100%	100%
2006	5,379	66.3%	54.5%
2007	5,984	84.6%	69.3%
2008	4,241	38.5%	31.9%
2009	3,958	32.9%	27.3%
2010	10,129	100%	100%
2011	9,768	100%	100%
2012	8,686	100%	100%
2013	5,455	68.5%	56.3%
2014	9,909	100%	100%
2015	4,727	49.5%	40.8%
2016	7,971	100%	100%
2017	6,725	100%	90.1%
2018	11,795	100%	100%
2019	4,754	50.0%	41.3%
2020	5,381	66.4%	54.6%
2021	3,368	22.8%	19.0%
2022	9,000	100%	100%
2023	13,262	100%	100%
2024	6,754	100%	91.0%
2025	10,257	100%	100%
2026	7,162	100%	100%
2027	6,526	100%	84.2%
2028	7,615	100%	100%

Average Shortfall (Percentile) = 1607.4 (95.6%)
Cumulative Drought (Percentile) = 19,290 (95.2%)

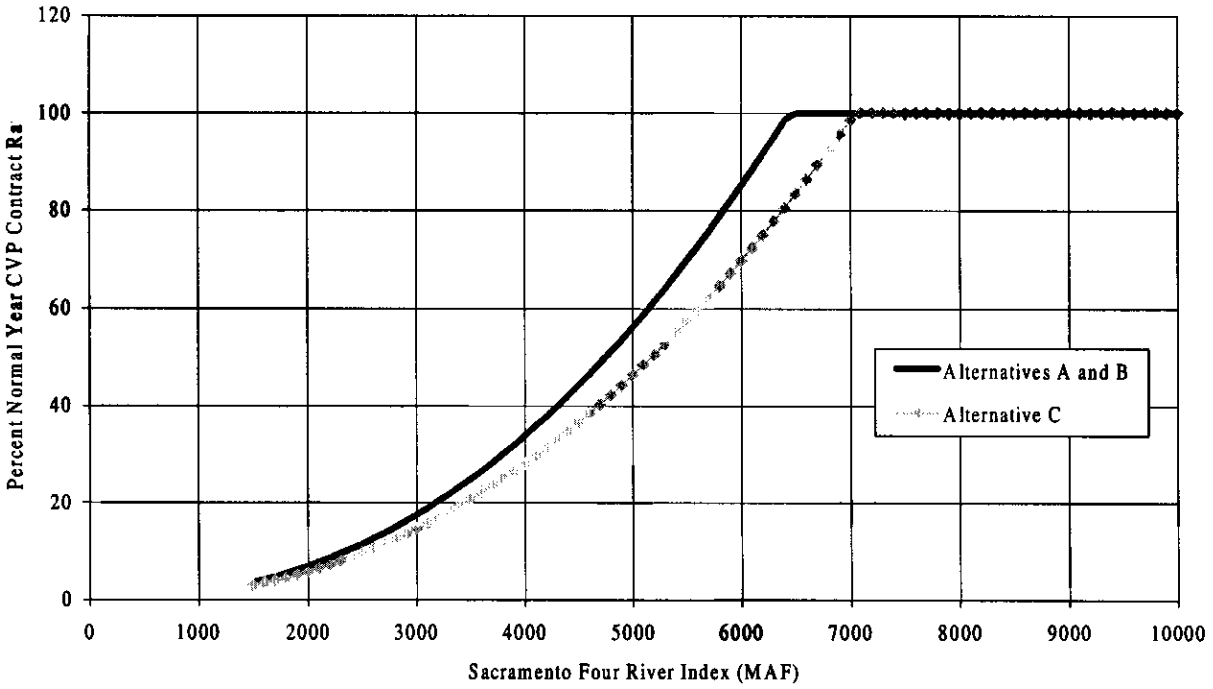

Figure 38 - Management Alternatives.

Table 5 - Alternative B Proposed Water Budget From Belitz and Phillips, 1995

Subarea	Area (mi^2)	Surface Water Delivery (ft/yr)	Groundwater Pumpage (ft/yr)	Groundwater Recharge (ft/yr)
Firebaugh	73	1.85	0.5	0.47
Panoche	48	1.58	0.5	0.56
Broadview	16	1.99	0.5	0.52
Tranquility	30	1.88	0.8	0.71
San Luis	30	1.24	0.9	0.67
Westlands				
Depth to Water<10 ft	97	133	0.9	0.39
10 ft< Depth to Water < 20 ft	42	1.58	0.96	0.63
Depth to Water > 20 ft				
with surface water	163	1.79	0.75	0.8
without surface water (1980)	30	1.23	1.23	0.86

Table 6 -- Comparison of Alternatives for Normal and Example Drought Years

Subarea	*Normal Water Year (SFRI>7000)* Total Applied Water (ft/yr)	Surface Water Delivery (ft/yr)	Groundwater Pumpage (ft/yr)	*Drought Year (SFRI=4600)* Total Applied Water (ft/yr)	Surface Water Delivery (ft/yr)	Groundwater Pumpage (ft/yr)
Alternative A						
Firebaugh	2.63	2.63	0.0	1.99	1.22	0.77
Panoche	2.48	2.48	0.0	1.88	1.15	0.73
Broadview	2.75	2.75	0.0	2.08	1.28	0.81
Tranquility	2.81	2.51	0.30	2.13	1.16	0.96
San Luis	2.26	1.86	0.40	1.71	0.86	0.85
WestLands						
Depth to Water < 10 ft.	2.68	2.43	0.25	2.03	1.13	0.90
10 ft< Depth to Water <20 ft.	2.65	2.19	0.46	2.01	1.02	0.99
Depth to Water > 20 ft.						
with surface water	2.68	2.43	0.25	2.03	1.13	0.90
without surface water (1980)	2.46	1.23	1.23	1.86	0.57	1.29
Alternative B						
Firebaugh	2.35	1.85	0.5	1.78	0.86	0.92
Panoche	2.08	1.58	0.5	1.58	0.73	0.84
Broadview	2.49	1.99	0.5	1.58	0.73	0.84
Tranquility	2.68	1.88	0.8	2.03	0.87	1.16
San Luis	2.14	1.24	0.9	1.62	0.58	1.05
WestLands						
Depth to Water < 10 ft.	2.23	1.33	0.9	1.69	0.62	1.07
10 ft< Depth to Water <20 ft.	2.54	1.58	0.96	1.92	0.73	1.19
Depth to Water > 20 ft.						
with surface water	2.54	1.79	0.75	1.92	0.83	1.09
without surface water (1980)	2.46	1.23	1.23	1.86	0.57	1.29
Alternative C						
Firebaugh	2.63	2.63	0.0	1.99	1.01	0.99
Panoche	2.48	2.48	0.0	1.88	0.95	0.93
Broadview	2.75	2.75	0.0	2.08	1.05	1.03
Tranquility	2.81	2.51	0.30	2.13	0.96	1.17
San Luis	2.81	2.51	0.30	2.13	0.96	1.17
WestLands						
Depth to Water < 10 ft.	2.30	1.9	0.40	1.74	0.73	1.01
10 ft< Depth to Water <20 ft.	2.65	2.19	0.46	2.01	0.84	1.17
Depth to Water > 20 ft.						
with surface water	2.68	2.43	0.25	2.03	0.93	1.10
without surface water (1980)	2.46	1.23	1.23	1.86	0.47	1.39

4.3 Optimization Model

A linear optimization model was formulated to find the maximum increase in ground water withdrawl without causing any inelastic compaction during the 30-year planning horizon. In order to eliminate the nonlinearity associated with subsidence, heads area allowed to fluctuate only within the region of elastic compaction. This is accomplished by setting the preconsolidation head as the lower bound for groundwater levels in the confined aquifer. For simplicity in computation and implementation, the optimization model assumes uniform pumping over each pumping subarea and heads are only monitored at one characteristic location in each subarea.

A response function approach (Gorelick, 1983; Yeh, 1992) is used in the model formulation. In this approach, the calibrated simulation model is used to generate response coefficients. The model is first allowed to reach a steady state under normal-year pumping conditions. Each pumping subarea is then separately subjected to a unit impulse of additional pumpage in the first period with no disturbance thereafter, and the system response to each excitation is monitored over the entire planning period. All the responses are then assembled in a response matrix. This response matrix can subsequently be used in the formulation of the following optimization model.

The objective function of the optimization model maximizes the total groundwater withdrawl at all production wells during the forecast period:

$$Max\ Z = \sum_{n=1}^{NTS} \sum_{k=1}^{NOW} Q(k,n) \qquad (6)$$

in which Z is the value of the objective function (L); Q(k,n) is volume of water withdrawn from the k^{th} well field (L^3/T); NTS is the total number of periods; NOW is the total number of well fields; and n is the time index.

The constraint set of the model includes the following conditions and specifications:

1. The projected additional ground water demand above the normal year demand, GWD(n), needs to be met:

$$\sum_{k=1}^{NOW} Q(k,n) \geq GWD(n) \qquad \forall n \qquad (7)$$

2. Ground water withdrawals are related to drawdowns through the response function coefficients:

$$s\ (l,n) = \sum_{i=1}^{NTS} \sum_{k=1}^{NOW} \beta(l,k,n-i+1) \cdot Q(k,\ i) \qquad \forall l,\ \forall n \qquad (8)$$

In which $s(l,n)$ is the drawdown at the l^{th} observation point; and $\beta(.)$ are the response coefficients.

3. Drawdown cannot exceed the maximum permissible drawdown (difference between the initial water level and the preconsolidation head level), and minimum and maximum pumpage rates at the production wells need to be satisfied:

$$s(l,n) \le s_{MAX}(l) \qquad \forall n \qquad (9)$$

$$Q_{MIN}(k) \le Q(k,n) \le Q_{MAX}(k) \qquad \forall n \qquad (10)$$

Maximum pumpage rates are set at 1.3 ft/year for all subareas. This bound was chosen to both limit the amount of pumping from any one subarea and to reflect number of existing wells.

The total area and maximum allowable drawdown for each water budget subarea are given in Table 7. Two different sets of maximum allowable drawdown are used in the optimization model in wet and dry periods. The maximum allowable drawdown in wet years corresponds to the preconsolidation head in the bottom sub-layer of the clay interbed unit. This is the maximum preconsolidation head for any compressible layer. Because of the low conductivity of the clay layer, however, piezometric head levels in the confined aquifer may drop below this value for short periods without causing inelastic subsidence. To take advantage of this additional capacity, the maximum allowable drawdown during dry years corresponds to the preconsolidation head in the outermost layer of the clay interbed unit. This adjustment provides for additional drawdown during periods of drought, but sustains long-term head levels above all values of preconsolidation head.

The calibrated MODFLOW (McDonald and Harbough, 1992) model was used to derive the response coefficients. The optimization model formulated above is a linear programming model and was solved using GAMS (Brook et al., 1992). The pumping rates calculated by the optimization model were then returned to the simulation model to estimate land subsidence.

Table 7 -- Maximum Drawdown and Areas for Pumping Subareas

	Water Budget Subareas								
	1	6	8	9	10	11a	11b	11c	11d
S_{max}-dry (feet)	141.6	124.8	152.8	172.5	225.2	153.1	168.1	195.3	269.7
S_{max}-wet (feet)	95.9	8.34	97.5	109.6	175.8	98.8	105.4	116.9	214.2
Area (mi^2)	73	30	48	16	30	98	41	148	45

4.4 Results

Figures 39-44 present the model predictions of total subsidence for the years 1999 to 2028 at the six extensometer locations used for calibration. Contour maps of land subsidence across the entire study area are shown as Figures 45-47.

Alternative A causes very little subsidence. Although there is some elastic subsidence during years of drought, the overall trend is toward rebound. Alternative B causes significant subsidence, especially in the northwest corner of the model. At extensometers 13/12-20D1, 15/13-11D2, and 16/15-34N1, subsidence occurs predominantly during periods of drought. At the other extensometer locations, subsidence continues during normal water years as well. Alternative C produces subsidence similar to that of Alternative A. In general, the compaction is elastic and long-term subsidence is minimal. A small increase in inelastic compaction during periods of drought accounts for the difference between the two alternatives. The optimization results produce subsidence similar to that of Alternatives A and C. The only major difference is a period of little change during the final seven years while Alternatives A and C show significant rebound.

The maximum ground water withdrawal for each water budget subarea found in the optimization model is shown in Figure 48. Ground water withdrawal can be significantly increased without causing any inelastic compaction in Subareas 1 (Firebaugh) and 6 (Tranquillity). These subareas are located along the river in the eastern side of the basin. In contrast, withdrawals cannot be increased above the minimum required rate over the next two decades without leading to inelastic subsidence in Subareas 10 and 11 along the no-flow boundary to the west. Ground water supplies are intensely operated in almost all of the subareas during the last years of the future scenario. This is the result of one of the major assumptions of the optimization model. Since the optimization model has perfect foresight, following the final drought period it must no longer plan for future drought and can increase pumping until ground water levels reach the point of maximum drawdown. In general, from the standpoint of land subsidence, there is greater potential for increased withdrawal of ground water supplies on the eastern side of the basin than on the western side. Because, the eastern side is bounded by a running water which acts like a permanent water supply to the nearby ground water overdraft areas, whereas the western side is bounded by no-flow zone.

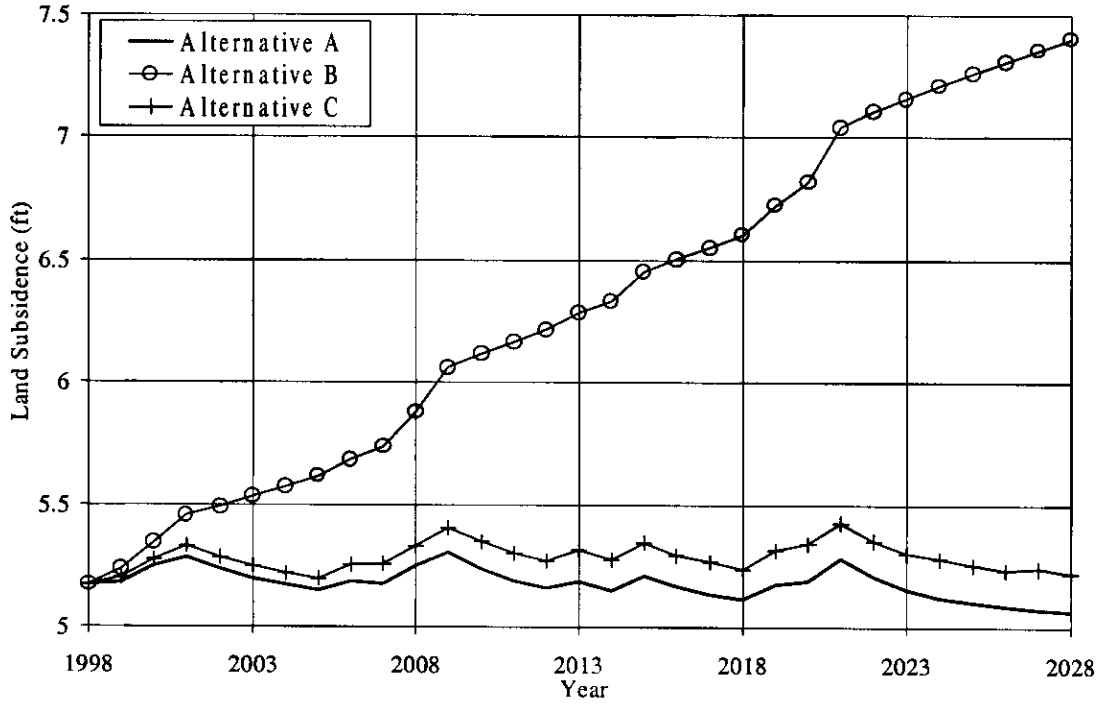

Figure 39 -- Model Predictions of Total Subsidence for 1999-2028 at Extensometer 1.

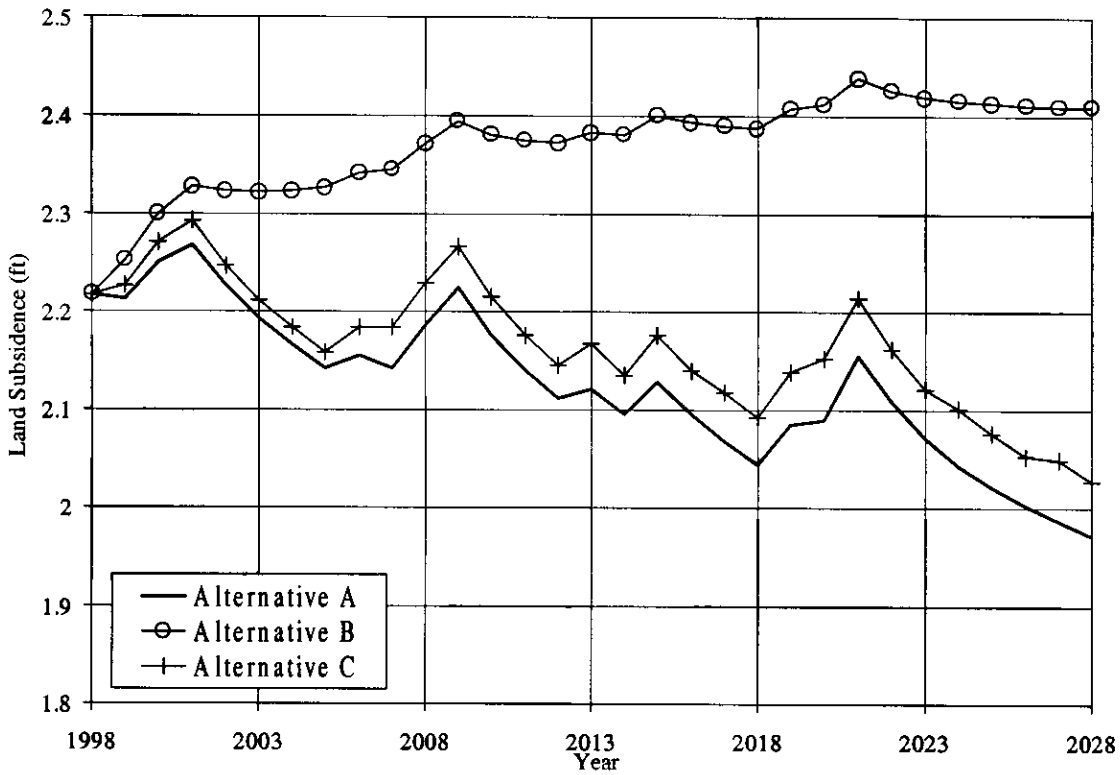

Figure 40 -- Model Predictions of Total Subsidence for 1999-2028 at Extensometer 2.

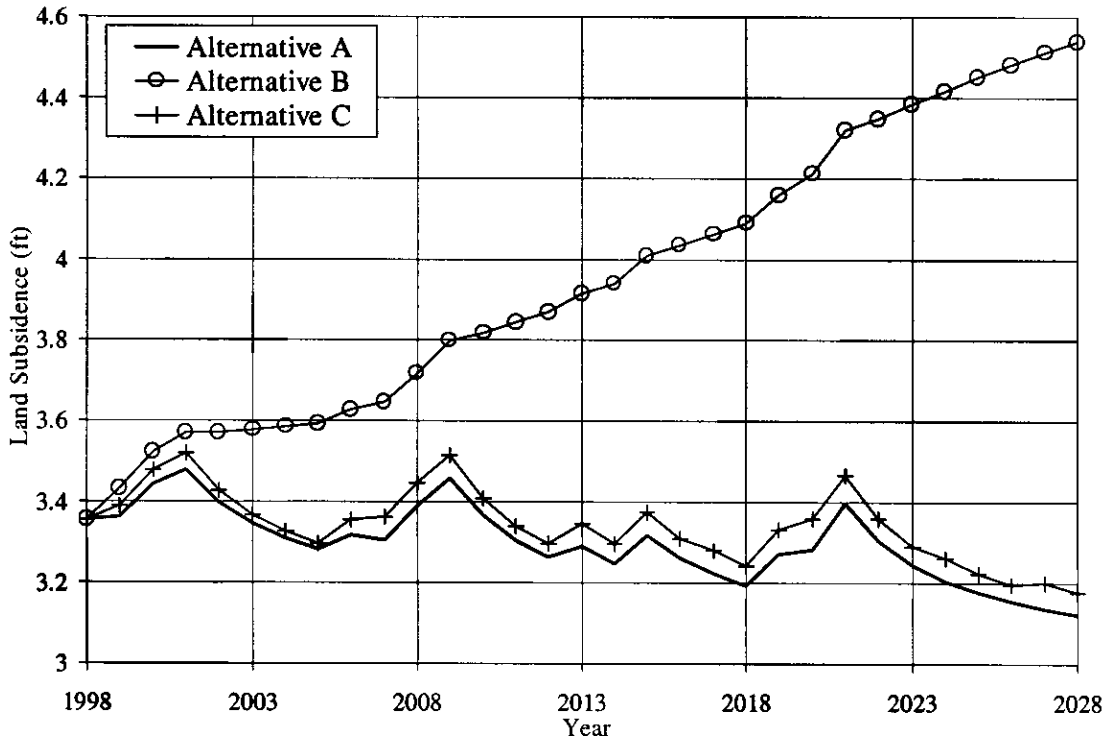

Figure 41 -- Model Predictions of Total Subsidence for 1999-2028 at Extensometer 3.

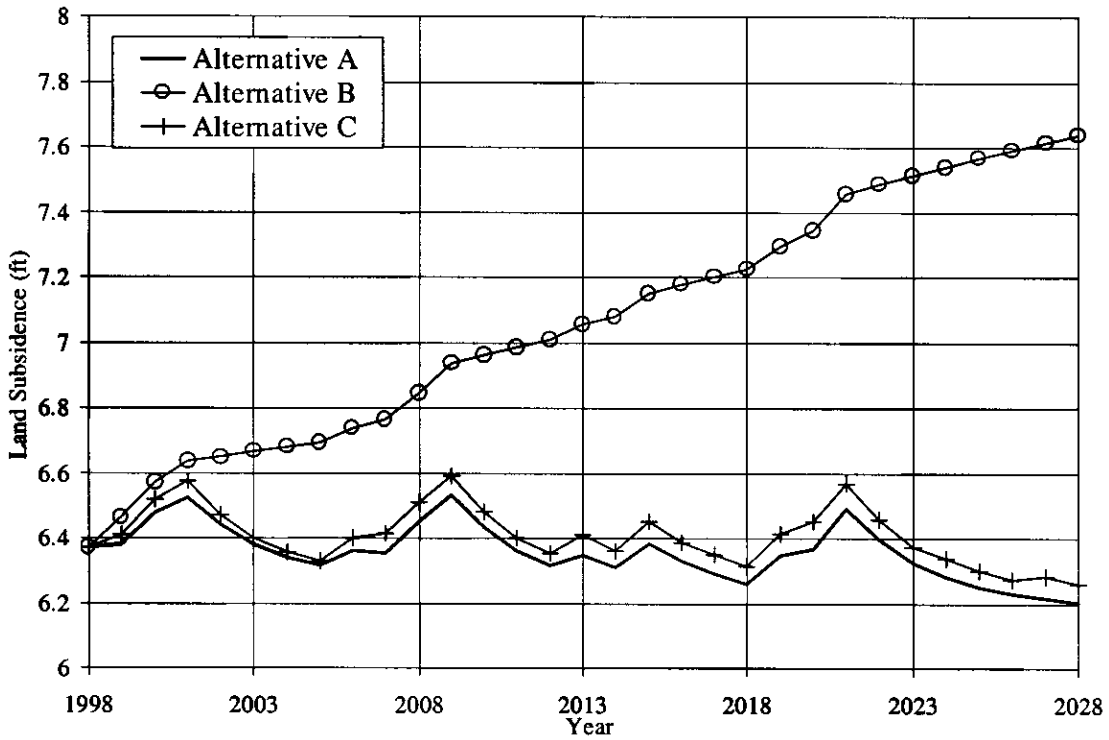

Figure 42 -- Model Predictions of Total Subsidence for 1999-2028 at Extensometer 4.

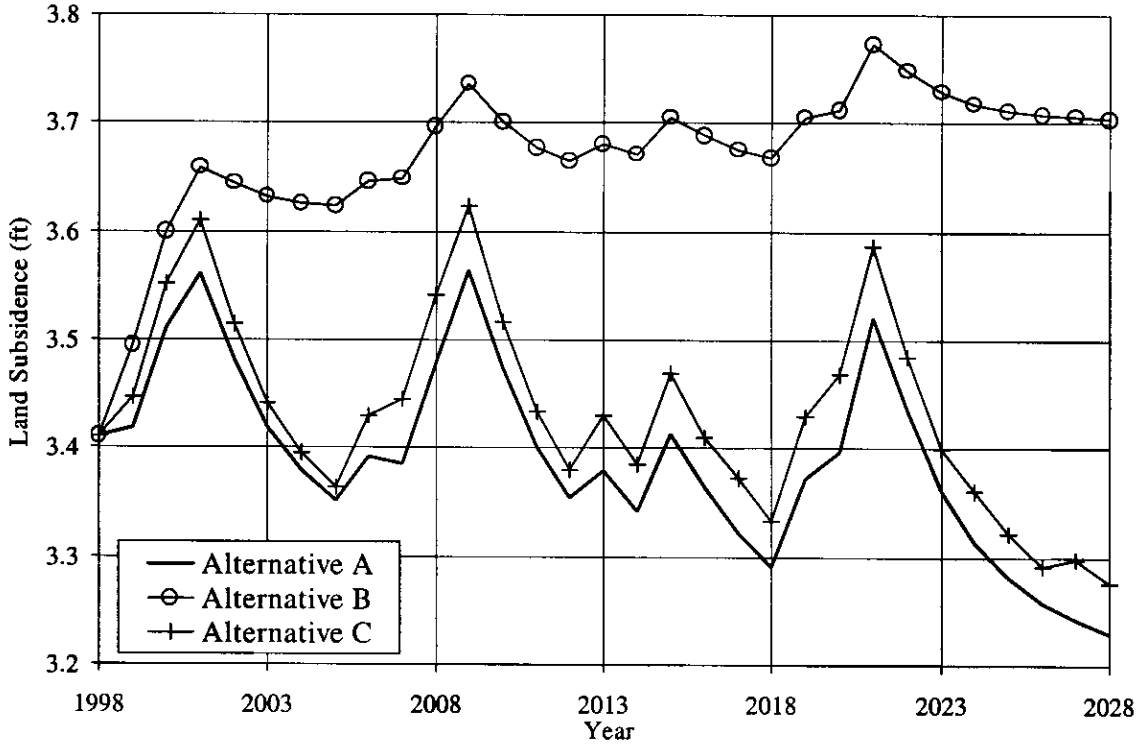

Figure 43 -- Model Predictions of Total Subsidence for 1999-2028 at Extensometer 5.

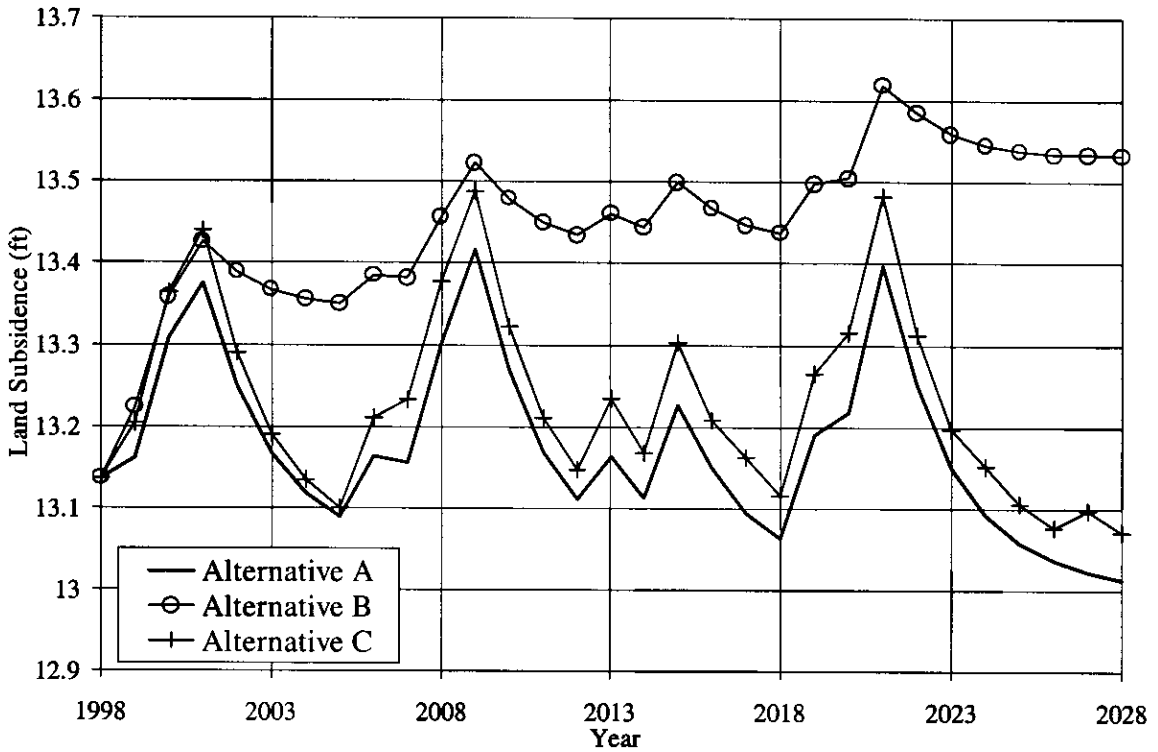

Figure 44 -- Model Predictions of Total Subsidence for 1999-2028 at Extensometer 6.

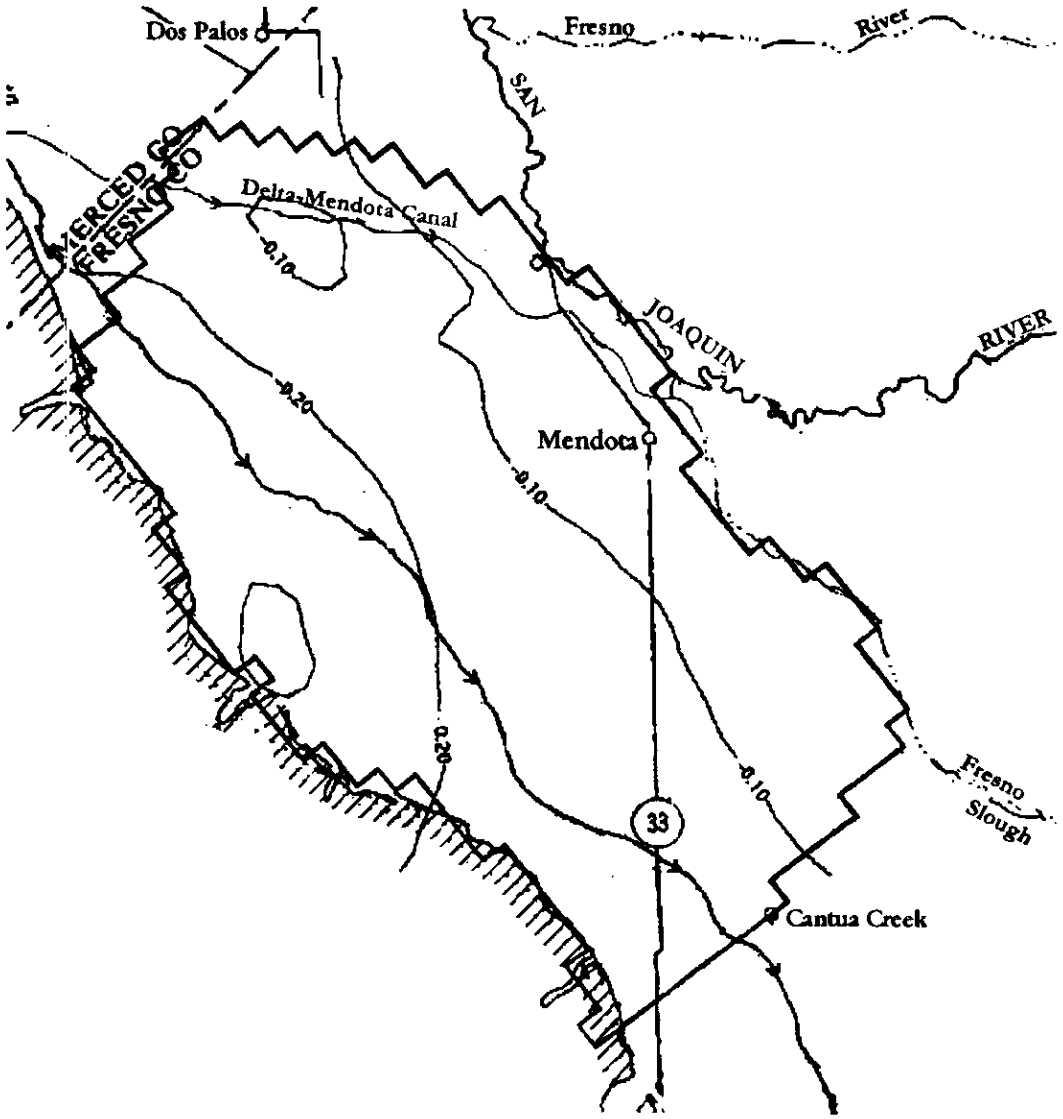

Figure 45 -- Simulated Subsidence (in feet), 1999-2028 (Alternative A).

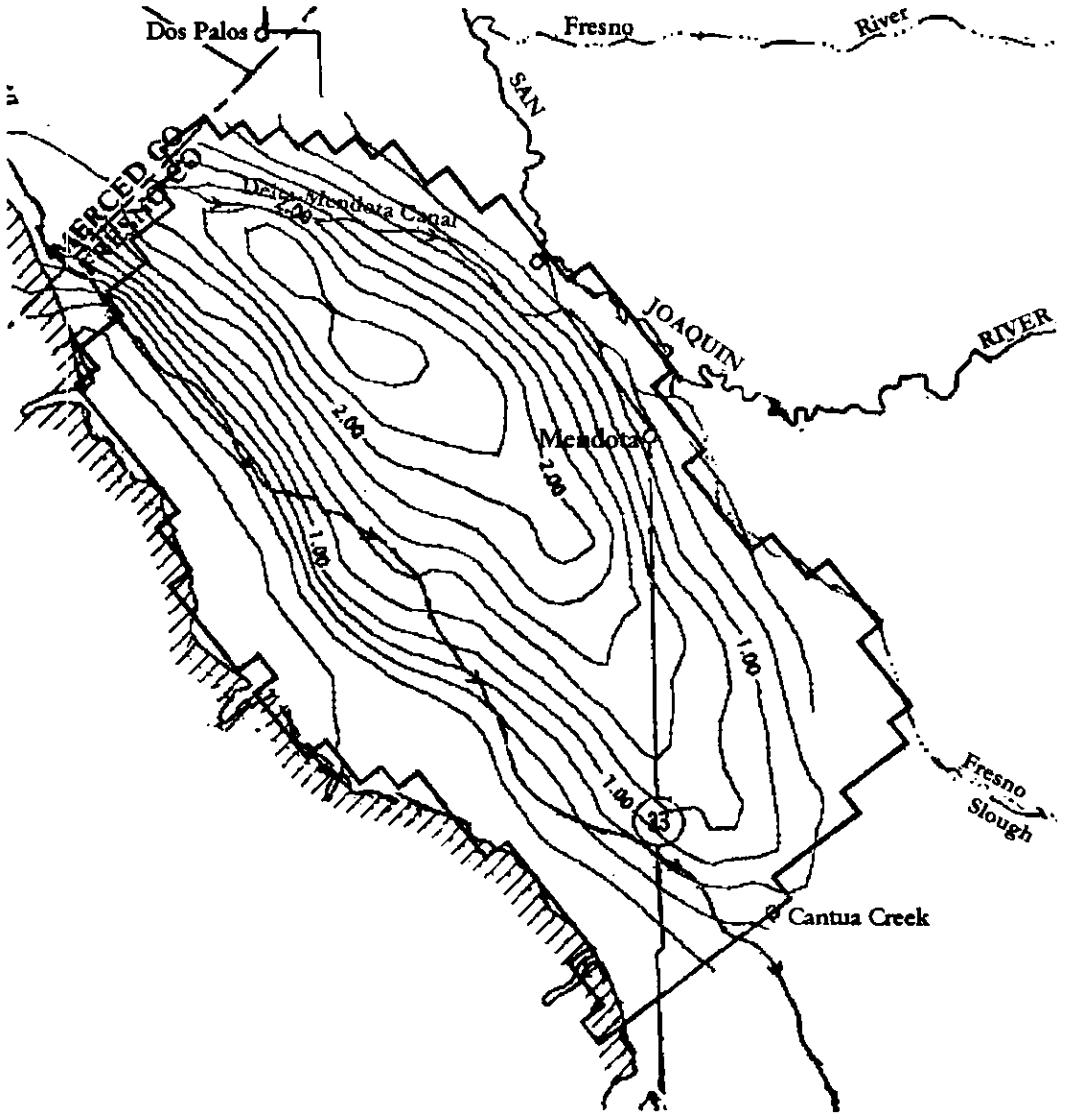

Figure 46 – Simulated Subsidence (in feet), 1999-2028 (Alternative B).

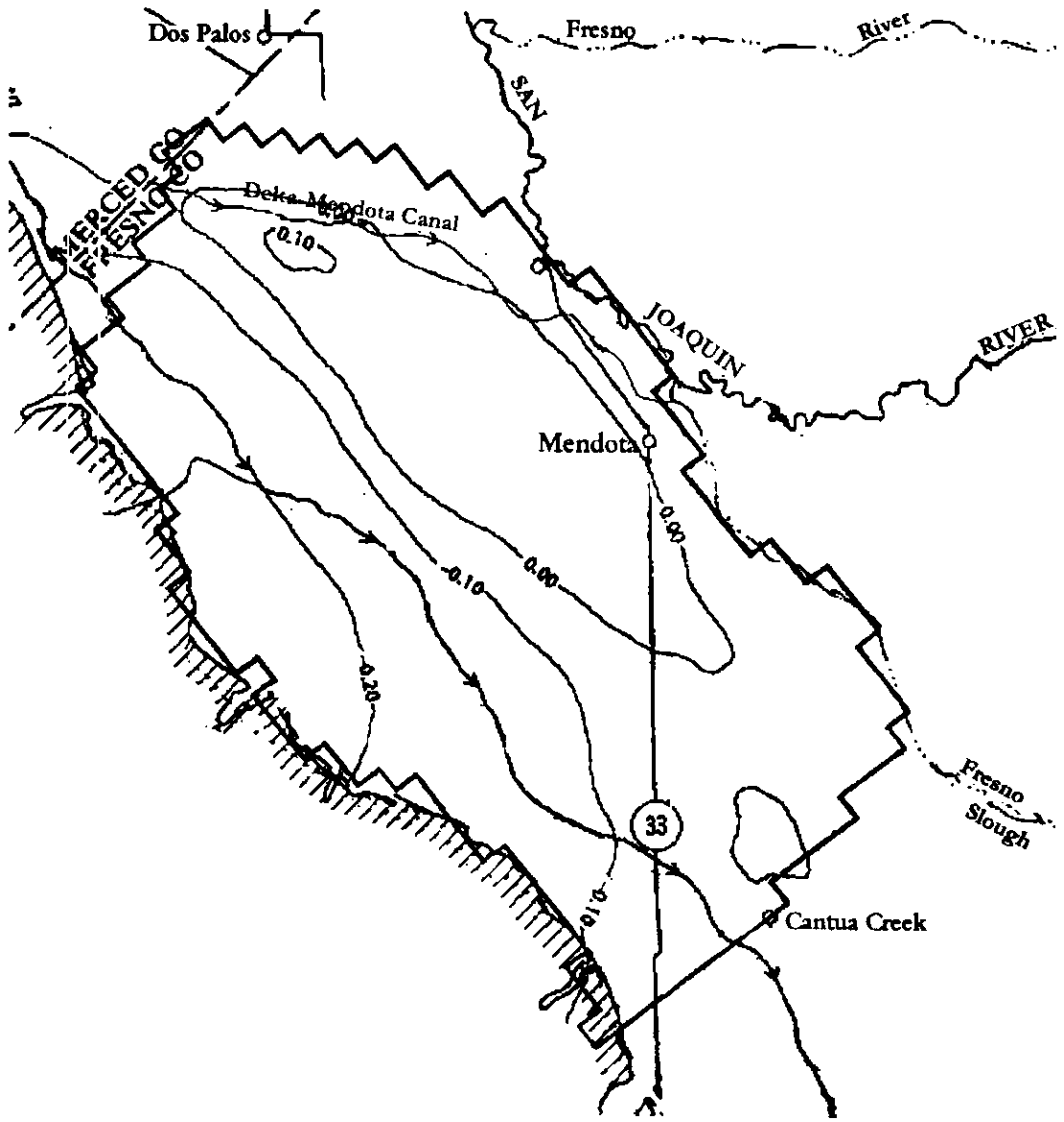

Figure 47 -- Simulated Subsidence (in feet), 1999-2028 (Alternative C).

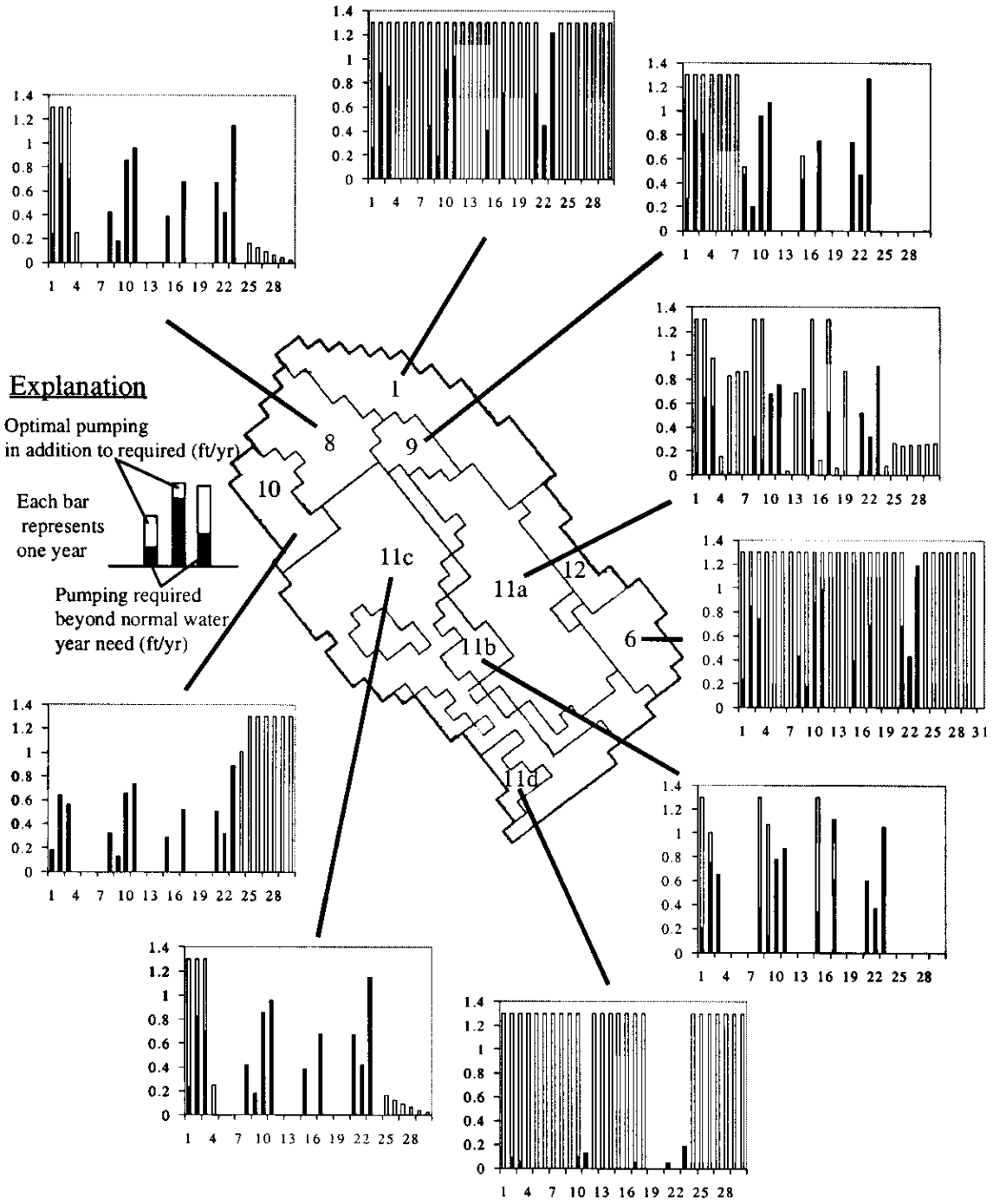

Figure 48 -- Maximum Groundwater Withdrawl from Optimization Model.

5. CONCLUSIONS AND RECOMMENDATIONS

For the foreseeable future, land subsidence will remain a concern for water managers in the San Joaquin Valley. To avoid the costly and serious damage associated with land subsidence, it is vital to consider the effects of all proposed water use alternatives. The groundwater-subsidence model presented herein provides a method for evaluating each alternative.

The success of a model is mainly measured by its ability to reproduce observed data. Although it cannot represent the complex ground water system in its entirety, the Los Banos-Kettleman City model is a simplified conceptual model that successfully matches observed head and subsidence values on an annual time scale. Because of the limited amount of data available and the corresponding large number of calibration variables, however, it is possible that other model parameters could produce equally appropriate matches to the observed data. Although it is probably not unique, the current calibrated model appears to be useful for the evaluation of future water management alternatives.

If present practices can be sustained for the Los Banos-Kettleman City area, the model indicates that land subsidence will not be a serious problem in the next thirty years. Although head levels are significantly reduced and some elastic compaction does occur during periods of drought, there is enough storage in the underlying aquifers to prevent most unrecoverable subsidence. However, with the continued growth of urban populations to the south and increased restrictions on water exportation from the north, current practices may not be sustainable.

The alternative water budget proposed by Belitz and Phillips (1995) achieves a reduction in surface water dependency by increasing irrigation efficiency and groundwater pumping. This proposal is also meritorious for its positive effect on drainage problems in the region. Unfortunately, this alternative produces significant inelastic compaction during the future scenario considered in this report.

There are two possible reasons the Belitz and Phillips report (1995) did not recognize the proposed water budget's potential for subsidence. First, in their analysis, subsidence was assumed to occur only when the piezometric head in the confined aquifer falls below its historic minimum. This neglects the presence of residual pore pressure, which will cause inelastic compaction to begin at heads much greater than the past aquifer minimum. Second, in the water budget used by Belitz and Phillips (1995), the surface water delivery rate was assumed to be constant for the next 45 years. Much of the predicted subsidence would be eliminated using the same assumption for our model. The proposed water budget lowers head values just enough, however, that when drought years are included, there is not enough storage to prevent subsidence from occurring. Hence, the frequency of drought has an immense importance in such analysis.

The final alternative examined was a shift in the relationship between available surface water (SFRI) and the amount of CVP water used in the region. Like Alternative A, this alternative limits subsidence to a significantly reduced rate. Although it does not reduce the surface water required during wet years, it does reduce the area's dependence on surface water during years of drought. This or any other alternative that involves an increase in pumping is potentially limited by water quality problems (e.g., TDS, salinity).

Although the modest increases in pumping included here are probably acceptable (Belitz and Phillips, 1995), additional work would be required to determine the long-term impact of such changes on water quality.

A linear optimization model was constructed to predict the maximum potential groundwater pumpage from each subarea above the predicted water demands for the next 30 years. Although perfect foresight limits the implementation of the optimization model in practice, the model indicates that groundwater supplies of certain subareas in the eastern portion of the study area can be operated far above the target demand rates without leading to inelastic compaction. In contrast, little increase in groundwater withdrawal is possible for subareas on the western side due to their proximity to running waters, which act as permanent water supplies to the nearby ground water withdrawal areas.

There are at least four areas in which further work could improve the quality of the model. First, the thickness of the layer representing the interbeds was assumed to be uniform across the study area. Additional field data regarding the composition of the confined aquifer may allow for a better estimation of the spatial distribution of interbed thickness. Stratigraphic data in combination with additional computational capacity may also allow for the replacement of the fictional interbed layer with modeling layers more closely representing the physical system. A second improvement could be achieved by considering smaller stress periods. Some detail is lost as pumping is averaged over the entire year. A seasonal or monthly model may capture more accurately the groundwater fluctuations leading to subsidence. Third, the time delay of consolidation was adequately captured using the IBS1 package (Leake, 1991) by sub-dividing the compressible layers. However, equally valid and numerically more efficient results may also be attainable using a package which analytically considers time delay, such as the IDP package (Shearer and Kitching, 1994). Finally, this report has used land subsidence as its only criteria for evaluating management alternatives. Since any management scheme implemented in the region must address both the subsidence and drainage problems facing the region, a composite model is needed to consider both of these important issues.

REFERENCES

American Farmland Trust. 1995. *Alternatives for Future Urban Growth in California's Central Valley: The Bottom Line for Agriculture and Taxpayers.* Washington, D. C., U.S.A.

Belitz, K., and Heimes, F.J. 1990. *Character and evolution of the ground water flow system in the central part of the western San Joaquin Valley, California.* U.S. Geological Survey Water-Supply Paper 2348: 28p.

Belitz, Kenneth, Phillips, S. P., and Gronberg, J. M. 1992. *Numerical Simulation of Ground-Water Flow in the Central Part of the Western San Joaquin Valley, California.* U. S. Geological Survey Open-File Report 91-535: 71 p.

Belitz, Kenneth and Phillips, Steven P. 1995. *Alternatives to Agricultural Drains in California's San Joaquin Valley: Results of a Regional-Scale Hydrogeologic Approach.* U. S. Geological Survey Open-File Report 91-535: 71 p.

Bull, W. B., and Miller, R. E. 1975. *Land subsidence due to ground water withdrawal in the Los-Banos Kettleman City area, California. Part 1, Changes in the hydrologic environment conducive to subsidence.* U.S. Geological Survey Professional Paper 437-E: 71p.

Bumb, A. C., Mitchell, J. l., and Gifford, S. K. 1997. Design of a ground-water extraction/re-injection system at a superfund site using MODFLOW. *Ground Water* 35(3):400–408.

California Department of Water Resources. 1998. *Compaction Recorded by Extensometer-Wells Since 1984 in the West San Joaquin Valley, California.* Sacramento, California.

California Department of Water Resources. 1999. *California Water Plan Update,* Bulletin 160-98, v. 1

Casagrande, A. 1932. The Structure of Clay and its Importance in Foundation Engineering, *Journal of the Boston Society of Civil Engineers,* April; reprinted in *Contributions to Soil Mechanics 1925-1940,* BSCE:72-113

De Marsily, Ghislain. 1986. *Quantitative Hydrogeology – Groundwater Hydrology for Engineers.* Academic Press, San Diego California: 440 p.

Gronberg, J. M. and Belitz, Kenneth. 1992. *Estimation of a Water Budget for for the Central Part of the Western San Joaquin Valley, California.* U. S. Geological Survey Water-Resources Investigation Report 91-4192: 22 p.

Holtz, Robert D. and Kovacs, William D. 1981. *An Introduction to Geotechnical Engineering.* Prentice Hall, Englewood Cliffs, New Jersey: 733 p.

Holzer, T. L. 1989. State and Local Response to Damaging Land Subsidence in United States Urban Areas. *Engineering Geology* 27:449-466.

Hua, Z., Tiezhu, L., and Xinhong, L. 1993. Economic benefit risk assessment of land subsidence in Shanhai. *Environmental Geology* 21:208-211.

Hubbell, J. M., Bishop, C. W., Johnson, G. S., and Lucas, J. G. 1997. Numerical groundwater flow modeling of Snake river plain aquifer using superpostion technique. *Ground Water* 35(1):59-66.

Ireland, R. L., Poland, J. F. and Riley, F. S. 1984. *Land Subsidence in the San Joaquin Valley, California, as of 1980.* U. S. Geological Survey Professional Paper 437-I: 93p.

Ireland, R. L. 1986. *Land subsidence in the San Joaquin Valley, California, as of 1983.* Prepared in cooperation with the California Department of Water Resources, Sacramento, California. U.S. Geological Survey, Denver, CO: 50 p.

Irrigation Training and Research Center, California Polytechnic State University. 1994. *Grassland Basin Irrigation and Drainage Study.* Prepared for the California Regional Water Quality Control Board – Central Valley Region, contract # 1-078-150-1. San Luis Obispo, California

Johnson, A. I., Moston, R. P., and Dorris, D. A. 1968. *Physical and hydrologic properties of water-bearing materials in subsiding areas in the central California.* U.S. Geological Survey Professional Paper 497-A: 71p.

Laudon, J., and Belitz, K. 1991. Texture and depositional history of Late Pleistocene-Holocene alluvium in the central part of the western San Joaquin Valley, California. *Bulletin of the Association of Engineering Geologist* 28(1):73-88.

Leake, S. A. 1990. Interbed storage changes and compaction in models of regional ground water flow. *Water Resources Research* 26:1939-1950.

Leake, S. A., and Prudic, D. E. 1991a. *Documentation of a computer program to simulate aquifer-system compaction using the modular finite-difference ground water flow model.* U.S. Geological Survey Techniques of Water Resources Investigation, Book 6, Chapter A2: 68 p.

Leake, S. A. 1991b. Simulation of vertical compaction in models of regional groundwater flow. pp. 565-574. In: *Proceedings of the fourth international symposium on land subsidence, May 1991.* IAHS Publication no. 200.

Lofgren, B. E. 1979. Changes in Aquifer-system Properties with Ground Water Depletion. pp. 26-46. In: *Procedings, International Conference on Evaluation and Prediction of Land Subsidence, Pensacola, December 1978.* American Society of Civil Engineers.

McDonald, M. G., and Harbaugh, A. W. 1988. *A modular three-dimensional finite-difference ground-water flow model.* U. S. Geological Survey Techniques of Water Resources Investigations, Book 6, Chapter A1: 586 p.

Miller, R. E., Green, J. E., and Davis, G. H. 1971. *Geology of the compacting deposits in the Los Banos-Kettleman City Area, California.* U.S. Geological Survey Professional Paper 497-E: 46p.

Onta, P. R., and Gupta, A. D. 1995. Regional management modeling of a complex ground water system for land subsidence control. *Water Resources Management* 9:1-25.

Page, R. W. 1986. *Geology of the fresh ground water basin of the Central Valley, California, with texture maps and sections.* U.S. Geological Survey Professional Paper 1401-C: 54p.

Phillips, Steven P. and Belitz, Kenneth. 1991. Calibration of a Texture-Based Model of a Ground-Water Flow System, Western San Joaquin Valley, California. *Ground Water* 29(5):702-715

Poland, J.F., Lofgren, B.E., Ireland, R.L., and Pugh, R.G. 1975. *Land Subsidence in the San Joaquin Valley, California, as of 1972.* U.S.G.S. Professional Paper #437-H. U.S. Government Printing Office, Washington D.C., U.S.A.

Poland, J. F. 1981. *The Occurrence and Control of Land Subsidence Due to Ground-Water Withdrawal with Special Reference to the San Joaquin and Santa Clara Valleys, California.* Ph.D.–Dissertation, Stanford University, Palo Alto, California

Reynolds, J. W., and Spruill, R. K. 1995. Ground-water simulation for management of a regulated aquifer system: A Case study in the North Carolina Coastal Plain. *Ground Water* 33(5):741-758.

Shearer, T. R., and Kitching, R. 1994. *A numerical model of land subsidence caused by ground water abstraction at Hangu in the peoples of republic of China.* British Geological Survey, Technical report WC/94/46

Shen, H. W. and Tabios, G. Q. 1996. *Modeling of Precipitation-Based Drought Characteristics Over California.* Technical Completion Report. Water Resources Center, Contribution No. 204. Water Resources Center. University of California, Davis

Terzaghi, K. 1925. Principles of soil mechanics: IV Settlement and consolidation of clay. In: Eng. News-Rec, McGraw-Hill, New York:874-878.

Westlands Water District. 1998. *Water Conservation Plan.* Fresno, California

Williamson, A. K., Prudic, D. E., and Swain, L. A. 1989. *Ground water flow in the Central Valley, California.* U.S. Geological Survey Professional Paper 1401-D: 127 p.

APPENDIX

	1	2	3	4	5	6	7	8	9	10	11	12	13	14	15	16	17	18	19	20
1	--	--	--	--	--	--	--	--	--	--	--	--	--	--	--	--	--	--	--	--
2	--	--	--	--	--	--	--	--	--	--	101	102	--	--	--	--	--	--	--	--
3	--	--	--	--	--	--	--	--	--	104	101	101	102	--	--	--	--	--	--	--
4	--	--	--	--	--	--	--	118	112	107	103	101	101	102	--	--	--	--	--	--
5	--	--	--	--	--	151	138	119	111	106	105	101	102	102	103	--	--	--	--	--
6	--	--	--	-18	152	150	128	115	108	105	104	102	102	102	103	104	--	--	--	--
7	--	--	-21	-19	160	149	119	107	103	100	102	102	101	102	103	104	105	--	--	--
8	--	--	-22	-21	145	142	114	101	96	94	97	99	101	101	103	104	105	--	--	--
9	--	--	-24	-23	135	128	110	98	93	90	92	97	99	101	102	104	105	106	--	--
10	--	--	-28	-27	121	109	102	97	94	91	93	97	99	100	102	103	105	106	--	--
11	--	--	-31	93	103	94	93	92	90	91	93	97	98	99	101	103	105	105	106	--
12	--	--	-36	89	92	84	82	82	80	84	89	95	97	98	100	102	104	105	106	--
13	--	-44	-42	72	79	70	71	72	71	76	83	90	93	96	98	101	103	105	106	--
14	--	-46	77	65	66	57	59	61	64	70	78	86	90	93	96	99	102	104	105	--
15	-51	-48	68	53	55	51	51	55	60	66	74	82	87	91	94	98	101	103	104	99
16	-53	101	72	61	49	44	48	51	57	63	71	78	84	88	92	95	99	102	103	101
17	-54	136	76	58	45	42	47	50	55	62	68	75	81	85	89	93	98	101	102	101
18	-55	95	58	40	36	40	45	49	54	60	65	73	78	83	87	91	96	100	102	98
19	--	66	18	6	26	36	43	48	54	58	64	70	76	80	85	89	95	98	101	97
20	-58	48	-11	-9	17	30	40	47	53	57	63	69	73	79	84	88	93	97	99	--
21	-57	28	-32	0	9	22	35	45	53	58	63	68	73	79	84	88	92	97	100	--
22	60	39	26	3	3	11	28	42	51	57	62	67	73	79	84	88	91	95	99	--
23	--	80	32	8	3	9	25	39	49	54	59	65	71	77	81	85	90	94	--	--
24	--	79	32	12	9	14	28	38	46	52	56	61	68	73	78	83	88	93	--	--
25	--	--	34	17	16	25	34	39	45	50	55	60	66	71	77	82	88	92	--	--
26	--	--	--	12	19	30	39	42	45	50	54	60	65	70	76	82	88	92	--	--
27	--	--	--	11	17	31	41	44	44	49	54	60	66	71	77	82	87	91	94	--
28	--	--	--	24	17	29	41	45	46	49	54	60	66	71	76	81	85	89	93	--
29	--	--	--	18	2	23	41	48	50	51	55	60	65	70	75	80	83	87	91	95
30	--	--	--	--	8	16	39	48	53	53	56	59	63	68	73	78	82	86	90	94
31	--	--	--	--	6	12	35	46	53	54	57	59	63	67	73	78	82	85	90	95
32	--	--	--	--	1	14	32	46	53	56	57	60	64	68	73	78	82	85	90	--
33	--	--	--	--	-13	18	38	47	54	58	59	62	66	69	74	78	81	82	84	--
34	--	--	--	--	-24	15	36	47	54	58	61	63	67	70	74	78	81	80	79	--
35	--	--	--	-5	-5	14	31	45	54	59	62	64	68	72	75	78	80	81	--	--
36	--	--	--	-25	5	12	29	43	55	61	64	65	69	73	78	--	--	--	--	--
37	--	--	-49	-24	9	5	24	41	57	63	67	--	--	--	--	--	--	--	--	--

Preconsolidation Heads (in feet) -- Layer 6

	1	2	3	4	5	6	7	8	9	10	11	12	13	14	15	16	17	18	19	20
1	--	--	--	--	--	--	--	--	--	--	--	--	--	--	--	--	--	--	--	--
2	--	--	--	--	--	--	--	--	--	--	57	62	--	--	--	--	--	--	--	--
3	--	--	--	--	--	--	--	--	--	44	50	58	64	--	--	--	--	--	--	--
4	--	--	--	--	--	--	--	33	32	37	45	52	62	65	--	--	--	--	--	--
5	--	--	--	--	--	37	29	23	26	29	41	47	61	63	67	--	--	--	--	--
6	--	--	--	-46	27	30	19	15	18	27	36	46	58	61	67	71	--	--	--	--
7	--	--	-52	-49	28	22	5	4	11	18	33	45	53	58	65	70	75	--	--	--
8	--	--	-57	-52	17	10	-10	-7	2	11	28	42	50	56	63	69	74	--	--	--
9	--	--	-62	-60	3	-12	-21	-21	-6	7	23	40	47	54	61	67	72	76	--	--
10	--	--	-70	-69	-18	-24	-25	-24	-11	4	21	36	44	50	58	64	71	75	--	--
11	--	--	-81	-32	-32	-36	-32	-27	-18	--	15	32	41	48	56	63	70	73	77	--
12	--	--	-96	-45	-42	-43	-40	-33	-27	-9	9	28	37	45	53	61	68	72	77	--
13	--	-118	-114	-64	-56	-51	-46	-38	-34	-17	0	22	32	43	49	58	67	71	76	--
14	--	-124	-71	-76	-72	-67	-54	-47	-38	-24	-7	15	28	39	46	55	64	69	75	--
15	-131	-128	-80	-90	-91	-80	-64	-53	-41	-28	-12	8	24	35	43	52	61	67	74	75
16	-136	-72	-88	-99	-110	-99	-72	-55	-44	-32	-16	2	18	30	39	47	58	64	70	75
17	-140	-64	-91	-100	-113	-99	-71	-57	-46	-33	-20	-3	12	24	34	43	53	62	66	73
18	-145	-86	-100	-106	-106	-89	-68	-55	-46	-34	-24	-8	5	19	31	39	50	59	64	67
19	--	-98	-117	-116	-98	-78	-61	-53	-44	-35	-24	-11	1	13	26	37	48	55	61	62
20	-152	-106	-129	-121	-99	-79	-61	-51	-44	-35	-25	-12	0	12	26	36	46	54	60	--
21	-152	-114	-137	-120	-107	-85	-63	-50	-40	-31	-21	-9	4	16	28	37	45	52	58	--
22	-102	-108	-113	-121	-111	-97	-68	-51	-39	-28	-18	-6	7	17	28	36	43	49	56	--
23	--	-90	-109	-115	-108	-96	-69	-53	-41	-31	-20	-8	5	15	22	30	39	47	--	--
24	--	-89	-105	-105	-101	-90	-64	-53	-42	-31	-23	-14	-2	8	17	24	35	45	--	--
25	--	--	-100	-98	-91	-75	-59	-50	-40	-32	-24	-15	-3	3	13	23	36	45	--	--
26	--	--	--	-97	-84	-70	-56	-48	-39	-30	-22	-12	-3	5	16	28	39	46	--	--
27	--	--	--	-97	-84	-70	-56	-48	-40	-30	-19	-8	2	11	20	32	40	46	52	--
28	--	--	--	-92	-85	-72	-58	-48	-40	-28	-17	-6	5	12	22	32	40	46	52	--
29	--	--	--	-95	-92	-73	-61	-49	-39	-27	-15	-6	4	12	21	31	38	44	51	58
30	--	--	--	--	-93	-82	-64	-53	-38	-27	-16	-8	2	10	18	28	37	44	52	59
31	--	--	--	--	-102	-89	-70	-58	-43	-31	-19	-10	-1	9	18	28	36	45	52	61
32	--	--	--	--	-123	-94	-79	-63	-47	-32	-23	-12	-1	9	21	32	39	46	55	--
33	--	--	--	--	-140	-98	-76	-65	-49	-36	-23	-10	2	11	23	34	40	45	52	--
34	--	--	--	--	-151	-101	-74	-67	-51	-38	-22	-9	3	13	24	34	41	45	51	--
35	--	--	--	-169	-141	-103	-80	-66	-50	-36	-22	-9	4	14	25	35	43	45	--	--
36	--	--	--	-180	-135	-102	-81	-64	-46	-33	-21	-8	5	16	27	--	--	--	--	--
37	--	--	-210	-178	-127	-103	-81	-58	-37	-28	-20	--	--	--	--	--	--	--	--	--

Preconsolidation Heads (in feet) -- Layer 7

	1	2	3	4	5	6	7	8	9	10	11	12	13	14	15	16	17	18	19	20
1	--	--	--	--	--	--	--	--	--	--	--	--	--	--	--	--	--	--	--	--
2	--	--	--	--	--	--	--	--	--	--	28	38	--	--	--	--	--	--	--	--
3	--	--	--	--	--	--	--	--	--	4	15	31	42	--	--	--	--	--	--	--
4	--	--	--	--	--	--	--	-21	-21	-10	6	20	38	44	--	--	--	--	--	--
5	--	--	--	--	--	-25	-35	-39	-30	-25	-3	11	36	40	47	--	--	--	--	--
6	--	--	--	-60	-40	-37	-47	-50	-43	-27	-12	7	30	36	46	54	--	--	--	--
7	--	--	-69	-65	-42	-51	-66	-65	-53	-39	-16	6	21	31	43	51	58	--	--	--
8	--	--	-76	-69	-53	-69	-90	-80	-63	-48	-21	3	17	28	40	49	57	--	--	--
9	--	--	-83	-80	-71	-98	-106	-104	-75	-52	-27	1	12	24	36	45	54	61	--	--
10	--	--	-93	-94	-100	-105	-110	-106	-84	-58	-31	-5	8	19	31	42	51	59	--	--
11	--	--	-110	-102	-112	-117	-115	-109	-93	-64	-40	-11	4	15	28	39	50	56	62	--
12	--	--	-133	-122	-122	-124	-120	-113	-104	-76	-47	-17	-2	12	23	36	48	54	61	--
13	--	-161	-160	-145	-139	-129	-124	-115	-109	-85	-59	-25	-8	8	18	32	45	52	60	--
14	--	-171	-157	-161	-160	-149	-131	-124	-112	-92	-69	-34	-14	4	14	28	42	50	59	--
15	-175	-177	-167	-179	-188	-168	-145	-129	-115	-97	-74	-44	-18	-1	10	22	36	46	57	61
16	-180	-168	-184	-200	-219	-200	-157	-131	-117	-101	-79	-52	-27	-10	4	16	32	42	51	60
17	-189	-178	-193	-201	-221	-201	-156	-133	-119	-101	-83	-59	-36	-18	-3	10	25	37	44	57
18	-198	-191	-196	-199	-202	-180	-148	-129	-117	-102	-88	-64	-46	-26	-9	4	20	34	39	48
19	--	-194	-201	-195	-181	-156	-134	-124	-112	-100	-87	-68	-52	-35	-15	1	17	26	35	39
20	-207	-196	-204	-194	-177	-153	-131	-119	-111	-99	-87	-69	-53	-35	-15	0	14	25	35	--
21	-207	-198	-206	-198	-184	-157	-130	-115	-102	-92	-78	-63	-45	-28	-12	2	14	22	31	--
22	-195	-197	-199	-202	-187	-170	-132	-114	-99	-85	-72	-57	-38	-25	-11	1	10	19	29	--
23	--	-192	-199	-195	-180	-166	-129	-114	-101	-87	-73	-58	-41	-28	-19	-8	4	15	--	--
24	--	-191	-192	-179	-171	-157	-121	-111	-99	-86	-77	-67	-50	-37	-27	-18	-2	13	--	--
25	--	--	-183	-170	-159	-137	-116	-107	-94	-86	-77	-69	-52	-44	-31	-18	1	13	--	--
26	--	--	--	-165	-149	-133	-114	-105	-93	-83	-73	-62	-51	-41	-26	-10	7	15	--	--
27	--	--	--	-165	-148	-133	-116	-105	-94	-81	-69	-56	-43	-31	-19	-2	10	17	24	--
28	--	--	--	-166	-150	-136	-120	-107	-95	-79	-65	-52	-38	-28	-14	-1	10	19	26	--
29	--	--	--	-170	-154	-136	-126	-111	-96	-79	-63	-51	-38	-27	-16	-2	8	17	27	35
30	--	--	--	--	-160	-147	-131	-118	-98	-81	-64	-54	-41	-30	-19	-6	8	18	28	38
31	--	--	--	--	-176	-157	-139	-125	-107	-88	-71	-58	-45	-31	-18	-4	7	20	30	42
32	--	--	--	--	-212	-169	-153	-134	-113	-91	-78	-61	-46	-30	-13	4	14	24	34	--
33	--	--	--	--	-231	-177	-150	-139	-118	-98	-79	-59	-42	-27	-8	8	18	25	36	--
34	--	--	--	--	-242	-178	-146	-142	-120	-102	-78	-57	-39	-24	-7	9	20	26	37	--
35	--	--	--	-279	-233	-179	-152	-138	-118	-98	-77	-57	-38	-22	-6	10	23	26	--	--
36	--	--	--	-283	-225	-173	-152	-133	-112	-93	-75	-54	-35	-20	-5	--	--	--	--	--
37	--	--	-316	-279	-211	-170	-149	-121	-95	-85	-73	--	--	--	--	--	--	--	--	--

Preconsolidation Heads (in Feet) -- Layer 8

	1	2	3	4	5	6	7	8	9	10	11	12	13	14	15	16	17	18	19	20
1	--	--	--	--	--	--	--	--	--	--	--	--	--	--	--	--	--	--	--	--
2	--	--	--	--	--	--	--	--	--	--	19	31	--	--	--	--	--	--	--	--
3	--	--	--	--	--	--	--	--	--	-9	4	22	35	--	--	--	--	--	--	--
4	--	--	--	--	--	--	--	-38	-37	-25	-7	10	30	37	--	--	--	--	--	--
5	--	--	--	--	--	-45	-55	-58	-48	-41	-17	-1	28	32	40	--	--	--	--	--
6	--	--	--	-65	-62	-59	-68	-70	-62	-43	-26	-5	21	28	39	48	--	--	--	--
7	--	--	-74	-70	-65	-74	-88	-87	-73	-57	-31	-7	11	23	36	45	53	--	--	--
8	--	--	-82	-74	-76	-94	-115	-103	-84	-66	-36	-9	7	19	32	42	51	--	--	--
9	--	--	-90	-87	-95	-125	-134	-129	-97	-70	-42	-11	1	15	28	38	48	56	--	--
10	--	--	-100	-102	-127	-131	-137	-132	-106	-77	-47	-18	-3	9	23	34	45	53	--	--
11	--	--	-120	-124	-138	-143	-141	-134	-116	-84	-57	-25	-8	5	19	31	43	50	57	--
12	--	--	-144	-147	-148	-149	-145	-137	-127	-97	-65	-32	-14	1	14	28	41	48	56	--
13	--	-175	-175	-172	-165	-153	-149	-138	-132	-105	-78	-39	-21	-3	8	24	38	46	55	--
14	--	-186	-185	-188	-188	-175	-155	-147	-135	-113	-88	-49	-27	-7	4	19	35	43	54	--
15	-190	-193	-195	-207	-218	-196	-170	-153	-137	-118	-94	-60	-32	-12	-1	13	29	39	51	57
16	-195	-200	-215	-232	-253	-231	-184	-154	-139	-122	-99	-69	-41	-22	-7	6	24	34	45	55
17	-205	-215	-225	-233	-254	-232	-183	-156	-141	-122	-103	-76	-51	-31	-15	-1	16	30	37	51
18	-215	-225	-227	-229	-232	-209	-173	-152	-139	-122	-108	-82	-62	-39	-21	-7	11	26	32	41
19	--	-226	-228	-220	-207	-180	-156	-146	-134	-121	-107	-86	-68	-50	-28	-11	7	17	27	32
20	-225	-226	-228	-217	-201	-176	-153	-140	-132	-119	-106	-87	-69	-49	-28	-11	4	16	27	--
21	-225	-226	-228	-223	-209	-180	-151	-135	-122	-111	-96	-79	-60	-42	-24	-9	4	13	23	--
22	-225	-226	-227	-228	-211	-193	-152	-133	-118	-102	-89	-72	-53	-38	-23	-10	--	9	20	--
23	--	-224	-227	-220	-203	-188	-148	-133	-119	-105	-89	-73	-56	-42	-32	-20	-7	5	--	--
24	--	-224	-220	-203	-193	-178	-139	-130	-117	-103	-93	-83	-65	-51	-40	-31	-13	3	--	--
25	--	--	-210	-193	-180	-157	-134	-125	-112	-103	-93	-85	-67	-59	-45	-31	-10	3	--	--
26	--	--	--	-187	-170	-153	-133	-123	-110	-100	-89	-77	-66	-55	-40	-22	-3	6	--	--
27	--	--	--	-187	-168	-153	-135	-124	-112	-98	-84	-70	-57	-44	-31	-13	0	8	16	--
28	--	--	--	-190	-170	-156	-140	-126	-113	-96	-81	-66	-51	-41	-26	-11	1	10	18	--
29	--	--	--	-194	-173	-155	-146	-131	-115	-96	-78	-65	-51	-40	-27	-12	-1	9	19	28
30	--	--	--	--	-181	-167	-152	-138	-117	-97	-80	-68	-55	-43	-31	-16	-1	10	21	31
31	--	--	--	--	-200	-179	-161	-146	-127	-105	-87	-72	-59	-44	-29	-14	-2	13	22	35
32	--	--	--	--	-239	-192	-176	-156	-134	-109	-95	-76	-60	-43	-23	-6	5	16	27	--
33	--	--	--	--	-259	-202	-174	-162	-139	-118	-96	-74	-56	-39	-18	-1	10	18	30	--
34	--	--	--	--	-271	-203	-168	-165	-142	-122	-95	-73	-53	-36	-16	1	13	19	32	--
35	--	--	--	-314	-262	-203	-175	-161	-140	-117	-94	-72	-51	-34	-15	2	16	20	--	--
36	--	--	--	-316	-254	-195	-174	-155	-132	-112	-92	-69	-48	-31	-15	--	--	--	--	--
37	--	--	-349	-311	-238	-192	-170	-141	-114	-103	-90	--	--	--	--	--	--	--	--	--

Preconsolidation Heads (in feet) -- Layer 10

	1	2	3	4	5	6	7	8	9	10	11	12	13	14	15	16	17	18	19	20
1	--	--	--	--	--	--	--	--	--	--	--	--	--	--	--	--	--	--	--	--
2	--	--	--	--	--	--	--	--	--	--	21	32	--	--	--	--	--	--	--	--
3	--	--	--	--	--	--	--	--	--	-5	8	24	36	--	--	--	--	--	--	--
4	--	--	--	--	--	--	--	-34	-32	-20	-3	13	32	38	--	--	--	--	--	--
5	--	--	--	--	--	-44	-52	-53	-43	-35	-12	3	29	34	41	--	--	--	--	--
6	--	--	--	-65	-62	-57	-64	-64	-56	-38	-21	-1	23	29	40	48	--	--	--	--
7	--	--	-74	-70	-65	-72	-83	-80	-66	-51	-26	-3	14	25	37	45	53	--	--	--
8	--	--	-82	-74	-75	-90	-108	-95	-76	-59	-31	-5	10	21	34	43	51	--	--	--
9	--	--	-90	-87	-93	-120	-126	-120	-89	-63	-36	-7	4	17	29	39	48	56	--	--
10	--	--	-100	-101	-123	-126	-129	-124	-98	-70	-41	-14	0	11	24	35	46	53	--	--
11	--	--	-119	-122	-134	-138	-133	-126	-108	-76	-51	-20	-5	7	21	33	44	50	57	--
12	--	--	-142	-144	-144	-143	-137	-129	-118	-88	-58	-27	-10	4	16	30	42	48	56	--
13	--	-173	-172	-167	-160	-147	-141	-130	-123	-97	-70	-35	-17	0	10	25	39	47	55	--
14	--	-183	-181	-183	-181	-167	-147	-138	-126	-105	-80	-44	-23	-4	7	21	36	44	54	--
15	-189	-190	-191	-201	-209	-187	-161	-144	-128	-110	-86	-54	-28	-9	2	15	30	40	51	57
16	-195	-198	-210	-224	-242	-220	-173	-145	-130	-114	-91	-63	-36	-18	-4	9	25	36	46	55
17	-203	-211	-219	-225	-243	-220	-172	-147	-132	-114	-95	-69	-46	-26	-11	2	18	31	38	52
18	-213	-221	-221	-221	-222	-198	-163	-144	-131	-114	-100	-75	-56	-34	-17	-3	14	28	34	43
19	--	-221	-222	-213	-199	-172	-148	-138	-126	-113	-99	-79	-62	-45	-23	-7	10	19	29	34
20	-223	-221	-222	-211	-194	-168	-145	-132	-124	-112	-99	-80	-63	-44	-23	-7	7	18	29	--
21	-223	-221	-222	-216	-201	-173	-144	-128	-116	-105	-90	-73	-55	-37	-19	-5	7	16	25	--
22	-222	-221	-221	-221	-204	-185	-146	-127	-112	-97	-84	-67	-48	-33	-19	-6	3	12	22	--
23	--	-219	-220	-213	-197	-181	-143	-128	-114	-100	-84	-68	-51	-37	-27	-16	-3	8	--	--
24	--	-218	-214	-197	-187	-173	-135	-125	-112	-98	-88	-77	-60	-46	-35	-26	-9	6	--	--
25	--	--	-204	-188	-175	-152	-131	-121	-107	-98	-88	-79	-62	-54	-40	-26	-6	6	--	--
26	--	--	--	-182	-165	-148	-129	-119	-105	-95	-84	-72	-61	-50	-35	-18	0	9	--	--
27	--	--	--	-182	-164	-148	-131	-119	-107	-93	-79	-65	-52	-39	-27	-10	3	10	18	--
28	--	--	--	-184	-165	-152	-135	-121	-108	-91	-76	-62	-46	-37	-22	-8	3	12	20	--
29	--	--	--	-187	-168	-150	-141	-126	-110	-91	-73	-60	-46	-36	-23	-9	1	11	21	29
30	--	--	--	--	-175	-161	-146	-133	-112	-92	-75	-64	-50	-39	-27	-13	1	12	22	33
31	--	--	--	--	-192	-172	-155	-140	-121	-100	-82	-67	-54	-40	-26	-11	--	14	24	36
32	--	--	--	--	-229	-184	-169	-150	-128	-104	-89	-71	-55	-39	-21	-4	7	17	28	--
33	--	--	--	--	-248	-194	-167	-156	-133	-112	-90	-69	-51	-36	-16	0	11	19	30	--
34	--	--	--	--	-260	-195	-162	-158	-136	-116	-90	-68	-49	-33	-15	2	13	19	32	--
35	--	--	--	-303	-253	-197	-169	-155	-134	-112	-90	-68	-47	-31	-14	3	16	20	--	--
36	--	--	--	-306	-246	-190	-168	-149	-127	-107	-88	-65	-45	-29	-13	--	--	--	--	--
37	--	--	-339	-302	-233	-187	-165	-137	-110	-99	-87	--	--	--	--	--	--	--	--	--

Preconsolidation Heads (in feet) -- Layer 11

	1	2	3	4	5	6	7	8	9	10	11	12	13	14	15	16	17	18	19	20
1	--	--	--	--	--	--	--	--	--	--	--	--	--	--	--	--	--	--	--	--
2	--	--	--	--	--	--	--	--	--	--	28	36	--	--	--	--	--	--	--	--
3	--	--	--	--	--	--	--	--	--	7	17	30	39	--	--	--	--	--	--	--
4	--	--	--	--	--	--	--	-22	-18	-6	10	22	36	41	--	--	--	--	--	--
5	--	--	--	--	--	-43	-44	-38	-27	-19	2	14	34	37	43	--	--	--	--	--
6	--	--	--	-65	-62	-52	-53	-48	-37	-21	-6	11	29	34	42	49	--	--	--	--
7	--	--	-74	-70	-64	-64	-69	-61	-46	-32	-10	9	22	30	40	46	53	--	--	--
8	--	--	-81	-74	-72	-80	-89	-74	-55	-40	-14	7	19	27	37	44	52	--	--	--
9	--	--	-88	-86	-88	-104	-103	-95	-66	-44	-19	4	13	23	33	41	49	55	--	--
10	--	--	-100	-99	-112	-110	-106	-98	-75	-49	-24	-2	9	18	30	38	47	53	--	--
11	--	--	-115	-117	-122	-121	-111	-101	-83	-55	-32	-8	5	15	26	36	45	51	57	--
12	--	--	-136	-135	-132	-126	-116	-104	-92	-65	-39	-14	0	12	22	34	44	49	56	--
13	--	-167	-162	-155	-145	-129	-120	-106	-97	-72	-49	-20	-6	8	18	31	42	48	55	--
14	--	-175	-171	-169	-161	-145	-124	-113	-100	-80	-57	-28	-11	4	15	27	39	46	54	--
15	-187	-182	-180	-184	-184	-161	-135	-117	-102	-84	-62	-37	-16	0	11	22	34	43	52	57
16	-194	-190	-195	-202	-210	-186	-143	-119	-104	-89	-68	-44	-23	-7	6	17	31	40	49	56
17	-200	-201	-203	-203	-210	-184	-141	-121	-106	-90	-72	-51	-31	-13	0	12	25	36	42	54
18	-206	-208	-204	-200	-194	-168	-136	-119	-106	-91	-77	-56	-39	-20	-4	7	21	33	39	47
19	--	-209	-205	-194	-176	-148	-125	-115	-103	-91	-78	-60	-44	-28	-10	4	18	27	35	39
20	-216	-209	-205	-193	-173	-147	-124	-111	-103	-92	-79	-61	-45	-28	-10	4	16	26	35	--
21	-215	-208	-204	-197	-180	-152	-124	-110	-97	-87	-72	-56	-39	-23	-7	5	16	24	31	--
22	-214	-207	-203	-200	-183	-164	-128	-110	-96	-82	-68	-52	-34	-21	-7	4	12	20	29	--
23	--	-203	-201	-193	-178	-162	-129	-112	-98	-84	-69	-52	-37	-24	-14	-3	7	17	--	--
24	--	-200	-195	-180	-171	-156	-124	-111	-97	-83	-72	-60	-44	-31	-21	-12	2	15	--	--
25	--	--	-186	-172	-160	-140	-121	-108	-94	-84	-72	-61	-45	-37	-25	-13	4	15	--	--
26	--	--	--	-166	-151	-136	-119	-107	-93	-81	-69	-55	-45	-35	-21	-6	9	17	--	--
27	--	--	--	-165	-149	-135	-120	-107	-94	-79	-65	-50	-38	-26	-15	0	11	18	25	--
28	--	--	--	-166	-150	-137	-122	-108	-95	-77	-62	-47	-33	-24	-12	1	11	19	26	--
29	--	--	--	-167	-151	-135	-126	-112	-96	-77	-60	-46	-34	-24	-13	-1	9	17	26	33
30	--	--	--	--	-156	-143	-130	-117	-97	-78	-61	-49	-37	-27	-17	-4	8	17	26	36
31	--	--	--	--	-170	-152	-137	-124	-104	-84	-66	-53	-40	-28	-16	-4	7	18	28	39
32	--	--	--	--	-199	-162	-148	-131	-110	-87	-72	-56	-41	-28	-13	1	10	20	31	--
33	--	--	--	--	-216	-170	-148	-137	-115	-94	-74	-55	-38	-26	-10	4	12	20	30	--
34	--	--	--	--	-228	-174	-145	-140	-117	-98	-74	-55	-38	-24	-9	5	14	20	31	--
35	--	--	--	-271	-226	-178	-151	-137	-116	-96	-75	-56	-37	-23	-9	5	16	20	--	--
36	--	--	--	-277	-224	-175	-152	-133	-110	-93	-76	-55	-36	-22	-8	--	--	--	--	--
37	--	--	-312	-276	-217	-174	-149	-122	-98	-88	-78	--	--	--	--	--	--	--	--	--

Preconsolidation Heads (in feet) -- Layer 12

	1	2	3	4	5	6	7	8	9	10	11	12	13	14	15	16	17	18	19	20
1	--	--	--	--	--	--	--	--	--	--	--	--	--	--	--	--	--	--	--	--
2	--	--	--	--	--	--	--	--	--	--	39	43	--	--	--	--	--	--	--	--
3	--	--	--	--	--	--	--	--	--	25	33	40	44	--	--	--	--	--	--	--
4	--	--	--	--	--	--	--	-4	5	16	28	35	42	44	--	--	--	--	--	--
5	--	--	--	--	--	-41	-32	-15	-2	7	24	31	41	43	46	--	--	--	--	--
6	--	--	--	-65	-61	-45	-37	-22	-9	4	18	29	39	41	45	49	--	--	--	--
7	--	--	-75	-69	-63	-53	-46	-32	-15	-4	15	28	35	39	44	48	53	--	--	--
8	--	--	-80	-75	-68	-63	-59	-41	-22	-10	12	24	32	36	42	46	52	--	--	--
9	--	--	-87	-84	-79	-80	-67	-55	-31	-13	8	21	28	32	40	45	51	54	--	--
10	--	--	-100	-95	-95	-86	-71	-59	-38	-18	3	16	24	29	37	43	49	53	--	--
11	--	--	-110	-108	-104	-96	-77	-62	-45	-22	-3	11	19	27	35	42	48	52	56	--
12	--	--	-126	-122	-114	-99	-83	-66	-52	-29	-9	7	15	24	32	40	47	51	56	--
13	--	-157	-146	-136	-122	-102	-87	-68	-56	-34	-16	2	11	21	29	38	46	50	55	--
14	--	-162	-155	-147	-131	-112	-88	-73	-59	-41	-21	-4	7	16	27	36	43	49	54	--
15	-185	-169	-162	-157	-144	-120	-94	-76	-61	-45	-27	-10	3	14	24	34	41	47	53	58
16	-192	-178	-172	-168	-159	-134	-96	-78	-64	-50	-32	-16	-2	10	22	30	39	46	52	58
17	-194	-185	-176	-168	-159	-129	-94	-80	-66	-52	-37	-21	-7	7	18	26	35	43	49	57
18	-196	-190	-177	-167	-150	-120	-92	-80	-67	-55	-42	-27	-12	3	14	23	33	42	48	53
19	--	-190	-178	-165	-141	-110	-89	-79	-67	-58	-45	-30	-16	-3	11	21	31	39	45	48
20	-206	-190	-178	-165	-141	-113	-90	-78	-70	-62	-48	-31	-17	-3	11	21	29	38	44	--
21	-203	-187	-176	-166	-147	-120	-94	-80	-69	-59	-45	-30	-14	-2	12	20	29	36	41	--
22	-201	-185	-175	-167	-151	-132	-100	-83	-70	-58	-43	-28	-13	-1	11	20	27	33	39	--
23	--	-178	-171	-163	-150	-132	-106	-88	-74	-60	-45	-28	-15	-3	7	15	23	30	--	--
24	--	-173	-166	-153	-144	-131	-107	-89	-74	-60	-48	-33	-19	-8	2	9	19	29	--	--
25	--	--	-159	-147	-137	-121	-105	-90	-74	-61	-48	-34	-20	-12	-1	8	20	28	--	--
26	--	--	--	-142	-130	-117	-104	-89	-74	-59	-45	-30	-20	-11	0	12	23	29	--	--
27	--	--	--	-140	-127	-116	-102	-88	-75	-58	-43	-27	-16	-7	4	15	23	30	35	--
28	--	--	--	-138	-126	-115	-101	-88	-74	-56	-41	-25	-14	-6	4	15	23	30	35	--
29	--	--	--	-137	-126	-112	-102	-90	-74	-55	-39	-25	-14	-6	3	13	21	27	35	40
30	--	--	--	--	-127	-116	-104	-93	-73	-56	-39	-27	-16	-8	-1	9	18	26	33	41
31	--	--	--	--	-135	-121	-109	-98	-77	-59	-42	-30	-18	-10	-1	9	17	25	34	42
32	--	--	--	--	-153	-127	-116	-103	-82	-62	-45	-33	-19	-11	-1	8	16	24	34	--
33	--	--	--	--	-167	-135	-118	-108	-87	-67	-47	-32	-19	-10	0	8	14	21	30	--
34	--	--	--	--	-178	-142	-119	-110	-88	-70	-49	-34	-20	-10	-1	9	15	22	30	--
35	--	--	--	-222	-185	-150	-124	-109	-88	-71	-53	-37	-21	-10	-1	9	16	20	--	--
36	--	--	--	-232	-189	-152	-126	-106	-85	-71	-58	-40	-22	-12	-1	--	--	--	--	--
37	--	--	-268	-235	-193	-153	-125	-100	-79	-71	-64	--	--	--	--	--	--	--	--	--

Preconsolidation Heads (in feet) -- Layer 13

	1	2	3	4	5	6	7	8	9	10	11	12	13	14	15	16	17	18	19	20
1	--	--	--	--	--	--	--	--	--	--	--	--	--	--	--	--	--	--	--	--
2	--	--	--	--	--	--	--	--	--	--	54	52	--	--	--	--	--	--	--	--
3	--	--	--	--	--	--	--	--	--	50	53	54	50	--	--	--	--	--	--	--
4	--	--	--	--	--	--	--	21	35	45	54	54	50	49	--	--	--	--	--	--
5	--	--	--	--	--	-39	-15	17	32	42	53	54	50	50	49	--	--	--	--	--
6	--	--	--	-65	-60	-35	-14	13	29	38	50	54	52	50	49	50	--	--	--	--
7	--	--	-75	-68	-61	-38	-15	8	27	34	49	53	53	51	49	50	53	--	--	--
8	--	--	-78	-75	-63	-41	-18	4	22	31	46	48	50	49	49	50	53	--	--	--
9	--	--	-84	-82	-67	-47	-19	-1	17	28	44	44	47	45	49	49	53	53	--	--
10	--	--	-100	-91	-72	-54	-23	-6	11	25	40	40	43	44	48	49	52	53	--	--
11	--	--	-103	-96	-79	-61	-31	-10	6	22	35	37	39	42	46	49	51	53	55	--
12	--	--	-112	-103	-89	-63	-39	-14	3	20	31	34	36	40	45	49	51	53	55	--
13	--	-144	-126	-110	-91	-65	-43	-18	-1	17	28	32	34	39	44	49	51	53	55	--
14	--	-145	-134	-116	-89	-66	-40	-19	-4	11	27	29	31	33	43	49	49	52	54	--
15	-181	-151	-139	-120	-90	-65	-39	-21	-6	8	22	27	28	33	43	48	50	53	55	58
16	-190	-163	-141	-122	-91	-64	-33	-24	-10	3	16	22	26	33	42	47	50	54	57	60
17	-186	-164	-141	-122	-90	-55	-29	-25	-12	-1	10	18	25	33	41	46	50	53	58	60
18	-182	-164	-141	-123	-90	-56	-34	-27	-15	-6	6	13	24	33	40	45	49	53	59	61
19	--	-165	-141	-125	-93	-59	-40	-30	-19	-12	0	11	22	31	39	44	48	54	58	60
20	-192	-165	-141	-127	-98	-68	-45	-34	-26	-20	-5	9	21	30	38	43	48	53	56	--
21	-188	-160	-139	-125	-103	-78	-52	-41	-31	-21	-8	6	19	27	38	41	47	52	55	--
22	-183	-155	-137	-124	-108	-88	-62	-46	-35	-26	-9	4	15	25	36	41	46	50	54	--
23	--	-144	-131	-121	-112	-92	-75	-55	-41	-27	-14	4	15	25	35	41	44	49	--	--
24	--	-136	-127	-116	-109	-96	-84	-60	-43	-29	-15	4	14	24	33	37	42	48	--	--
25	--	--	-122	-114	-106	-95	-85	-64	-47	-30	-15	4	14	22	31	36	41	47	--	--
26	--	--	--	-109	-101	-92	-83	-64	-48	-30	-14	4	14	21	29	36	42	46	--	--
27	--	--	--	-106	-97	-89	-78	-63	-48	-30	-12	5	14	20	29	36	40	45	50	--
28	--	--	--	-100	-95	-85	-74	-61	-47	-28	-12	5	13	20	26	34	38	45	48	--
29	--	--	--	-95	-92	-81	-70	-60	-45	-26	-11	4	12	19	24	31	36	41	46	49
30	--	--	--	--	-88	-79	-69	-61	-41	-25	-10	3	12	17	21	28	33	38	42	48
31	--	--	--	--	-88	-79	-71	-63	-41	-26	-10	1	11	15	20	25	31	34	42	47
32	--	--	--	--	-92	-81	-74	-65	-45	-27	-9	-2	10	13	15	18	24	29	39	--
33	--	--	--	--	-102	-86	-77	-69	-49	-30	-12	-1	8	10	13	15	18	24	30	--
34	--	--	--	--	-112	-98	-83	-71	-50	-33	-16	-6	4	9	11	14	17	24	28	--
35	--	--	--	-157	-130	-112	-87	-72	-51	-37	-23	-12	1	8	10	13	16	20	--	--
36	--	--	--	-171	-143	-121	-91	-71	-51	-42	-34	-19	-3	3	9	--	--	--	--	--
37	--	--	-210	-180	-161	-125	-92	-70	-54	-48	-45	--	--	--	--	--	--	--	--	--

Preconsolidation Heads (in feet) -- Layer 14